UNIVERSITY OF
KWAZULU-NATAL

INYUVESI
YAKWAZULU-NATALI

NUCLEATION INDUCED BY HIGH FREQUENCY SOUND FOR THE PRODUCTION OF SUGAR REFINERY SEED CRYSTALS

Shaun Madho

BSc Eng (Chemical)

University of KwaZulu-Natal

This dissertation is submitted in fulfillment of the academic requirements for the degree of Master in Science in Engineering (Chemical) at the School of Engineering, University of KwaZulu-Natal

Supervisor

Prof. Maciej Starzak

August 2016

DECLARATION

I, Shaun Madho, declare that:

(i) The research reported in this dissertation, except where otherwise indicated, is my original work.

(ii) This dissertation has not been submitted for any degree or examination at any other university.

(iii) This dissertation does not contain other persons' data, pictures, graphs or other information, unless specifically acknowledged as being sourced from other persons.

(iv) This dissertation does not contain other persons' writing, unless specifically acknowledged as being sourced from other researchers. Where other written sources have been quoted, then:
   a. Their words have been re-written but the general information attributed to them has been referenced;
   b. Where their exact words have been used, their writing has been placed inside quotation marks, and referenced.

(v) Where I have reproduced a publication of which I am an author, co-author or editor, I have indicated in detail which part of the publication was written by myself alone and have fully referenced such publications.

(vi) This dissertation does not contain text, graphics or tables copied and pasted from the internet, unless specifically acknowledged, and the source of being detailed in the thesis and in the Reference sections.

31 JULY 2017

Shaun Madho Date

As the candidate's supervisor I agree/do not agree to the submission of this dissertation.

31 July 2017

Prof. Maciej Starzak Date

ABSTRACT

The crystallisation process is the second oldest unit operation in existence and a *sine qua non* in the production of crystalline sugar. It comprises two distinct phases viz. nucleation and the growth of the subsequent crystal. The former is conventionally achieved by either shock- or replaced by slurry-seeding, and is not a very well understood process in the sugar industry. It is generally accepted then that the adopted industrial nucleation processes have been derived more out of experience than from scientific fundamentals.

The use of sound waves has the potential to create repeatable numbers of seed crystals from supersaturated sucrose solutions, that can be grown to a robust size in the absence of evaporation, for a controlled full seeding technique. This study describes benchtop-scale trials performed at the Sugar Milling Research Institute NPC (SMRI) that explored the usage of sound waves for seed crystal formation. The range of suitable operating conditions which could enable this process to produce seed for conventional panboiling was investigated by calculation. Using this range of operating conditions as a specification, an extensive benchtop scale laboratory investigation identified the equipment and operating conditions that could be able to produce acceptable seed crystals in a continuous process. As part of the investigation it was been necessary to develop appropriate techniques for measuring crystal sizes, size distributions and number densities.

The results of the laboratory tests show that acceptable seed crystal sizes, with an acceptable crystal size distribution, can be achieved by growth at constant temperature. During the growth phase the nuclei exhaust the available supersaturation of the mother liquor from which they have been nucleated. The crystal number densities obtained are high enough to achieve a range of acceptable densities by the addition of extra mother liquor after nucleation if desired. It was concluded that the process is technically feasible for refinery seed production.

Various classical crystal growth theories were modelled on Matlab®. The results predicted for the empirical n^{th}-order kinetics with concentration-based driving force, compared well with the experimental results for growth of crystals obtained from sound induced secondary nucleation.

Potential benefits of the full continuous seed production system include:

- Addressing the skills shortage associated with batch panboiling (a skill recognised by the Agricultural Sector Educational and Training Authority (AGRISETA) of South Africa to be the only unique skill in the sugar industry). Poor recoveries of sucrose have been experienced during panboiling due to diminishing skills in this area. A new full continuous seed production system without evaporative crystallisation involved will make batch seed pans obsolete and eliminate the pan skills issue.
- Steam savings from elimination of the slurry nuclei conditioning phase in panboiling. Elimination of this phase would also improve the capacity utilisation of pans.
- Improved sugar quality through narrower crystal size distributions. This will also improve drying and conditioning operations.
- Improved sugar recovery in centrifuges as the narrower size distribution will reduce the amount of smaller crystals escaping through screen perforations into the lower value molasses.
- Elimination of multi-storey crystallisation plants due to eliminating the need to discharge large quantities of seed hydraulically from pans in short times. The proposed seed system could lead to a ground floor crystallisation operation with large structural savings for new factories.

ACKNOWLEDGEMENTS

Before the many people I am grateful to are acknowledged, I bow my body, mind and soul to the light and energy that guides my loved ones and myself. In the same breath it has to be said that I am also forever indebted to the support my family and friends have given me through the completion of this work, and in pursuing further studies.

Savar Kailash Madho, you are the sun to me, and my daily inspiration.

This research has been conducted over the course of many years at the Sugar Milling Research Institute NPC (SMRI). The project developed from a proposal by Dr Barbara Muir (SMRI) to use high frequency sound to form slurry nuclei in order to replace ball-milled slurries, as found in papers on this topic (uptake of this technology into industry could not be verified). A Project Team recognised the potential of the technology to produce crystal seeds instead of slurry crystals, which would be of greater benefit to the sugar industry. This project was led by myself, Shaun Madho, as a senior process engineer at the SMRI. The project was supported by an Advisory Research Committee to the SMRI comprising senior representatives of the South African sugar milling companies. The Technology Group of Tongaat Hulett Sugar (THS) subsequently became technology partners for the project and co-funding for the work was received from the South African Department of Science and Technology (this funding was managed by the Technology Innovation Agency).

As the technology and commercial partners, THS were active in establishing the industrial requirements of the process proposed. Dr Dave Love, of THS, and part of the Project Team, is specifically acknowledged in the pages of this work for his individual contributions to the project.

At the SMRI, Steve Davis, Dr Janice Dewar, Sayed Rahiman and Dr Richard Loubser constituted the remaining members of the Project Team. They are all sincerely thanked

for their technical and strategic guidance throughout the course of the project. In particular Sayed Rahiman is singled out for his meticulous work and attention to detail in assisting with the running of the laboratory test work and also the analysis of the product obtained.

Prof. Maciej Starzak, my supervisor for this research, gave very useful guidance on crystal growth mechanisms. I would also like to thank him for his continuous support.

TABLE OF CONTENTS

LIST OF FIGURES

LIST OF TABLES

COMMONLY USED ABBREVIATIONS

AGRISETA	Agricultural Sector Educational and Training Authority
CSD	Crystal Size Distribution
CSPS	Continuous Seed Production System
CV	Coefficient of Variance
MA	Mean aperture (crystal size)
SMRI	Sugar Milling Research Institute NPC
SSC	Supersaturation coefficient
THS	Tongaat Hulett Sugar
VHP	Very High Pol

GLOSSARY

agglomerate	Inter-grown cluster of several crystals. Also referred to as conglomerates.
brix	(Refractometer brix) - The term used when a refractometer, equipped with a scale and based on the relationship between refractive indices at 20°C and the percentage by mass of total soluble solids of a pure aqueous sucrose solution, is used instead of a hydrometer to test the solids concentration of a sucrose containing solution.
cavitation	The formation and implosion of bubbles upon insonation at certain frequencies and intensities.
compression	A forward motion by a wave in an area of increased pressure and density.
conglomerates	Inter-grown cluster of several crystals. Also referred to as agglomerates.
crystallisation	Formation of solid particles within a homogeneous phase.
dry solids	In most cases, moisture free solids.
false grains	Undesirable small crystals formed in the intermediate or labile zones of supersaturation.
frequency	The number of vibrations that a molecule in a medium makes per second.
gravity purity	Ratio of sucrose to brix percentage.
horns	A component of an insonation system that amplifies the vibrating motion generated by a transducer. Also referred to as a waveguide.
insonation	The application of a high frequency sound wave.
intermediate zone	In this zone of supersaturation, sugar crystals will continue to grow but new nuclei will form in the presence of sugar crystals.
irradiation	The application of a high frequency sound wave.
labile zone	In this zone of supersaturation, new crystals will form spontaneously.
magma	A mixture of sugar and a sugar solution that is prepared by mechanical means. Usually used as a seed for A-massecuite pans.

massecuite	Mass of sugar crystals together with the surrounding liquor. From the French words masse cuite (cooked mass).
metastable zone	In this zone of supersaturation, sugar crystals will grow but no new nuclei will form.
molasses	The sucrose solution around the sugar crystal from which no more sucrose can be deposited onto the crystal.
movement water	Condensate used in the evaporative crystallisation process to wash away small crystals.
nucleation	Generation and development of small crystals capable of growth.
pan	Vessel used for the growth of crystals by evaporative crystallisation, usually under a vacuum.
panboiling	Crystallisation operation where massecuites are grown.
period	The time taken for a complete vibration of a point in the path of the wave.
pol	Apparent sucrose content determined using a polarimeter.
purity	Ratio of pol to brix.
rarefaction	A backward wave movement resulting in a zone of decreased molecular density and low pressure.
rawhouse	That part of a sugar mill which produces a brown sugar from sugar juices.
refinery	A sugar factory that removes impurities from a brown sugar to produce a white sugar.
saturated	A solution that contains the total quantity of a substance that it can dissolve at a particular temperature.
seed	A footing or mixture of grown crystals for further growth in massecuite pans.
slurry	Minute sugar specs or nuclei, usually suspended in an organic solvent.
solubility	The concentration of a solute in a solvent.
solute	A substance dissolved in another substance, forming a solution e.g. dissolved sugar in water.
supersaturated	The ratio of the concentration of sucrose to the solubility of sucrose at

	the same temperature (for pure sucrose solutions).
syrup	A concentrated sugar solution, usually at approximately 65-70% sucrose content.
transducer	A component of an insonation system that converts electrical energy into mechanical energy.
wave guide	A component of an insonation system that amplifies the vibrating motion generated by a transducer. Also referred to as a horn.

CHAPTER 1 - INTRODUCTION

Despite advances in the chemical and engineering disciplines, sucrose still cannot be created in a factory. It is created in the plant, be that plant sugar cane or sugar beet or otherwise. In the factory, it is merely separated from the plant, usually in the crystalline form.

Crystallisation in raw sugar factories and refineries is very much at the heart of the process. All preceding unit operations are simply preparatory processes, performed to achieve a high quality raw material for crystallisation – one of the oldest unit operations in existence. The fundamentals of the process have not changed much since its inception, a characteristic which is shared with most processes in the sugar industry. Shreve's Chemical Process Industries (Austin GT, 1984), a renowned chemical engineering reference book that details the chemical processing of raw materials into useful and profitable products, introduces the manufacture of sugar [*sic*] as follows, "The major processing methods used for refining cane sugar today have been worked out for many years and are unlikely to change drastically soon. Alterations to conserve energy and perhaps reduce the use of some reagents are to be expected, but major process changes seem unlikely". Nucleation in sugar crystallisation is certainly one such process.

In conventional industrial sucrose crystallisation all product crystals are grown from small seed crystals purposely added at the start of the crystallisation process. The ideal situation is that of "full seeding" where a known quantity of seed crystals all grow into product crystals, without any of the seed crystals dissolving or any new crystals being generated by unwanted nucleation. This ideal situation is seldom achieved by either of the conventional processes of "shock seeding" (where crystals are formed spontaneously at very high supersaturations) or "slurry seeding" (where the nuclei for sugar formation are introduced in the form of a few litres of ball-milled refined sugar crystals). Controlled nucleation of seed crystals, induced by sound waves, has the potential to create reproducible numbers of nuclei that can be grown to a robust size of seed crystal in the

absence of any evaporation and thereby provide a mechanism for achieving “full seeding”.

In the conventional processes the slurry is usually prepared in a ball-mill that crushes sugar crystals in a suspension of methylated spirits (Anon, 1985). Millions of broken crystals result and have a large variation in the sizes produced. These nuclei are then further grown to obtain sugar crystals, also of varying sizes. The size range is of severe consequence to the economics of the sugar mill as crystallisation rates are affected, as well as equipment capacities (evaporative crystallisers or pans and centrifugals). To limit the variation in size, the nuclei introduced into the pans are conditioned with condensate to wash away smaller crystals (same procedure applied to crystals formed from shock seeding). This process is naturally energy intensive, as any water introduced needs to be evaporated to achieve desired supersaturations. There is also little control over crystal number densities in the process. For these reasons, ultrasound is proposed as a method to induce nucleation in supersaturated sugar solutions, overcoming the energy requirement for the initiation of nucleation and possibly achieving more uniformly sized sugar nuclei. To date and to the best knowledge of the author, this method has not been commercialised and is not used anywhere in the world in the sugar industry. Not production related, but very advantageous to the sugar industry, would be the possibility of using the technology to overcome the skills shortage in crystallisation operations (panboiling) - panboiling was identified to be the only unique skill in sugar processing by Agricultural Sector Education Training Authority (AGRISETA). Furthermore, pans are placed high up in sugar factories to discharge large volumes of product rapidly (difficult to pump). A continuous full seed production system without the need for pans may eliminate the need for multi-storey factories (structural savings will be a game changer in the design of new factories).

It is assumed that those reading this work are well versed in the workings of the sugar industry. For those not familiar with the industry, the process of producing a raw/brown sugar or Very High Pol (VHP) sugar is adequately described by Pillay (1994). More detailed information can be obtained in texts such as Hugot (1986) and Rein (2007) – these would include the production of white refined sugar as well. For sugarbeet

processing van der Poel *et al*. (1998) can be referenced. As such this thesis describes the production of a seed for refined sugar manufacturing, a brief overview of the refining process follows: VHP sugar, as produced by a raw sugar mill, has a pol of over 99,3% and a moisture of 0,15%. This gives a brix of 99,85% (100-0,15%) and hence a non-pol content of 0,55% (brix-pol). This non-pol represents impurities in the VHP sugar. The purpose of the refinery is to remove impurities from sugar crystals. South African refineries, whether attached to a raw sugar mill (a backend refinery), or whether it stands separately as a "central" refinery, accepts VHP sugar as its raw material. The VHP sugar is dissolved (melted) into condensate or low brix process streams and the melt is processed. The melt purity is in excess of 99%. The impurities are in the form of colour compounds and ash (inorganic constituents). The melt colour is reduced by various clarification processes which also removes some ash. This process stream is then further decolourised and concentrated in evaporators to produce a liquor from which up to four crops of crystals can be boiled. The crystals from each of these boilings are combined to form commercial refined sugar. The resultant "final molasses" may be boiled to produce more crystals that will be remelted, may be recycled to rawhouse syrup (in backend refineries) or may be used as a by-product. Re-crystallisation alone is a powerful purification step that can substantially reduce colour. The general refining process is shown in Figure 1.1. (Madho, 2016).

The research proposal presented is done so in the partial fulfilment of a Master of Philosophy degree in Chemical Engineering at the University of KwaZulu Natal. It includes a literature survey on irradiation, its mechanisms and its applications, with particular reference to sono-nucleation. Also included in the survey are summaries of sucrose nucleation, typical slurries used and the benefits and marketplace of a new slurry preparation system producing a narrow size distribution of crystals. The findings of the experimental program are presented, as well as future recommendations for larger scale work. All experimentation was performed on a bench-top scale. Classical crystal growth theories were also modelled and compared to the experimental data obtained.

Generally, it should be noted that even though attention is given to the production of a seed for refinery usage, the process is also applicable to VHP and beet sugar processing.

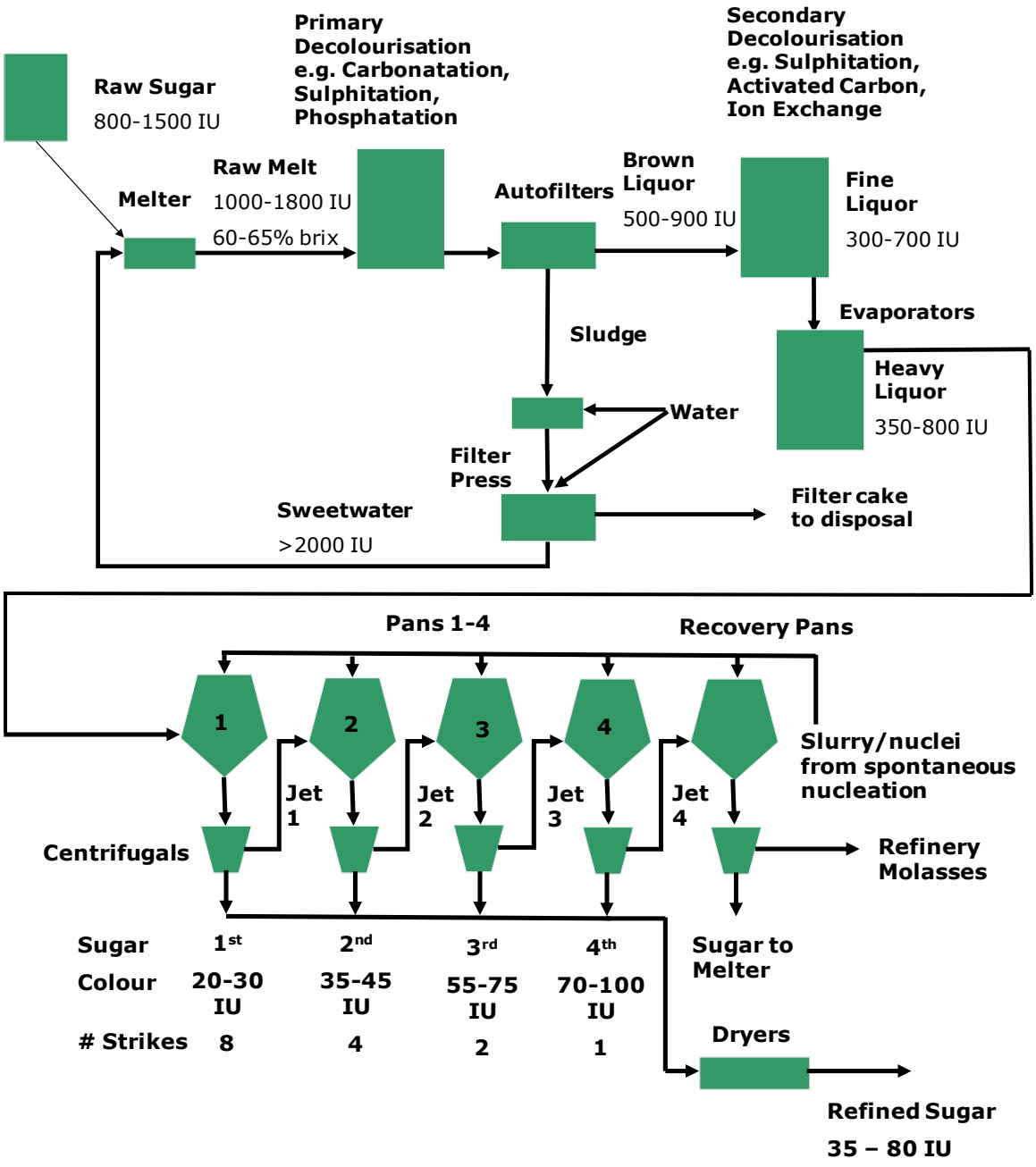

Figure 1.1. A simplified process flow diagram for the production of refined sugar (Madho, 2016)

CHAPTER 2 - ABOUT SOUND WAVES, IRRADIATION AND ULTRASOUND

Ultrasound can be defined as sound which is of a frequency above the limit to which the human ear can respond. The exact reported frequency at which this begins though varies, for example, Mason (1990) reported on the work of Galton who determined the limit to be about 16 kHz but Hedrick *et al*. (1995) define ultrasound as high frequency mechanical waves that humans cannot hear (greater than 20 kHz). Hedrick *et al*. also define infrasound as a frequency which humans cannot hear as frequencies below 20 Hz. It should be stated that sound, ultrasound and infrasound all have the same properties and are often used interchangeably in the description of physical and chemical interactions. In this chapter, as well as throughout this thesis, various terms have been used to denote the use of sound waves e.g. irradiation, insonation, ultrasound and sonication. Given that the exact start of the ultrasound range has not been verified, the other terms are used to denote the general use of sound waves, whether or not it is in fact used in the ultrasound range. The use of the term ultrasound has been maintained when reference is made to the work of others.

Irradiation is widely used in fields such as biology and biochemistry, dentistry, engineering, geology, medicine and plastics and polymers, as well as in industry. These are briefly discussed in this chapter with particular attention given to the use of ultrasound in nucleation (sono-nucleation), crystallisation (sono-crystallisation) and in general chemistry (sono-chemistry). The history and background of irradiation and ultrasound are discussed, as is the principles of cavitation and acoustic streaming, the factors influencing cavitation and typical equipment used.

2.1. The history of irradiation

Although certain applications of ultrasound are just beginning to emerge (Suslick, 1990), the origins of ultrasound or irradiation can be traced back to the early 1800's. In 1847, what is now known as magnetostriction, was identified by Joule when an increase in length was observed on applying a magnetic field to an iron bar (Mason, 1976).

Subsequently, sound waves are produced in the surrounding medium, or when an alternating field, by means of a solenoid, is applied across a ferromagnetic material (Schwikkard, 2001).

Galton, in 1883, determined the normal limit of human hearing (16-18 kHz) when he produced a whistle which generated sound at known frequencies (Mason and Lorimer, 1988 and Mason, 1990). The whistle is an example of an ultrasonic transducer, a device that transforms one form of energy into another. In Galton's case this would be from gas motion to ultrasound.

Mason (1990) also reports that the type of transducer used in most sono-chemical equipment today is based on the piezoelectric effect, which was discovered by the Curie brothers at the turn of the 19th century. The effect is found in some crystalline materials (e.g. quartz) and results in a potential difference across opposite faces when subjected to sudden compression. Modern transducers use an inverse effect where a rapidly alternating potential is placed across the faces of a piezoelectric crystal that generates dimensional changes, and thus converts electrical energy into vibrational or sound energy.

Suslick (1990) states that the most important nonlinear acoustic process for sono-chemistry is cavitation (the formation and implosion of bubbles upon insonation at certain frequencies and intensities). Its initial observation was made by Sir Thornycroft and Sydney Barnaby, in 1894, during speed trials on the propeller of the first modern destroyer, the H.M.S Daring. Bubble formation, severe vibration and propeller surface damage was reported. This was confirmed by Lord Rayleigh in 1917 (Suslick, 1989), who described the first mathematical model for the collapse of cavities in incompressible liquids and predicted local temperatures (10 000 K) and pressure (1 000 000 kPa) during such collapses. These conditions are different to what occurs in an ultrasonic field, however, but did form the basis for the development for ultrasonic cavitation theory (Neppiras, 1984).

In the 20th century ultrasound started to find several engineering, medical and chemical applications. Langevin used ultrasound, in 1917, for depth and submarine detection and discovered that small fish were killed upon application (Mason, 1976). Richards and Loomis (1927) pioneered the chemical effects of ultrasound and found that chemical transformations were accelerated by ultrasound in the explosion of nitrogen tri-iodide, mercury dispersion, lowering of boiling points of liquids, the hydrolysis of dimethyl sulfate and the iodine clock reaction. Frenzel and Schultes, in 1934, first reported the emission of light during sonication – sonoluminescence (Harvey, 1939).

2.2. Basic irradiation physics

2.2.1. Sound waves

Sound is mechanical energy that is transmitted through a medium. Since the motion of the molecules in the medium is repetitive, the term cycle is used to describe the sequence of changes in molecular motion that recurs at regular intervals.

The frequency of a wave is the number of vibrations that a molecule in the medium makes per second, or the number of times the cycle is repeated per second. For comparative purposes, a high frequency means that the cyclic motion is executed at a faster rate and more cycles are completed in a time interval than at a lower frequency.

The simple harmonic motion of a wave can be represented as Equation 2.1. (Hedrick *et al.*, 1995).

$$A = A_0 \cdot \sin(2 \cdot \pi \cdot f \cdot t) \qquad \textbf{…Equation 2.1.}$$

where A is the amplitude of the wave (m) at time t (s), A_0 is the peak amplitude (maximum distance from rest position) and f is the frequency in Hz.

The time taken for a complete vibration of a point in the path of the wave is called the period of the wave (τ) and is given as the inverse of the frequency. There are other terms

to describe waves such as crests and troughs. Crests are the top of the waves whilst troughs are their opposite. The distance between two crests or troughs is the wavelength (λ) which can be Equation 2.2. These terms are illustrated in Figure 2.1.

$$\lambda = \frac{c}{f} \qquad \text{…}\textbf{Equation 2.2.}$$

where λ is the wavelength in m, c is the speed of sound in the medium (m/s) and f is the frequency in Hz.

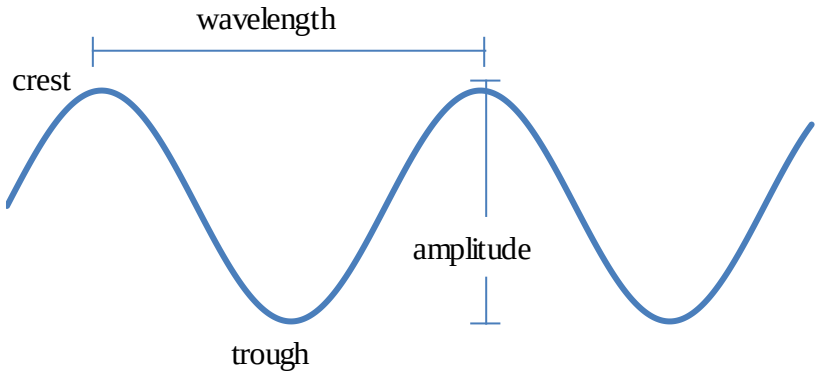

Figure 2.1. Sinusoidal wave illustrating wavelength, amplitude, crests and troughs

Waves in general can be divided into two categories viz. longitudinal and transverse waves. With longitudinal waves the particle motion is along the direction of the wave energy propagation and with transverse waves the motion is perpendicular. Sound waves are longitudinal (Hedrick *et al.*, 1995 and Bueche, 1986) and its velocity can be given by Equation 2.3. (Bueche, 1986).

$$v = \sqrt{\frac{\gamma \cdot P}{\rho}} \qquad \text{…}\textbf{Equation 2.3.}$$

where v is the velocity of sound (m/s), γ is the ratio of specific heat at a constant pressure and at a constant volume, P is pressure (N/m^2) and ρ is density of the medium (kg/m^3).

Another term used to describe sound waves is its intensity. The intensity (W/m^2) is defined as the power passing through a unit area erected perpendicular to the direction of propagation. For a person near the source of the sound a painful sound is about 1 W/m^2 or 120 dB (decibels – an intensity level scale given by Equation 2.4.). Other sound intensities include 10^{-2} W/m^2 for a jackhammer, 10^{-6} W/m^2 for an ordinary conversation and 10^{-12} W/m^2 for a barely audible sound or 100, 60 and 0 dB respectively (Bueche, 1986).

$$Intensity\ level\ in\ decibels\ (dB) = 10 \cdot \log\frac{I}{I_0} \quad \text{…}\textbf{Equation 2.4.}$$

where I is the intensity of the sound in W/m^2 and I_0 is a reference intensity, usually taken to be 10^{-12} W/m^2 (Bueche, 1986).

2.2.2. Compression, rarefaction and cavitation

It has been discussed that sound waves are pressure or mechanical waves that result in the movement of particles of a medium across or through their mean positions as is given in Equation 2.1. and illustrated in Figure 2.1. A forward motion results in an area of increased pressure and density and is termed compression. A backward movement results in a zone of decreased molecular density and this low pressure region is termed rarefaction. Through various cycles of compression and rarefaction, the molecules in the medium subjected to sound vibrate back and forth through their mean positions, a distance of only a few microns. These molecules do not travel from one end of the medium to the other i.e. there is no flow of molecules but rather the effect is transmitted over long distance from molecule-to-molecule or neighbour-to-neighbour interactions.

McCausland *et al*. (2001) states that the fundamental effect of ultrasound on a continuum fluid is to impose an oscillatory pressure on it. At low pressures the ultrasonic wave will induce motion and mixing within the fluid. This process is known as acoustic streaming. At high intensities, the local pressure in the rarefaction phase of the wave cycle falls below the vapour pressure of the fluid causing minute bubbles or cavities to grow. A

further increase in intensities creates negative transient pressures within the fluid enhancing bubble growth and producing new cavities by the tensioning effect of the fluid. During the compression phase of the cycle the increase in pressure either contracts the void or bubble to a smaller size or eliminates it by implosion. This process of acoustic bubble formation and implosion is known as cavitation (illustrated in Figure 2.2.), a process that is nonlinear in that the changes to the radius of the voids are not proportional to the variations in acoustic pressure.

Suslick (1990) reports that the collapse of the bubbles formed in cavitation results in an intense heating. The localised hotspots have temperatures of roughly 5 000^{o}C at pressures in excess of 50 000 kPa with a lifetime of only a few microseconds. Shock waves from the cavitation in liquid solids slurries can produce high velocity interparticle collisions, the impact of which is sufficient to melt most metals.

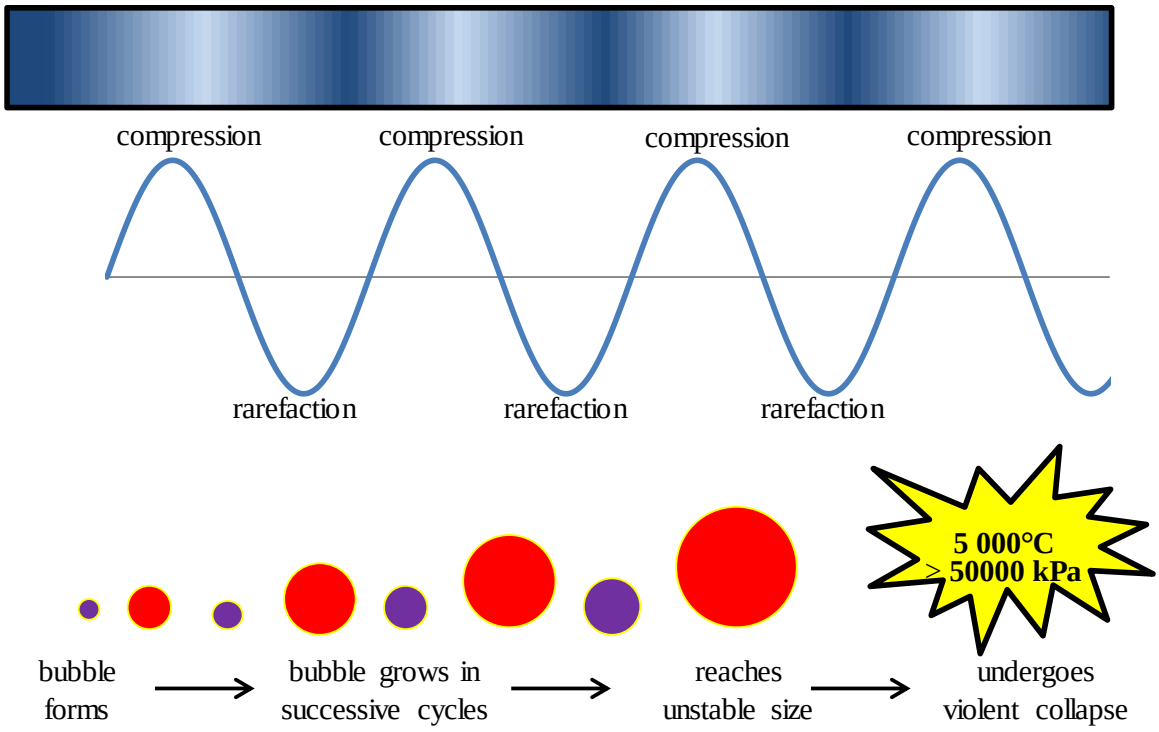

Figure 2.2. The cavitation process illustrated

McCausland *et al*. (2001) also report that there are two types of voids or cavities that form viz. stable or transient. The stable cavities exist over several cycles and oscillate, usually nonlinearly, around some mean equilibrium size. The transient cavities exist for only a single cycle (up to two cycles – Mason, 1990). They may enlarge to many times their original size during their expansion and collapse quite violently during compression. The implosion of gas-filled cavities generates a number of smaller bubbles, whilst a vapour-filled cavity will collapse with considerable violence, as there is no residual compressible gas to cushion the mechanical effect. Mason (1990) states that transient bubbles generally form with intensities greater than 10 W/cm^2.

The onset of cavitation is difficult to determine using theoretical or mechanistic criterion. Experimentally though cavitation can be observed to occur above a certain threshold in ultrasonic intensity. Delivery of irradiation by a probe will be at its highest intensity originating at its tip and falling off dramatically as the distance increases. The existence of cavitation can be detected by the pitting of a small test plate of metal foil in the liquid. In any application where irradiation is used, the majority of the visible bubbles would be as a result of stable cavitation, however, the most dramatic effects of irradiation, such as the pitting of foil upon insonation, are due to the unstable transient cavities and their collapse.

2.3. Cavitation and nucleation

Sucrose nucleation is dealt with in some detail in Chapter 3. True homogeneous nucleation is uncommon in practice, sucrose nucleation being no different, and only happens at high levels of supersaturation. Under such conditions, reversible clustering occurs. Generally, nucleation almost always occurs heterogeneously and it is believed to be associated with traces of suspended solids or imperfections in the container's or vessel's surfaces that function as nucleation sites.

McCausland *et al*. (2001) provide good experimental evidence that applying irradiation not only induces nucleation but also increases reproducibility. It is suggested that the

cavitational collapse during insonation may create a nucleation site analogous to that from a suspended solid or surface imperfection. The nucleation by insonation was shown in laboratory scale tests on the crystallisation of sorbitol hexaacetate by cooling in methanol (Price, 1997) as shown in Figure 2.3. When a saturated solution at 40^{o}C was cooled without any irradiation, nucleation occurred at 33.2^{o}C whereas when irradiation was applied, nucleation occurred at 36.8^{o}C. The reduced zone width (see Section 3.2.) of 3.6^{o}C is associated with better quality in terms of size and habit and a lesser propensity for the solute to "crash out" with the extensive formation of grains (McCausland *et al*., 2001). Another effect of irradiation on nucleation is shortening of the induction time between the establishment of supersaturation and the onset of nucleation and crystallisation.

In solid/liquid suspensions, the cavitational collapses tend to be focused at the solid/liquid interfaces. Continuing insonation in a solid/liquid system does not result in damage and disruptions but rather in further nucleation and inhibition of crystal growth. A smaller crystal size is thus obtained. It is possible that the further nucleation may be as a result of cavitationally induced disturbances at the solid surfaces.

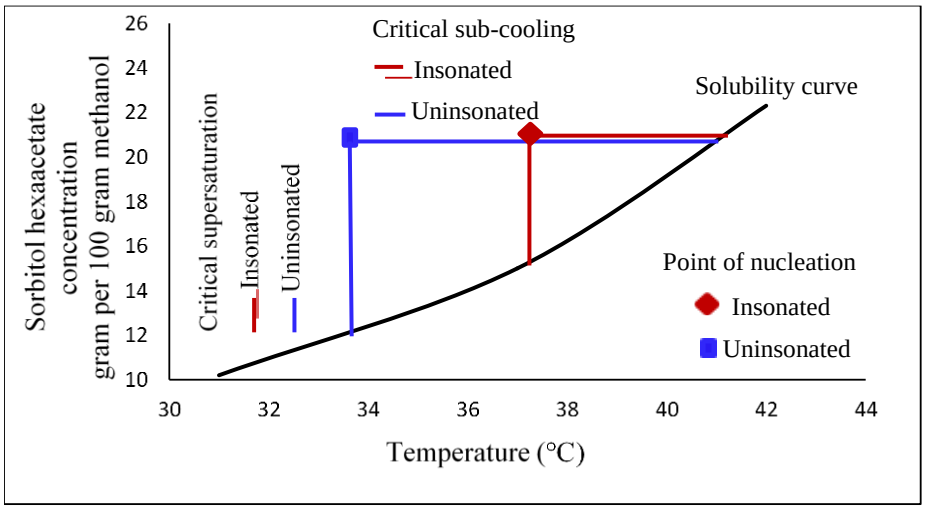

Figure 2.3. Nucleation induced by irradiation, at a reduced metastable zone width, in the crystallisation of sorbitol hexaacetate from methanol (Price, 1997)

2.4. Factors affecting cavitation

There are a number of experimental factors that affect cavitation formation and collapse upon insonation. These factors are of prime importance when considering an experimental design to investigate the uses of the ultrasonic cavitation and are discussed in this section.

2.4.1. The presence of gas

The majority of industrial liquids are heterogeneous solutions, containing a certain amount of dissolved gases as well as gas bubbles. The latter has a positive influence on cavitation as they act as nuclei for the growth of cavitation bubbles (Wilson, 1997). In the absence of these bubbles e.g. degassed liquids, a greater power intensity is required to overcome the cavitation threshold. Figure 2.4. (Mason, 1990) illustrates this by showing that at lower frequencies, the threshold can be overcome by increasing the power intensity for degassed or air free liquids, but that the increased intensity has little to no effect at higher frequencies.

The dissolved gases in liquids have a detrimental effect on cavitation as they tend to cushion the shock wave intensity or acoustic streaming provided by the collapse of bubbles in cavitation. This could be to the extent that a large quantity of the dissolved gases could outweigh the effect of the bubble collapse (Wilson, 1997).

Particulate matter can also lower the cavitation threshold by acting as sources of trapped vapour gas nuclei.

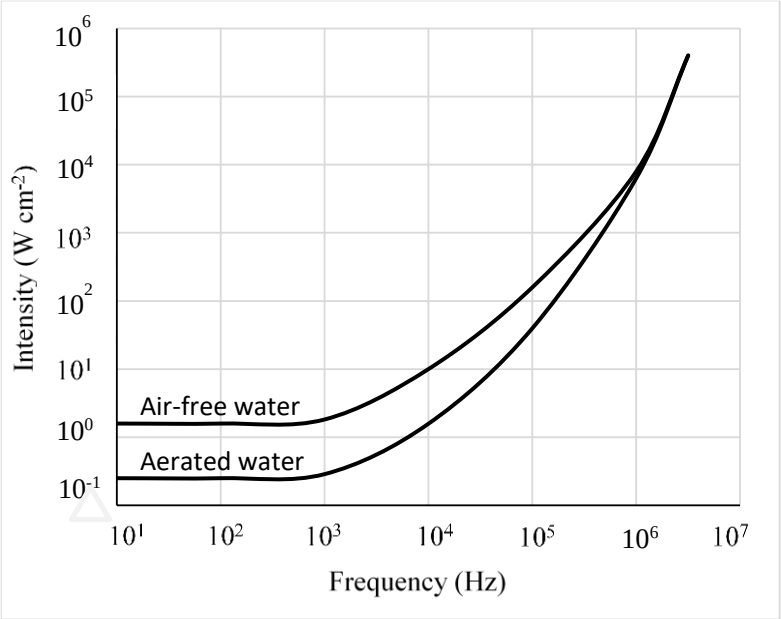

Figure 2.4. Cavitation thresholds for air-free and aerated water (Mason, 1990)

2.4.2. External pressure and irradiation intensity

Mason (1990) reports that the larger external pressures require the application of greater acoustic pressure and hence intensities to provide cavitation. Wilson (1997) reports that by increasing the irradiation power, the vibration amplitude is intensified. As a result, the collapsing pressure rises, causing faster and more violent transient implosions.

Due to engineering and practical considerations, there is a limit to the amount of power that can be applied. At sufficiently high acoustic intensities a decoupling phenomenon occurs, leading to a loss of power transfer into the medium. This is due to the source of the irradiation being unable to remain in contact with the liquid medium for the complete cycle. Increasing the power to a sufficiently high limit can also increase the number of cavitations per unit volume to the extent that a substantial amount of conglomeration can occur, leading to the formation of larger, stable bubbles. The stable cavitation has a cushioning effect as it passes through the medium causing a decrease in the impact of the irradiation.

Increasing the power intensity would also impact the transducer used. Any increase in intensity would require a greater dimensional change in the transducer material causing possible damage to the transducer, or drastically reducing its lifespan. A compromise which considers both optimum performance and longevity of the equipment is therefore necessary (Wilson, 1997).

2.4.3. Viscosity and surface tension

In order for cavitation to occur, it is necessary for the rarefaction pressure to overcome the cohesive forces in the irradiated medium. Thus, any increase in viscosity or surface tension will lead to an increase in the amount of energy required to separate the liquid for bubble formation. Table 2.1. represents the acoustic pressure for various oils for cavitation to occur as a function of their viscosities (Mason, 1990). Although an increase in viscosity does require larger amplitudes or acoustic pressure for cavitation, the effects are not dramatic.

Table 2.1. Sound pressure producing cavitation in various liquids under hydrostatic pressure of 1 atmosphere (Mason, 1990)

Liquid	Viscosity (Poise)	Density (kg/m^3)	Velocity of sound in medium (m/s)	Acoustic pressure (atm)
Castor oil	6.30	969	1 477	3.90
Olive oil	0.84	912	1 431	3.61
Corn oil	0.63	914	1 463	3.05
Linseed oil	0.38	921	1 468	2.36

2.4.4. Choice of solvent

The lower the vapour pressure for a given external pressure, the larger must be the acoustic pressure (Mason, 1990).

2.4.5. Temperature

In general, the threshold intensity required to produce cavitation is lowered by raising the temperature. This may be due to the lowering of the viscosity and/or surface tension of the medium insonated but is more likely to be due to a rising of the liquid vapour pressure (Mason, 1990). It is reported by Wilson (1997), however, that closer to a medium's boiling point, a substantial increase of vapour pressure occurs which may cushion the implosions during the compression cycles, and decrease the effect of the shock waves produced from the implosions.

In addition, Wilson (1997) also reports Figure 2.5. As tap water is heated to approximately 55ºC, an increase in the intensity of cavitation can be observed. A further increase in temperature, however, towards the boiling point, shows a reduction in the cavitation intensity due to the increase in the vapour pressure and its associated cushioning effect. Also observed is the hysteresis that occurs when the water is cooled after boiling (upper curve in Figure 2.5.). The intensity of the cavitation increases towards an optimum of about 60ºC, probably due to the degassing of dissolved gases when the water was boiled.

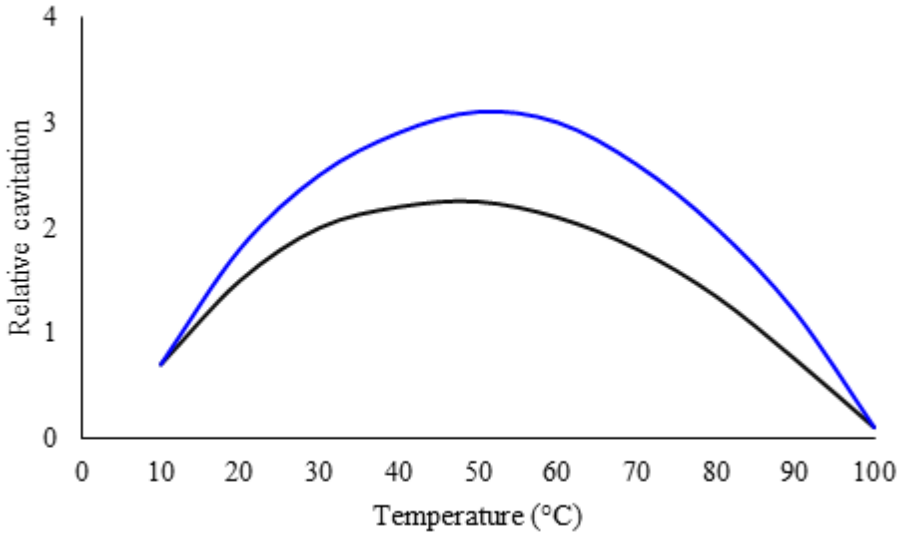

Figure 2.5. The effect of temperature on cavitation in tap water and its hysteresis (Wilson, 1997)

2.4.6. Frequency

To create and grow a bubble requires a finite time and is therefore dependent on the frequency of irradiation as it may be that the time required is less than that available during the rarefaction cycle. For example, at 20 kHz, one cycle or period occurs every 20 000th of a second or 50 µs (Section 2.2.1.) and the rarefaction phase only last 25 µs, peaking at 12.5 µs. For a 20 MHz insonation, the rarefaction phase only lasts 25 ns, which may be insufficient for bubble growth. Thus, as frequency increases, the production of cavitation bubbles becomes less likely. This can be partially overcome by the application of higher intensity sound waves (see Figure 2.4.).

2.5. Factors affecting the fate of a bubble under insonation

If a gas or vapour diffuses into a bubble or void during its growth then the complete collapse of the bubble may not occur and may oscillate in the applied field. Whether a bubble collapse or oscillates depends on several factors, such as temperature, frequency, solvent type and external pressure. Also influential is the acoustic amplitude or intensity, bubble size and gas content and type (Mason, 1990).

2.5.1. Frequency

If the sound wave is of sufficient intensity to create a bubble then the bubble must have sufficient time to collapse. Naturally high frequency sound waves will only have short compression cycles and the bubble may not have enough time to collapse totally (Mason, 1990). Neppiras (1984) gives the collapse time for a cavity by Equation 2.5.

$$Collapse\ time\ (s) = 0.915 \cdot Bubble\ size \cdot \left(\frac{density}{collapse\ pressure}\right)^{1/2} \quad \ldots \textbf{Equation 2.5.}$$

where bubble size is in centimetres, density in g/cm^3 and pressure in atmospheres.

2.5.2. External pressure

The effect of external pressure can be seen in Equation 2.5. The greater the external pressure, the greater the collapse pressure and the shorter and more violent the bubble collapse.

2.5.3. Bubble size

The principle of degassing can be explained if the bubble does not collapse totally. It may be that during the rarefaction cycle the bubble has grown so large that it does not have sufficient time to collapse fully. If the bubble contracts to a size which is larger than its original, then it could undergo a growth during the following cycles until it is sufficiently buoyant to be expelled from the liquid. This is the fundamental principle of degassing (Mason, 1990).

2.5.4. Intensity

The larger the intensity the larger the acoustic amplitude and the collapse pressure, and hence the faster and more violent the collapse of the bubble.

2.5.5. Temperature

Temperature can affect the collapse time of bubbles formed indirectly as it controls both the cavitation threshold and maximum radius that the bubble can grow.

Mason (1990) gives Equations 2.6. and 2.7. from which it is possible to determine the maximum temperature and pressure in the bubble at the moment of collapse.

$$T_{max} = \frac{T_0 \cdot P_m \cdot (\gamma - 1)}{p} \quad \text{…}\textbf{Equation 2.6.}$$

$$P_{max} = P \cdot \left[\frac{P_m \cdot (\gamma - 1)}{p}\right]^{\frac{\gamma}{\gamma - 1}} \quad \text{…}\textbf{Equation 2.7.}$$

Where T_{max} and P_{max} are the maximum temperature and pressure in the bubble, T_0 is the experimental temperature, P_m is the pressure in the liquid at the moment of collapse, γ is the ratio of specific heat at a constant pressure and at a constant volume and P is pressure.

It is also well known that an increase in temperature accelerates reaction rates. Quite remarkably, Mason (1990) reports that insonation increases reaction rates by lowering the vapour pressure and therefore also temperature.

When performing sono-chemical reactions, it should be noted that there are certain areas in the medium where a maximum effect can be observed. Pugin (1987) compared the erosion of a foil (due to the effect of cavitation) and the temperature developed in an ultrasonic bath as a function of distance from the irradiating surface (see Figure 2.6.).

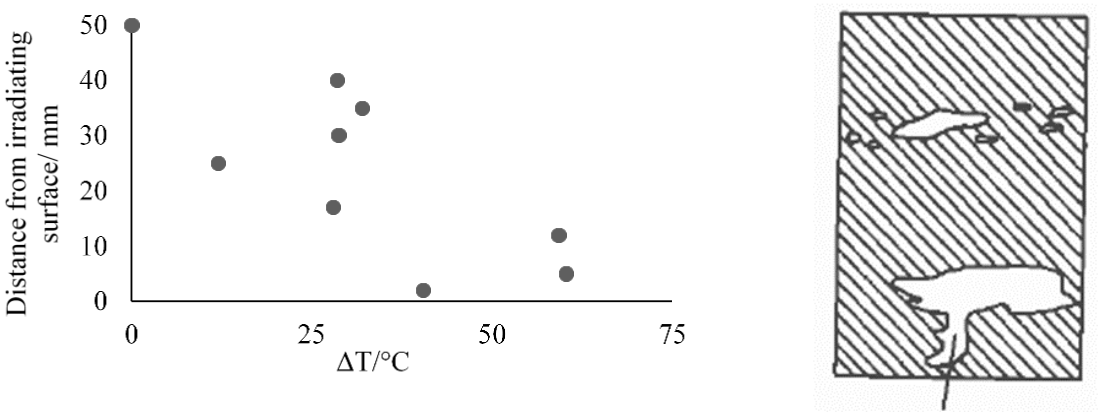

Figure 2.6. A comparison of thermocouple reading (left) and foil erosion (right) at various distances from the irradiating surface of an ultrasonic bath (Pugin, 1987)

Pugin's conclusion (1987) is that the maximum effect occurs at an odd multiple of a quarter of a wavelength [i.e. $(2n + 1)\cdot\lambda/4$] from the bath base. A frequency of 35 kHz was used for the experiments, giving a wavelength of 42.8 mm if a sound velocity of 1 500 m/s is used in Equation 2.2. As is evident from Figure 2.6. the maximum erosion and temperature is observed at approximately 10 mm and 33 mm or $\lambda/4$ and about $3\lambda/4$. Also

quite interesting is Mason's addition (1990) that flat bottom flasks provide a larger transfer of ultrasonic energy than round bottom flasks.

2.6. Summary of general principles of sono-chemistry

Mason (1990) gives the following useful summary of the general principles of irradiation in sono-chemistry:

(a) Sound waves produce an acoustic pressure, P_a, in addition to the normal atmospheric pressure P_h. The total pressure P is a sum of P_a and P_h.

(b) The acoustic pressure is time dependent as is shown in Equation 2.8.

$$P_a = P_A \cdot \sin(2 \cdot \pi \cdot f \cdot t) \quad \text{…Equation 2.8.}$$

where P_a is the acoustic pressure at time t (s), P_A is the peak acoustic pressure and *f* is the frequency in Hz.

(c) The peak acoustic pressure is given by Equation 2.9.

$$P_A = (2 \cdot I \cdot \rho \cdot c)^{\frac{1}{2}} \quad \text{…Equation 2.9.}$$

where I is the intensity of the source, ρ is the density of the medium and *c* is the speed of sound in the medium.

(d) Higher frequencies attenuate sound more rapidly than low frequencies which can be seen in Equation 2.10.

$$I = I_0 \cdot \exp\left[-2 \cdot l \cdot \left(\frac{8 \cdot \eta_s \cdot \pi^2 \cdot f^2}{3 \cdot \rho \cdot c^3}\right)\right] \quad \text{…Equation 2.10.}$$

where I is the intensity of the source, I_0 is the instantaneous intensity, *l* is the distance from the source, η_s and ρ are the kinematic viscosity (Stokes) and density

of the medium, *f* is the frequency of the sound and *c* is the speed of the sound in the medium.

(e) The formation and the type of bubble depends on various factors, such as the presence of gas, external pressure, viscosity, surface tension, vapour pressure and frequency.

(f) Transient bubbles only last 1-2 cycles and give high temperatures and pressures upon implosion. Produced at intensities above 10 W/cm^2.

(g) Stable bubbles have smaller temperatures and pressures upon implosion than transient bubbles, but have significant longer term chemical effects as they exist for several cycles e.g. increase of reaction rates by increasing the collision or diffusion of the reactant species. Produced at intensities of about 1-3 W/cm^2.

2.7. Monitoring of acoustic input

There are three possible ways of determining the acoustic power (Mason, 1990). These are discussed as follows:

2.7.1. Calorimetric method

This is simply the calculation of power input into the medium by measuring the rate of temperature rise in the system and using the thermal capacity of the medium.

2.7.2. Measurement of vibrational amplitude

This is the direct measurement of the amplitude of the working surface of the horn and yields a parameter that is at least proportional to the acoustic power, as can be seen by Equation 2.11.

$$P_{ac} = \frac{1}{2} \cdot \rho \cdot c \cdot \xi^2 \qquad \text{…}\textbf{Equation 2.11}$$

where P_{ac} = acoustic power, ρ is the density of the load, c is the local sound velocity and ξ is the transducer amplitude.

The amplitude can be directly measured by using a microscope and taking a measurement by looking at the end of a free transducer. This is clearly impractical though during a sono-chemical experiment. The amplitude can also be determined on a continuous basis using an electro-mechanical or purely electrical method. In the electro-mechanical method, the alternating stress in a resonant element is at a maximum in the centre and if a strain gauge is bonded at the centre then the output from this will be proportional to the amplitude of vibration. In the purely electrical method, the changes to resonant frequency in converting the electrical frequency at the mains to the desired operating frequency can be monitored.

2.7.3. Measurement of the real electric power to the transducer

This can be converted to the acoustic power if the overall acoustic transfer efficiency is known.

2.8. General irradiation equipment

A general insonation system will comprise the following components:

- Generator – provides the required electrical voltage to the transducer for generation of a sound wave at the required frequency. Insonation settings may be inputted on the generator or driven from a computer with some user interface.
- Transducer – converts electrical energy to mechanical energy.
- Horn – also referred to as an amplifier or waveguide and has the function of amplifying the vibrating motion generated by a transducer.
- Irradiating surface – that surface which is in contact with the medium to be insonated. This can be, for example, the tip of a horn or a specially designed flange or clamp.

These components are commercially available, either separately or sold as systems.

2.9. Irradiation in the sugar industry

2.9.1. Gao *et al*. (1992)

Gao *et al*. (1992) described using a combination of an organic solvent and irradiation to afford nucleation in sugar solutions. Figure 2.7. represents slurry and subsequent crystals produced after an hour by irradiation and Figure 2.8. shows a slurry and one-hour crystals when the ball milling method was used. The solvent was not disclosed but described as a mixed organic solvent consisting of mainly low molecular weight alcohols, surfactants and stabilisers. In the industrial tests, a 25-40 kHz transducer was used, with 1-2 kW power generated.

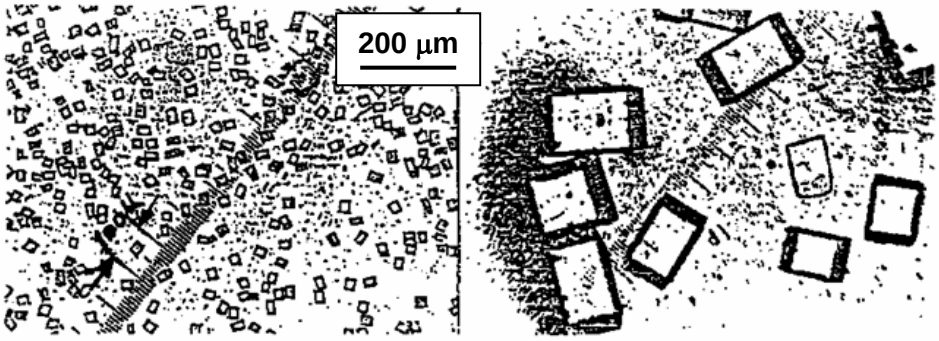

Figure 2.7. Microscope image of nucleation using irradiation and crystals after an hour (Gao *et al*., 1992)

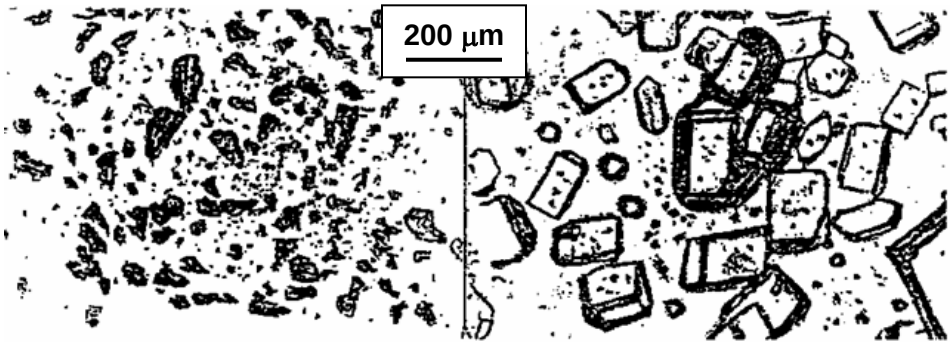

Figure 2.8. Microscope image of nucleation using ball milling and crystals after an hour (Gao *et al*., 1992)

It is claimed that the new slurry preparation method was subsequently used during the 1989/90 season at two cane sugar factories in China. The following advantages were reported compared to using a ball-mill slurry and other conventional seeding methods:

• The absence of irregular grains reduced the time, water and steam usage significantly since there was no need for the wash treatment of these grains. In general, the boiling times were reduced from 4.8 hours to 3.9 hours (B-pans). Vapour consumption was reduced by 10%.

• More sucrose was extracted in the pan boiling process, resulting in a drop of about 4% of sucrose in the final molasses.

• An increase in A-, B- and C-sugar quality was recorded. The quality parameters included colour, impurities, fines, brightness and uniformity of the crystals and a lower degree of conglomeration.

It was claimed that the technology was adopted by more than 50 cane and beet sugar factories in the People's Republic of China after 1990. Illovo Sugar Limited (RSA) recently acquired a sugar factory in China. Chinese sugar mills contacted via Illovo Sugar Limited reported that they were not aware of this method presently being used.

Interestingly, the sugar and patent literature is void of any further mention of this technique or work in the area after this initial paper. It is therefore not clear whether this has been commercialised or if work is continuing.

2.9.2. Tai-quin (1993) and Taiqiu (*sic*) *et al*. (1994).

Tai-quin (1993) and Taiqiu (*sic*) *et* al. (1994) report that the process of nucleation of sucrose solutions may be markedly influenced by sonic fields. Nucleation by insonation was carried out under low supersaturation in a refinery. The crystal size distribution of the final product was much improved and reduced pan boiling times.

The industrial tests indicated that the crystal number density obtained did not meet the industrial production requirement. Tai-quin (1993) recommended the combination of a continuous slurry preparation setup (as opposed to larger seed crystal production) with a product pan for higher nucleus density. The arrangement would have a moderate emission power yet higher than that used in his tests (100 W generated at frequencies of 6.10 - 6.25 kHz).

2.9.3. McCausland and Cains (2003)

A commercial technology using sono-crystallisation was described by McCausland and Cains (2003). The report was non-technical but did show that irradiation can be used to reduce the metastable zone widths at 50^{o}C for various sugars viz. xylose, sucrose, lactose and maltose. For the saturated sucrose solution at 50^{0}C it was shown that crystals were formed at below 40^{o}C without irradiation and at 47^{0}C with irradiation, upon cooling.

The company that holds this technology at the moment is Prosonix (United Kingdom). No patents were found particularly referring to the nucleation of sucrose.

2.10. Health and safety aspects

Health and safety aspects need to be considered as the cavitation effects during insonation leads to a wide spectrum of noise that is radiated to the atmosphere. Generally, an exposure limit of 85-90 decibels is permitted over an eight-hour period. Shorter exposure times permit higher pressure levels e.g. a four-hour exposure would have the limit increased by about 3 decibels and a two-hour exposure by six decibels and so on, up to a maximum of 120 decibels. Equation 2.4., discussed in Section 2.2.1., can be used to convert power intensities used to decibels to gauge if applications fall within the specified exposure limits. Using ear muffs or an acoustic screen around the apparatus may be ways of guarding against any noise generated.

2.11. General scaling up of equipment

The type of industrial process will naturally govern the choice of transducer energy density required viz. a low intensity or a high intensity sonication (Mason, 1990).

In the case of a low intensity application, the liquid/s could be passed through an ultrasonic tank with multiple transducers and out over a weir to the next process. Tanks in series could also be used. The transducers could be bonded on to a stainless steel or titanium plate and bolted with a gasket into the tank. Alternatively, a sealed submersible transducer assembly could be employed. For high intensity applications it is possible to couple a probe transducer into a flow pipe by means of a "T" section. Again, a number of transducers can be employed with the actual number and position in the process line having to be determined during the process development phase (Mason, 1990).

McCausland (2001) report that for scaling up purposes probe systems with intensities of 5×10^4-10^6 W/m^2 at frequencies of 20-60 kHz suffer the disadvantage that the intense cavitation field cannot be transmitted for more than a few centimetres beyond the end of the probe. Even banks of probes have been found incapable of transmitting cavitation through distances of 100-700 mm. In order to achieve the high density fields in large volumes, it is preferable to operate at a lower intensity (~104 W/m^2) over an extended area. In pharmaceutical and fine chemicals manufacture, where nucleation of large batches is needed, a simple arrangement that uses a jacketed, stirred tank reactor can be applied with the insonator located in a pump-around loop outside of the tank.

CHAPTER 3 - SUCROSE CRYSTALLISATION

Crystallisation is one of the oldest unit operations, and is still widely used, probably due to the highly purified and attractive form of a chemical solid which is obtained from relatively impure solutions (Wei, 2008 and Perry, 1999). In the sugar industry, crystallisation is still exclusively used to produce a solid sugar.

The process of the solution crystallisation consists of two major steps viz. nucleation and growth (Wei, 2008). The former, as well as, sucrose solubility, supersaturation and the concept of full seeding are discussed in this chapter. Also included is a section on the linear dimensions and shape factors of sucrose crystals. The theory on classical batch crystal growth systems is discussed.

As VHP sugar with a purity of about 99.8% is used as the input to the refinery, and the purity of the lowest bagged sugar is typically greater than 99.7%, only pure solutions are discussed in this chapter. In the manufacture of brown sugar purities as low as 30% are typical.

3.1. Solubility of sucrose in pure solutions

The sucrose molecule contains eight hydroxyl groups; three groups are involved in intramolecular hydrogen bonds and the other five are involved in intermolecular hydrogen bonds (Mathlouthi, 1981). The latter is responsible for sucrose crystal formation in the crystallisation process, or the solvation of sucrose molecules by water molecules during the dissolution step. The high solubility of sucrose in water is due to the fact that the hydroxyl groups can form hydrogen bonds with water molecules (van der Poel *et al.*, 1998). Figure 3.1. below shows the intramolecular hydrogen bond formation in a sucrose molecule (Lichtenthaler *et al.*, 1991).

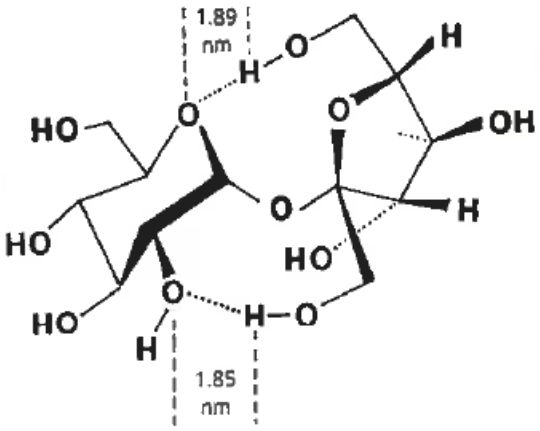

Figure 3.1. Schematic diagram of a sucrose molecule (Lichtenthaler *et al.*, 1991).

Allen *et al*. (1974) reported that in dilute solutions each sucrose molecule is surrounded by up to eleven water molecules. Love (2002) reported that removal of the water molecules from the solution will eventually result in insufficient water molecules to satisfy all the attraction sites of the sucrose present and the attraction between sucrose molecules would begin.

The solubility of pure sucrose in water is known to increase with an increase in temperature (Hugot, 1986). When the solution contains the total quantity of sucrose which it can dissolve, it is said to be saturated at that temperature. Culp (1981) gives the ratio of water to sucrose molecules at saturation as Equation 3.1. below.

$$N = 10.65 - 0.0674 \cdot T$$ ...**Equation 3.1.**

where N = the water/sucrose ratio and T = Temperature of the solution (^{o}C).

Peacock (1995) reports on the extensive work done by Vavrinecz (1960) on sucrose solubility, the most accurate of which was a correlation (Equation 3.2.) constructed to fit the experimental data of Grut (1937).

$$B = 63.753 + 0.13542 \cdot T + 0.0008869 \cdot T^2 - 2.222x10^{-6} \cdot T^3$$ … **Equation 3.2.**

where B = concentration of sucrose in the aqueous solution (% Brix) and T = temperature of the solution (^{o}C).

For Equation 3.2. it is assumed that the Brix content of the solution is the same as the dry solids or sucrose content of a pure solution, the former of which can be seen in the Batterham *et al*. (1973) relationship in Equation 3.3. below.

$$Dry\ solids\%solution = Brix\%solution - 8.86\left(1 - \frac{Purity}{100}\right) \quad \ldots \textbf{Equation 3.3.}$$

3.2. Supersaturated solutions

A supersaturated solution contains more solute at a certain temperature than a saturated solution at the same temperature. Supersaturated solutions can be prepared by evaporating water from a saturated solution or by cooling the saturated solution. Equation 3.4. gives the supersaturation coefficient (SSC) which shows whether a solution is unsaturated (SSC<1), saturated (SSC=1) or supersaturated (SSC>1). It results from the division of the ratio of the mass fractions of sucrose to water in a solution by the ratio of the mass fractions of sucrose to water in a saturated solution at a given temperature (van der Poel *et al.*, 1998).

$$SSC = \frac{{}^{w_s}/_{w_w}}{\left({}^{w_s}/_{w_w}\right)_{at\ saturation}} \quad \ldots \textbf{Equation 3.4.}$$

where SSC = Supersaturation coefficient, w_s = mass of sugar in the solution and w_w = mass of water in the solution.

The solubility of pure sucrose solutions is shown in Figure 3.2. (adapted from Rein, 2007).

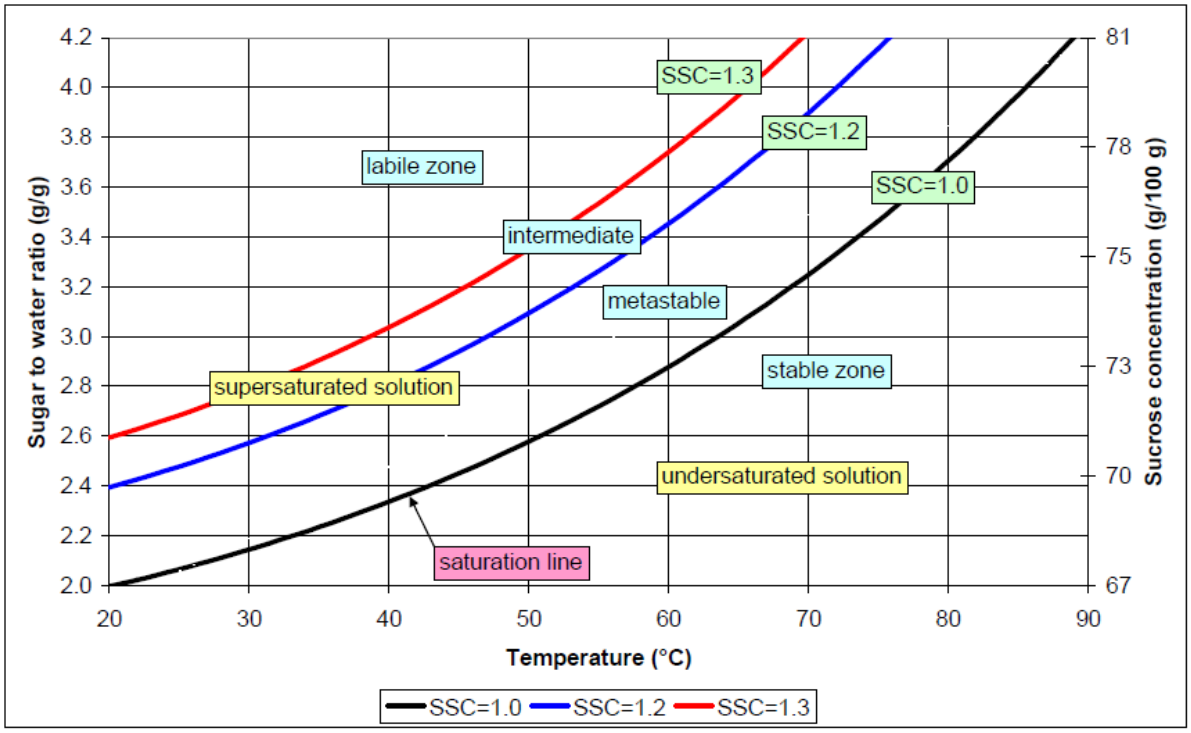

Figure 3.2. Solubility graph of pure sucrose solutions adapted from Rein (2007)

Saturation is represented by the curve SSC=1 in Figure 3.2. The region of supersaturation between SSC = 1 and 1.2 is known as the metastable zone of supersaturation. In this zone of supersaturation, sugar crystals will grow but no new nuclei will form. The region between SSC's of 1.2 and 1.3 is known as the intermediate region and above 1.3 as the labile region. In the intermediate region of supersaturation, sugar crystals will continue to grow but new nuclei will form in the presence of sugar crystals or sugar crystal fragments (called heterogeneous or secondary nucleation - van der Poel *et al*., 1998). In the labile region, new crystals will form spontaneously (Rein, 2007). There is little control over the amount or quality of the crystals that are formed in the intermediate and labile zones of supersaturation and hence panboiling or crystal growth operations operate in the metastable zone. In the sugar industry, the unwanted crystals formed in the intermediate and labile zones are known as false grains. These widen the CV of the massecuite formed which makes separation of the crystals difficult in centrifuges and inevitably leads to poor sucrose recoveries.

3.3. Nucleation and crystal growth

The crystallisation process is made up essentially of two steps viz. a phase separation or "birth" of new crystals called nucleation and then the growth of these crystals into larger sizes. Crystallisable solute molecules are considered by Broadfoot and Wright (1972) to be in a low energy state once bound in a crystal lattice whilst molecules in solution have a random movement and are in a higher state of energy. The driving force for crystallisation is the difference between the free energies of the liquid and the solid states. When a sufficient number of these freely-moving molecules form a stable configuration then a nucleus is formed onto which further solute molecules can be deposited.

It is also considered that the molecules in their random movement through the solution encounter another molecule by chance to create a molecular arrangement corresponding to the configuration of the crystal lattice. The release of the kinetic energy of the molecules will only result in a stable nucleus for agglomerates that are larger in size than the critical size. Smaller crystals will tend to dissolve back into solution and thus a nucleus will only form if the driving force of supersaturation is sufficient to overcome the tendency to dissolve. Such nucleus formation is termed as homogeneous nucleation. Van Hook (1959) estimated the radius of the critical nucleus to be about 190 nm, which corresponds to a sphere containing about 80 sucrose molecules. van der Poel *et al*. (1998) showed that the nucleation rate is very dependent on temperature and supersaturation. Myserson (2002) reports that homogeneous nucleation forms part of primary nucleation, which is nucleation in the absence of crystalline surfaces. Homogeneous nucleation rarely occurs in practice. Heterogeneous primary nucleation is typically induced by the presence of dissolved impurities, whilst secondary nucleation involves the presence of crystals and its interaction with the surrounding environment e.g. impellers, reactor walls, etc.

The rate of crystal growth (or crystallisation velocity) is usually measured in milligrams of sucrose deposited per minute per square metre of crystal surface or mg/min/m^2 (Anon, 2011). Rein (2007) describes the crystallisation rate to be dependent on mainly two processes viz. the diffusion of the sucrose molecule to the crystal and then their

incorporation into the crystal lattice. The latter also comprises adsorption into the surface layer of the crystal, migration to a suitable site on the surface and attachment to the crystal lattice itself. The nucleation process can be catalysed by seed crystals in the solution (Broadfoot and Wright, 1972). The solute molecules in the solution may adsorb onto the crystal surface of the seed crystals rather than into a crystal lattice. The activation energy is thereby reduced and a smaller driving force or supersaturation would be required. Love (2002) makes reference to Figure 3.3. produced from published data by Maurandi *et al*. (1988) which shows the activation energy for sucrose growth.

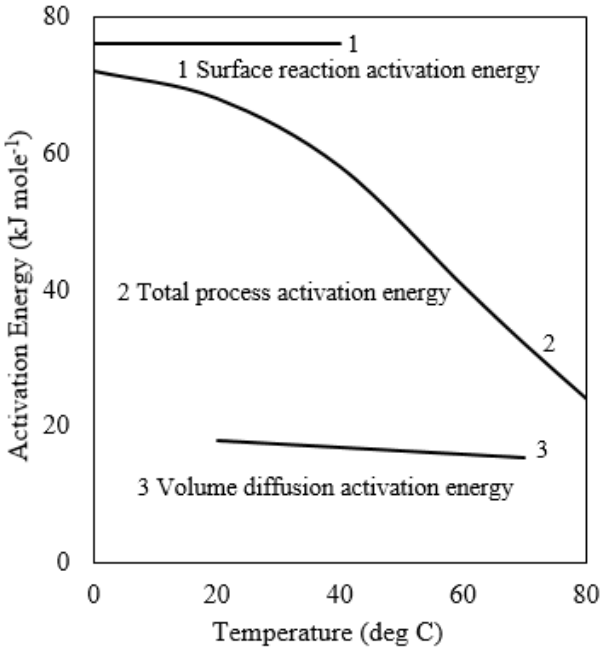

Figure 3.3. Activation energy for sucrose growth (Love, 2002)

The crystallisation rate can be expressed as Equation 3.5. below (Rein, 2007).

$$\frac{dm}{d\tau} = k_G \cdot A \cdot \left(c - c_{eq}\right)^n \qquad \text{…Equation 3.5.}$$

where m = mass (g), τ = time (minutes), k_G = rate constant (cm/min), A = crystal surface area (cm^2), c and c_{eq} are the concentrations of the bulk of the solution and at equilibrium respectively (g/cm^3) and n = a value between 1 and 2 at low concentration differences but tending towards a first order process at the higher concentrations.

The rate constant k_G can be expressed as an Arrhenius type relationship which is dependent on temperature (Equation 3.6.)

$$k_G = k_0 \cdot exp\left(\frac{-E_A}{R \cdot T}\right) \quad \text{…Equation 3.6.}$$

where k_0 is the pre-exponential factor, E_A = activation energy, R = universal gas constant or 8.314 kJ/(kmol·K) and T is the absolute temperature.

Typical crystal growth rates in industry are shown in Table 3.1. below (Rein, 2007).

Table 3.1. Typical industrial linear crystal growth rates in refineries (Rein, 2007)

Massecuite type	**Mother liquor purity (%)**	**Linear growth rate (µm/h)**	**Source of data**
Refinery – industrial	99	300	Wright (1983)
Refinery – industrial (early stages)	99	890	Lionnet (1999)
Refinery – industrial (late stages)	99	110	Lionnet (1999)
Refinery – pilot plant (early stages)	99	710	Lionnet (1999)
Refinery – pilot plant (late stages)	99	31	Lionnet (1999)

3.4. Dimensions and shape factors of sucrose crystals

Bubnik and Kadlec (1992) undertook an extensive study into the linear dimensions of sucrose crystals. Their work is summarised here.

The crystal characteristic dimension can be given by Equation 3.7. where it was assumed that the crystal length along the a-axis was equal to the length along the b-axis.

$$L = \sqrt[3]{L_b^2 . L_c} \quad \text{…Equation } \mathbf{3.7}.$$

These dimensions can be seen in Figure 3.4.

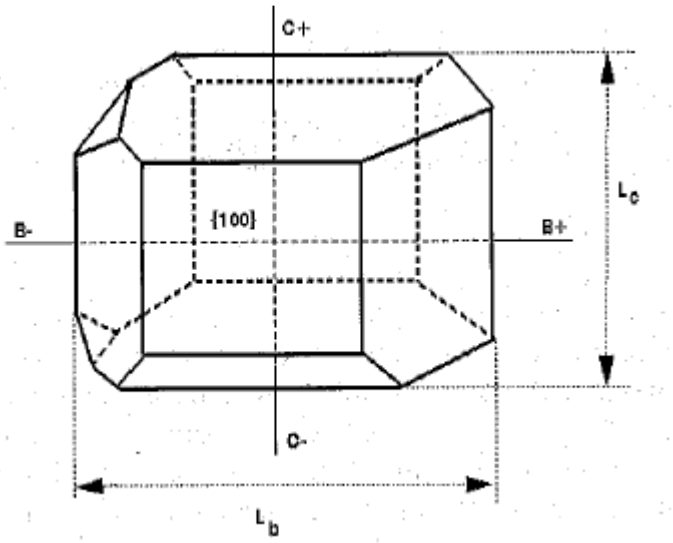

Figure. 3.4. Typical sucrose crystal with description of axis and characteristic linear dimensions L_b and L_c (Bubnik and Kadlec, 1992).

From the linear dimensions, it is possible to calculate the crystal mass (Equation 3.8.).

$$m = \alpha.\rho.L_b^2.L_c \quad \text{…}\textbf{Equation 3.8.}$$

where m is the mass of crystals, ρ is the density of sugar crystals and α is the volume shape factor defined as Equation 3.9.

$$V = \alpha.L^3 \quad \text{…}\textbf{Equation 3.9.}$$

where V is the volume of the crystal and the characteristic linear dimension L (which may be the mean aperture if sieve analysis is used to determine crystal mass fractions) can be obtained from Equation 3.10. The surface shape factor (β) can be obtained using the crystal surface area A.

$$A = \beta.L^2$$ …**Equation 3.10.**

It is also possible to use a crystal shape factor F ($mm^2.mg^{-2/3}$) from Equation 3.11.

$$F = \frac{A}{\sqrt[3]{m^2}} = \frac{\beta}{\sqrt[3]{(\rho.\alpha)^2}}$$ …**Equation 3.11.**

The shape factor F is commonly used in the research of sucrose crystallisation. An average value for this is 4.47 $mm^2.mg^{-2/3}$. Using this value and experiment performed, Bubnik and Kadlec (1992) calculated the volume and surface shape factors to be 0.75 and 5.02, respectively. This was using the sieving method to determine the mass fractions of sugar used. Lionnet (1998)[a], in his work on cane sugar crystals from a pilot crystalliser, reported a volume shape factor of 0.34 and a surface shape factor of 2.94 when image analysis was used instead of sieve analysis to determine the length of crystals. Lionnet also reported that Bubnik and Kadlec gave a volume shape factor of 0.31 when image analysis was used.

3.5. Crystallisation models

Classical batch crystal growth models are given below (Starzak, 2016 and Myerson, 2002). For these models the following assumptions are made:

- The crystal population (number of crystals) does not change.
- There is a uniform size distribution of the crystals.
- Crystal volume and surface shape factors during growth are constant.
- There is perfect mixing of liquor in the vessel during the batch operation.

3.5.1. First-order kinetics with supersaturation-ratio-based driving force

$$R_c = k_0 \exp\left(-\frac{E_c}{R(T+273.15)}\right)\left[S-(1+\varepsilon)\right]\rho_c \qquad \text{…Equation 3.12.}$$

where ε = 0.0046 for sucrose crystallisation, R_c is the rate of crystallisation, k_0 is a constant, E_c is the activation energy, S is the supersaturation ratio and ρ_c is the density of the crystals.

3.5.2. Solid on solid model, first-order kinetics, concentration-based driving force

$$R_c = k_o \exp\left(-\frac{E_c}{R(T+273.15)}\right)\sigma\ \rho_c \qquad \text{…Equation 3.13.}$$

where the concentration-based driving force σ can be calculated from brix data as:

$$\sigma = \frac{Brix}{Brix^*}\frac{\rho(Brix)}{\rho(Brix^*)} - 1 \qquad \text{…Equation 3.14.}$$

where

$Brix^* = 9.1103 \times 10^{-6}\ T^3 - 2.6192 \times 10^{-3}\ T^2 + 0.56428\ T + 48.337$ …Equation 3.15.

3.5.3. Empirical n^{th}-order kinetics with concentration-based driving force

$$R_c = k_o \exp\left(-\frac{E_c}{R(T+273.15)}\right)\sigma^n\ \rho_c \qquad \text{…Equation 3.16.}$$

3.5.4. Burton-Cabrera-Frank model – nonlinear kinetics, concentration-based driving force

$$R_c = k_0 \exp\left(-\frac{E_c}{R(T+273.15)}\right)\frac{\left[\ln(1+\sigma)\right]^2}{\sigma_c}\tanh\left[\frac{\sigma_c}{\ln(1+\sigma)}\right]\rho_c \qquad \text{…Equation 3.17.}$$

where σ_c is a constant.

3.5.5. Nuclei above nuclei model – nonlinear kinetics, concentration-based driving force

$$R_c = k_0 \exp\left(-\frac{E_c}{R(T+273.15)}\right)\sigma^{2/3}\left\|\ln(1+\sigma)\right\|^{1/6}\exp\left[\frac{-G}{\ln(1+\sigma)(T+273.15)^2}\right]\rho_c$$

…Equation 3.18.

where G is a constant.

3.5.6. Two-dimensional growth theories – polynuclear model (Myerson, 2002)

$$G = (C_1 / T^2\{\ln(S)^{3/2})\exp[-C_2 / T^2 \ln(S)] \qquad \text{…Equation 3.19.}$$

where G is the linear growth rate, C_1 and C_2 are empirical parameters obtained from experimental data.

3.5.7. Diffusion layer model (Myerson, 2002)

The basis of the diffusion layer model is that the solute diffuses through the boundary layer of the crystal and is then incorporated into the crystal.

A simplified relation is given for the rate of increase of the crystal mass (dm_c/dt):

$$\frac{dm_c}{dt} = K_G A \Delta C^g \qquad \text{…Equation 3.20.}$$

where C is the difference between the bulk and interfacial concentrations, g is a value between 1 and 2, A is the surface area of the crystal and K_G is approximately the diffusion coefficient divided by the thickness of the boundary layer.

CHAPTER 4 – REQUIREMENTS AND BENEFITS OF A FULL SEEDING TECHNIQUE

Full seeding is not practised in the cane sugar industry; therefore, in order to propose a technique, suitable conditions for its practice must be determined. Prior to this though, it is necessary to understand the concept of full seeding and undertake a review of full seeding systems trialed previously. The conditions that are predicted can also be used in the determination of factors to be investigated (and the ranges of the factors) for the testing of a new full seeding system. These concepts are described by Love *et al*. (2016), a paper in which the author of this dissertation is a co-author.

4.1. The concept of full seeding

The ideal situation for seeding is to be able to achieve “true seeding” or “full seeding”. This is where a known quantity of seed crystals is added at the beginning of the crystallisation process and every one of these seed crystals grows to become a product crystal, and no other seed crystals are inadvertently nucleated during the crystallisation process. Of the three conventional seeding techniques, slurry seeding comes closest to this ideal.

If full seeding can be achieved, adding the correct number of seeds at the beginning of the crystallisation process will result in the desired final crystal size. As a first approximation (neglecting the spread in crystal sizes around a mean crystal size), the number of product crystals can be calculated by dividing the total mass of product crystal produced by the mass of a single crystal. This is the number of seed crystals that will need to be added at the beginning of the crystallisation process.

Over the years there has been some contention about the suitability of slurry seeding to approach full seeding. James and Maslen (1964), in reference to tests at the Isis factory stated that “these figures make it abundantly clear that nothing approaching true seeding was achieved”. They also found poor repeatability between batches and stated that they

had “the distinct impression that the Isis low grade pan work is not inferior to any previously encountered” and that “It may well prove, therefore, that the results …are typical”. In discussing slurry seeding, Jensen (1967) stated that “today most operators in Queensland mills believe that they are true seeding; however, it is doubtful if any one of them is actually true seeding”. He goes on to quote instances where the number of product crystals is in some instances less than the number of seed crystals and in other instances greater than the number seed crystals. It is clearly possible that some techniques for slurry seeding can be associated with a degree of shock seeding, whilst in other instances, a proportion of the added seed crystals dissolve. Jensen (1967) emphasises the importance of adhering closely to standardised techniques that need to be developed to achieve the desired product crystal size.

Austmeyer and Schliephake (1983) are dismissive of the viability of slurry seeding, saying: “Because of the presence of the zones of under-saturation and high rate of seed crystal dissolution, it is concluded that the slurry seed method is of inadequate reproducibility for practical purposes”. This was contested by Payne (1984) who, based on successful practical application of the technique in Hawaii over a period of 30 years, stated that “Under a given set of controlled conditions, however, the survival (of slurry particles) is of sufficient statistical significance to provide a useful technique”. He also stated that “the order of magnitude of the surviving nuclei is about one third of those injected.”

The problems of obtaining consistent results from the slurry seeding technique are evident in an old, unpublished, industry survey done by the SMRI in 1977. The study compared the actual mass of seed added with the theoretical mass of seed required to achieve the product crystal size. The results covered the 18 factories operating in South Africa at the time and considered the seeding of both B and C massecuites in raw sugar factories. The percentage of surviving nuclei ranged from as low as 12% to as high as 500%! Values below 100% indicate dissolution of seed crystals whilst values above 100% indicate a degree of shock seeding or subsequent generation and growth of false grain.

Broadfoot and Steindl (1987) reported on the design and operation of a small, well controlled pan, dedicated to slurry seeding and the early stages of crystal growth. Although they had expected to achieve better consistency in the number of crystals established, the results achieved were similar to those achieved in an adjacent, conventional graining pan in the factory where the trials were conducted.

Bachan and Sanders (1987) reported on a simple technique for improving the conventional slurry seeding of a batch pan to more closely approach full seeding. This technique requires the presence of a stirrer within the pan (more conventionally available in refinery pans, but seldom available in raw cane sugar batch pans). Switching off the steam supply before graining with slurry effectively eliminates the possibility of dissolving crystals due to localised hot spots, addressing the reservations of Austmeyer and Schliephake (1983). After slurry addition the pan can be kept circulating using the stirrer, whilst allowing the seed crystals to grow as they exhaust the available supersaturation. Steam can be switched on again as the crystal growth begins to slow substantially, but by then the seed crystal size is much larger and crystals are far less likely to be destroyed by dissolution. Unfortunately, Bachan and Sanders (1987) do not provide any information on how well this technique approaches full seeding.

4.2. Seed production systems

The inability of the conventional slurry seeding technique to reliably achieve full seeding and the extent that the method relies on technique and the skill of the operator has led technologists to work on developing more robust seed production systems. Murphy *et al*. (1991) described how the conventional slurry seeding technique could be made to achieve acceptable results by careful control of supersaturation at the seeding point, low initial evaporation rates and very tight control of absolute pressure; however, they go on to state that “most of these difficulties are eased by using larger seed crystals from a seeding system to be discussed later in this paper”.

Although Randolph and Ziebold (1974) described a continuous nucleation system, based on secondary nucleation from a sucrose/water/ethanol system, for the production of seed, their system did not appear to gain any general acceptance in the sugar industry. Broadfoot and Wright (1992) reported that "the size spread of the crystals produced in this system was too broad for commercial application".

The beet sugar industry does use a batch seed production system that is based on a combination of slurry seeding and cooling crystallisation. This system was originally developed jointly by Sudzuker and Selwig & Lange. A comprehensive description of the development is given by van der Poel *et al*. (1984). The system can be installed as either a single stage system as done within British Sugar (Murphy *et al*.,1991) and at Raffinerie Tirlemontoise (Ruytings, 2005) or as a two stage system as implemented at Aarberg factory (Brunner *et al*., 1992).

Within the cane sugar industry Broadfoot and Hutchinson (1980) reported on the production of seed by slurry addition to A-molasses followed by cooling. Although some success was achieved with this system, it was not subsequently adopted by the cane sugar industry (Broadfoot and Wright,1992). Success has, however, been achieved with improving the quality of seed created as a magma from smaller crystals derived from lower grade crystallisations, as used in single and double magma boiling systems (Broadfoot and Petersen, 2005). This still leaves open the question of how to produce the seed necessary to grow into the crystals that will eventually become the seed magma.

There is clearly scope to develop a continuous seed production system that is based on a sound understanding of fundamentals, is robust, and can be easily adjusted to optimise the overall crystallisation process.

4.3. Potential benefits of a full continuous seed production system (CSPS)

The potential benefits of a full CSPS were investigated by the Project team overseeing the management of this SMRI project. Forming part of the Project Team and leading this aspect of the project was THS, the technology and commercial partners for the project. The THS support for the technology investigated was based on both the limitations of current methods of seeding sucrose crystallisation, and the potential benefits of a viable process for the continuous production of seed crystals.

Using controlled seeding as the basis for the production of crystalline sucrose is essential to ensure product crystal of the correct size and with a narrow size distribution. Due to the high viscosity of the mother liquor from which crystallisation takes place, it is not possible to remove and recycle fines that are generated by secondary nucleation during the process of growing the original seed crystals to the desired size (as is practiced in many industrial crystallisation processes). Starting the crystallisation with the correct quantity and quality of seed crystals, and thereafter avoiding any possibility of secondary crystallisation, is thus a critical aspect of sugar technology.

In conventional industrial production of crystalline sucrose (panboiling) seed crystals are either added in the form of very fine crystals suspended in alcohol as a slurry (generated by wet ball milling of white sugar for an extended period) or alternatively by “shocking” an unstable, highly supersaturated, sugar solution. When seeding is done by the addition of the fine crystals in alcohol (slurry seeding) there may be the destruction of some crystals by dissolution or alternatively the creation of extra crystals by secondary nucleation (i.e. partial shock seeding). The result is that both methods of seeding are usually highly dependent on operator skill and rely on procedures or “recipes” rather than the control of fundamental process parameters to achieve the required result. There is therefore a strong need in the industry for a reliable means of achieving “full seeding”. “Full seeding” is the ideal situation where the correct number and quality of seed crystals are added at the start of the crystallisation process and then, as the process of growing these seeds to the desired product crystal size, none of these seed crystals dissolve and no of extra seed crystals are formed by unwanted nucleation.

The technology under investigation for full and continuous seed production has the potential to provide a viable means of achieving reliable “full seeding” in both raw sugar factories and sugar refineries. This can help standardise and optimise performance, improving sugar recoveries and producing a better quality final product of crystalline sugar. It is also a solution to a skills shortage in terms of experienced operators who are able to reproducibly achieve acceptable results using standard techniques.

Within the South African Sugar Industry (and most other sugar industries) the initial seeding of the crystallisation process is done in batch mode in the first phase of the crystallisation process (in batch pans), even if subsequent crystallisation takes place as a continuous process (in continuous pans). In this application the continuous seed production process would be used to accumulate batches of seed material that would then be used to initiate the conventional first, batch, phase of the crystallisation process, replacing the current seeding process.

A major benefit of a continuous seed production system would be the ability to eliminate the batch aspect of the current crystallisation process altogether. This would be the biggest, although longer term, benefit of a successful outcome from the investigated CSPS. Much success has been achieved over the last 40 years within the South African Sugar Industry in converting from entirely batch evaporative crystallisation to using continuous evaporative crystallisation for a large portion of the crystallisation requirements. The proposed full seeding technique would also be an excellent fit in raw sugar factories and refineries that have replaced evaporative crystallisation with cooling crystallisation.

The benefit of a continuous seed production process would allow the elimination of the batch portion of the crystallisation process and the implementation of fully continuous crystallisation. This would not only extend the benefits that have been achieved by the replacement of batch evaporative crystallisation capacity with continuous processing described above, but could have major implications for overall factory design. Currently the use of batch evaporative crystallisation has required the design of “Pan Floors” where

large, batch, vacuum evaporative crystallisers (batch pans) are mounted relatively high up on steel work. The mounting of heavy dynamic loads high up is particularly demanding and requires very expensive structural steel supports. This need for mounting the batch pans high up is to allow for the rapid discharge of batches by gravity. A completely continuous process, with continuous product discharge, does not require any rapid discharge of vessels by gravity and this will allow the mounting of vessels close to ground level with the potential of major savings in the capital cost of new factories.

4.4. Investigating suitable operating conditions for a full seeding system

The full CSPS will need to grow the sound induced nuclei to a size that is "robust" enough to be fed to conventional pan boiling. The term "robust" refers to both being large enough to avoid inadvertent dissolution in the non-uniform conditions of pan boiling (dissolution due to areas of under-saturation) and also to have sufficient crystal surface area to avoid secondary nucleation (false grain) during the initial stages of pan boiling (if the crystal surface area is low then sucrose will form new nuclei in the bulk solution rather than depositing onto existing crystals). The ideal size will be a compromise between crystals that are large enough to be "robust" and small enough not to place a substantial crystallisation load onto the CSPS process. Indications from communications with senior South African sugar technologists and also from preliminary calculations are that an appropriate size is likely to be in the range of 50 to 100 µm. Crystals slightly less than 50 µm may also be deemed acceptable as these crystals can be grown to the more robust sizes with the addition of a supersaturated sugar processing streams to facilitate the crystal growth. It is also important that the seed produced by the CSPS process has an adequate crystal content since the lower the crystal content, the larger the quantity of seed that will be required to feed the subsequent crystallisation process. The possible crystal content can be determined by calculation if the operating conditions of the CSPS process are specified (see Figure 4.1.). This is done using the known solubility relationship for sucrose in water as a function of temperature (see Figure 3.2.).

A likely range of possible operating conditions is conveniently visualised on the graphs shown in Figure 4.1. (The calculations on which the graphs are based are described in Appendix A). The upper graph shows contours of constant supersaturation on a graph of temperature plotted against dry solids concentration of a pure sucrose solution. The lower graph represents sucrose solutions where the crystals and the mother liquor are as close to equilibrium as practically possible i.e. the mother liquor is practically at saturation with a low driving force for crystal growth (supersaturation coefficient (SSC) of 1.05). This lower graph shows contours of constant temperature on a graph of crystal content plotted against dry solids concentration of the combined (pure sucrose) mixture of crystal and mother liquor. The two graphs are aligned so that vertical lines can be drawn to demonstrate the consequences of crystallisation bringing about equilibrium between crystals and mother liquor in any specified sample. The temperature ranges cover both the conventional boiling temperatures for raw sugar and refinery pans (about 70 to 85°C).

For any selected crystal content of the seed, the required crystal number density can be determined from the desired crystal size. This is a relatively simple calculation (as described in Appendix A).

The third graph in Figure 4.1. (lower left) shows contours of constant crystal size on a plot of volumetric number density against crystal content. The graph is aligned horizontally with the adjacent graph, so that horizontal lines can be drawn at the appropriate crystal content and the required number density read off, depending on the chosen crystal size.

Figure 4.1. can be used to give an estimate of the required crystal number density for any particular set of operating conditions. Two possible scenarios are given to show the range of potential operating conditions for a commercially viable process:

A) Nucleation takes place in a solution at 70°C and an SSC of 1.10 (point 1). This is then allowed to come to equilibrium at 70°C (point 2), resulting in a crystal content of approximately 7%. If the desired crystal size is 50 µm (point 3), the required crystal

number density is approximately $5.5x10^5$ crystals/mL of seed. If the desired crystal size is 100 µm (point 4), the required crystal number density is approximately $7.0x10^4$ crystals/mL of seed.

B) Nucleation takes place in a solution at 85°C and an SSC of 1.20 (point 5) this is then cooled to 70°C and allowed to come to equilibrium (point 6), resulting in a crystal content of approximately 26%. If the desired crystal size is 50 µm (point 7), the required crystal number density is approximately $2.0x10^6$ crystals/mL of seed. If the desired crystal size is 100 µm (point 8), the required crystal number density is approximately $2.5x10^5$ crystals/mL of seed.

For the given scenarios, the acceptable crystal number densities were found to be $7.0\ x10^4$ crystals/mL and $2.0\ x10^6$ crystals/mL. Conditions of temperature and SSC lower than that stipulated in Scenario A is not likely to be a commercially viable process and thus the crystal number density of $7.0\ x10^4$ crystals/mL is set to be a minimum stipulated quality requirement for the seed to be produced. Scenarios A and B were estimated as likely typical operating conditions, however, as can be seen in Chapter 7, other scenarios yielded more desirable results. Generating nuclei at a crystal number density higher than the $2.0\ x10^6$ crystals/mL, as in Scenario B, is also viable because it is relatively easy to reduce the density to any (lower) required value by dilution by liquid processing streams.

Another critical measure to evaluate the quality of the seed produced is the crystal size coefficient of variation (CV), being the ratio of the standard deviation of the size distribution to the mean size expressed as a percentage. Again, senior South African sugar technologists were consulted and a target value of less than 50% CV was set for the seed to be produced. This value is set for CVs determined from image analyses by number rather than by the conventional sieving method which is based on mass.

Table 4.1. summarises the seed quality requirements desired for the full continuous seed production system, as determined from calculations and industry communications.

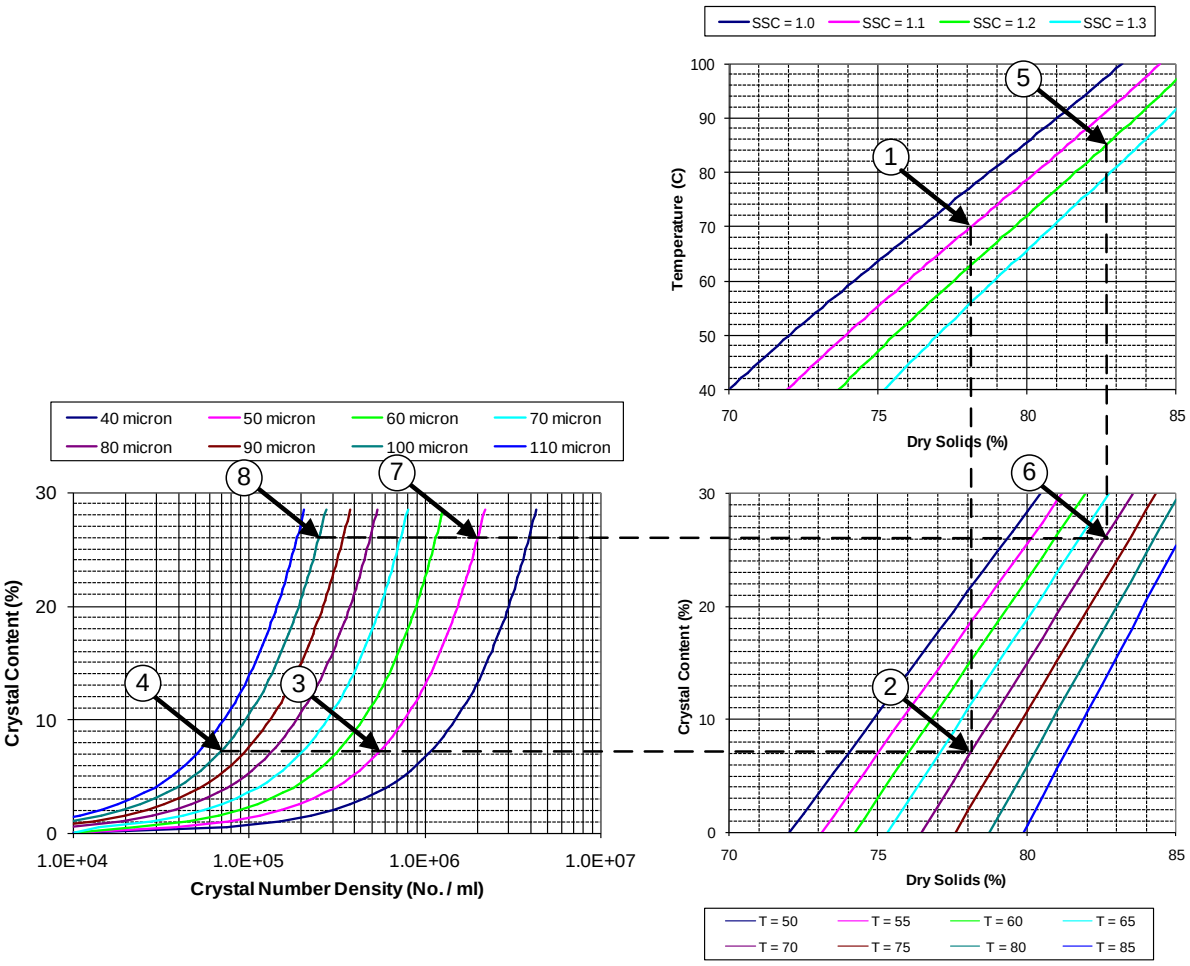

Figure 4.1. Graphical Estimation of Required Crystal number density for CSPS Process

Table 4.1. Quality requirements for seed from full continuous seed production system

Quality requirement for seed	**Stipulation**
Crystal number density (number of crystals/mL of seed)	> 7 X 10^4
Average crystal size (µm)	> 50
CV (%)	< 50

CHAPTER 5 – EVALUATION OF EXPERIMENTAL METHODS AND EQUIPMENT FOR ULTRASOUND APPLICATION

Discussed in this chapter is a review of experimental methods for the determination of the quality of the seed crystals produced. This includes comparisons between methods using laser diffractometry, a Coulter counter system and image analysis. The ultrasound equipment available for industrial usage is also reviewed. These include both direct and indirect methods of applying ultrasound to liquids.

5.1. Evaluation of methods to quantify crystal quality

The seed quality requirements for the full CSPS are described in Table 4.1. These include the crystal number density, average size and CV. The ability of laser diffractometry, Coulter counters and image analysis were evaluated to determine its suitability to quantify the seed quality requirements. Ball-milled slurry samples were used for the evaluation as these samples were easily stored without compromising the integrity of the samples. Ball-milled slurry crystals are typically greater than 3 μm in size; it was assumed that if the methods were able to detect these small crystals then it would also be able to quantify the quality of the larger seed crystals. This work was published by Rahiman *et al*. (2012), a paper which was co-authored by the author of this dissertation (also led the work done).

5.1.1. Laser diffractometry

This method utilises angular variation of light scattered by particles, to obtain a size distribution of the suspension. Modern laser diffractometry follows the Mie scattering theory which includes sensitivity to sizes smaller than 20 μm and a wide opacity range (Horiba Scientific, 2012) and provides an equivalent diameter based on light scattering.

The sub-sampled slurry was initially suspended in glycerol, followed by further suspension in ethanol. The result obtained from the instrument is simply a volume

distribution that can be fitted as a log-normal distribution. Figure 5.1. illustrates a typical slurry particle distribution obtained from laser diffractometry. The analyses were performed at the University of KwaZulu-Natal using a Malvern Mastersizer 2000 laser diffractometry instrument.

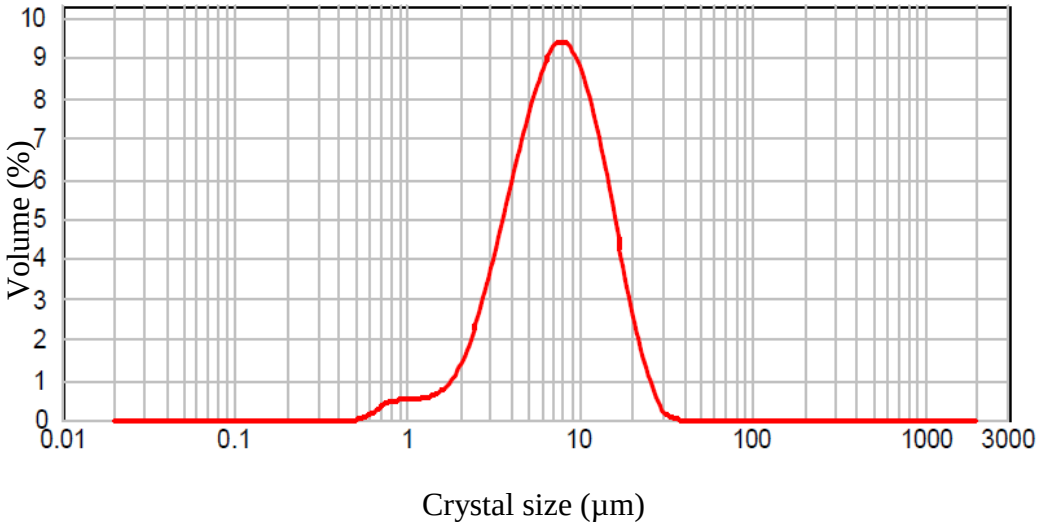

Figure 5.1. Laser diffractometry crystal size distribution of a ball-milled slurry.

The disadvantages of laser diffractometry are as follows:

- No direct evaluation of crystal number density and CV;
- It ignores crystal habit and assumes a spherical shape;
- A large amount of ethanol is required as a carrier for the particles and to avoid clusters of particles;
- Agglomerations are counted as single crystals (Horiba Scientific, 2012).

The advantages of this technique are that it is quick, repeatable and requires no calibration.

5.1.2. The Coulter counter method

This method was developed by WH Coulter in 1954 (Trottier *et al*., 2010), for the rapid counting of blood cells. According to Trottier *et al*. (2010), the principle involves passing

a controlled volume of particles suspended in an electrolyte through a given orifice through which current flows. The particles flowing through the orifice change the impedance across the orifice and the number of changes in electrical resistance across the orifice is related to the number of particles; the extent of the change correlates to the particle size. This method requires the particles to be adequately suspended, since agglomerates are counted as one crystal. The results obtained are in the form of a number distribution and a particle count. The advantages of this method are that it is rapid and it can measure complex distributions. A disadvantage is that the instrument is difficult to calibrate for a sample that has a large crystal size distribution (CSD).

For this work, the tests were performed on a Beckman Multisizer 3 Coulter counter that was made available by Biological Control Products SA and was calibrated using 20 µm beads. The slurry was suspended in saturated glycerol followed by further suspension in an ammonium thiocyanate electrolyte (van der Poel *et al*., 1985). The results obtained from the Coulter counter tests were not repeatable and there were many instances where the orifice was plugged despite the attention to crystal dispersion prior to the analysis.

5.1.3. Image analysis

This method is well known in the South African sugar industry as it is currently employed by the SMRI for CSD analyses of C-massecuites. The method utilises a transmittance light microscope equipped with a polariser and the relevant image analysis software (for the slurry analyses, Scope Photo® was the software used).

Due to the small visual differences in length and width of the slurry crystals in most samples, it was decided that the maximum distance across the crystal area be measured. The factory slurry was dispersed in saturated glycerol, and only 100 crystals were manually sized due to the hygroscopic nature of glycerol and the heat from the microscope dissolving smaller crystals when exposing the sample for too long. The crystal number density was measured by capturing pictures of a well dispersed slurry sample at various points on the slide, followed by manual counting of the crystals.

Results show that a mean size range of 7-9 μm was obtained, with an average crystal number density of 1.0×10^8 nuclei/mL of slurry. The crystals did not display defined crystal edges due to their small size and limitations to the available magnifications. The results of the image analysis compared well to the laser diffractometry results (also reported in a pharmaceutical application by Tinke *et al*., 2005); however, there were the added advantages, over laser diffractometry, of counting the number of crystals and evaluating their habit. Image analysis is a direct analytical method which allows measurement of various size parameters that may consider particle shape in certain instances, which overcomes a major weakness of laser diffractometry. The image analysis method used in these initial tests was, however, very tedious and was limited due to the time taken to analyse the sample, as well as the dispersion of crystals when counting. These constraints were overcome in the development of the image analysis method by the automatic counting of crystals from photomicrographs and from determining the appropriate amount of saturated glycerol to be used for the purpose of crystal dispersion.

Due to the ease of operation of the image analysis technique, further developmental work was performed to establish a repeatable method to quantify the crystal quality using the method. This is described in Appendix B (as reported by Rahiman *et al*. (2012)). Since this publication a slight modification to the procedure was introduced – this included the use of a feeler gauge on the microscope slide to ensure that a constant volume of sample was always used. The method in Appendix B can be modified as follows:

To prepare a microscopic slide for analysis, a representative sample of seed solution was taken from a sample bottle and placed in the centre of a glass microscope slide. A feeler gauge of 0.05 mm in thickness was then placed at each end of the slide before placing a second microscope slide on top of the sample. Squeezing the two slides together and allowing any excess sample to drain from the edges of the slides produced a film of seed slurry 0.05 mm thick trapped between the two glass slides.

5.2. Evaluation of various ultrasound systems

A brief description of commercially available insonation equipment and their components is given in Section 2.8. Each of these types of equipment were tested at the SMRI to evaluate sound wave induced nucleation for the production of the desired quantity and quality of seed crystals.

The insonation systems tested cover the two basic methods of applying acoustic power to liquid loads (Mason, 1990);

- A low power intensity system, such as a liquid filled vessel with multiple transducers around the base (see Figure 5.2.) or walls (see Figure 5.3.),
- A high power intensity system which transmits energy by means of a horn or velocity transformer (see Figure 5.4.).

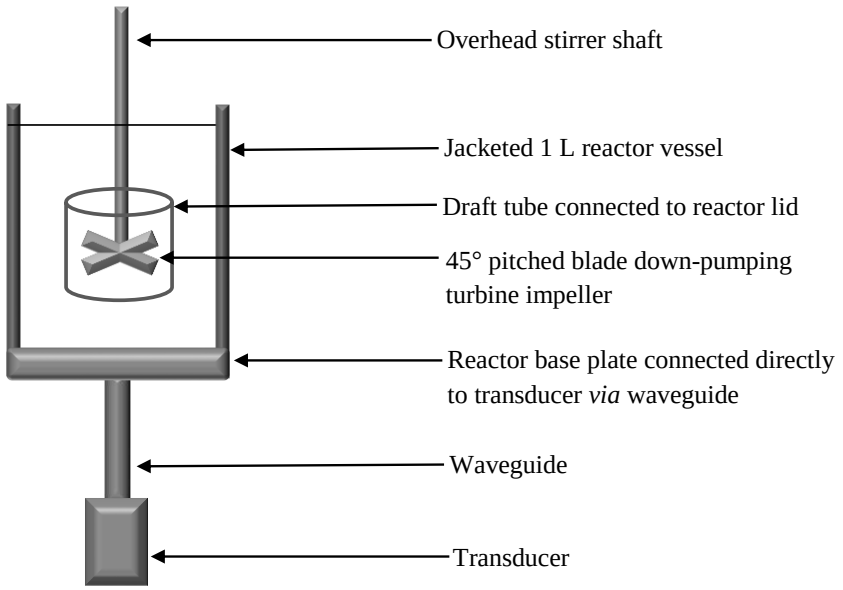

Figure 5.2. Low intensity ultrasound application with transducer at base of reaction vessel

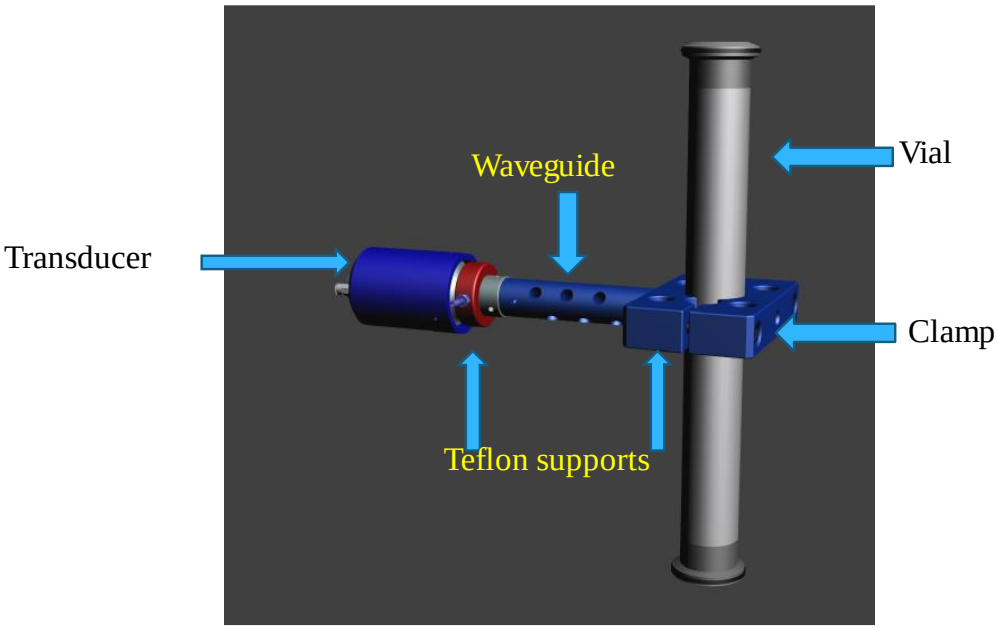

Figure 5.3. Low intensity ultrasound application with transducer around wall of flow through pipe

Figure 5.4. High intensity ultrasound application with horn in direct contact with liquid – seen here in a batch system, but also tested in a flow through system.

The first two insonation systems tested in the laboratory (Figures 5.2. and 5.3.) were low power intensity systems and contrary to the recommendations by suppliers of the units, these could not achieve the required crystal number densities. The required crystal number densities were, however, achieved with a high power intensity sonotrode system in both batch and continuous operations. A summary of the three systems tested appears in Table 5.1.

Table 5.1. Summary of the laboratory scale seed production tests using various insonation systems

Irradiating surface used	**Maximum Power Intensity (W/cm^2)**	**Desired crystal number density obtained at specified processing conditions**
Flange - at the bottom of a 1 litre vessel	3	No
Clamp - onto flow through pipe	6	No
Probe system – in batch vessels and flow through cells	130	Yes

The initial success of the high power intensity probe system, achieved with a 200W unit on loan from the supplier, was followed up with a planned set of batch insonation tests to cover a range of possible operating conditions and probe settings. This work then progressed into a continuous bench-top scale system, which forms the basis of the work presented in this dissertation.

CHAPTER 6 – DESCRIPTION OF EXPERIMENTAL APPARATUS, PROCEDURE AND DESIGN RATIONALE

Described in this chapter is the experimental apparatus used to assess if the desired seed quality can be produced on a continuous basis. The equipment used were of a bench-top scale, however, the flowrates used were typical of refinery requirements and sufficient to seed a full-scale refinery pan.

Also described are the experimental procedures used. These include the preparation of the sugar solution for insonation, general operating procedures and also the factors investigated to determine its influence on seed crystal quality.

6.1. Ultrasound equipment used in bench-top scale continuous seed production tests

The Hielscher 400W sonotrode system used in the bench-top scale tests is shown in Figure 5.4. Various horns can be purchased that retrofit the ultrasound unit. Standard probes with the unit included 7, 14 and 21 mm diameters. The sonotrode unit was very simple to operate compared to the low power units previously purchased. The frequency was fixed at 21 kHz, with control only over amplitude (%) and pulsing (% of a second).

For sonotrode systems, the horn is in direct contact with the liquid being treated. The supplier of the unit suggested an immersion depth of 10 mm for the probe. Observations of the acoustic intensity with various immersion depths were observed in beakers used for batch tests. The 10 mm immersion was confirmed visually to result in the greatest acoustic activity within the liquid treated. Batch tests were also used to show that the acoustic penetration was densest when the 14 mm probe was used. Limited tests with the different probes showed that the 14 mm probe gave the largest crystal number densities; this probe was subsequently used in all of the bench-top scale tests.

The 400W system was purchased as the power intensity was deemed to be sufficient for the application on bench-top and also pilot-scale tests.

6.2. Description and operation of bench-top scale continuous insonation system

The bench-top scale continuous insonation system was constructed around the high power sonotrode. This is shown schematically in Figure 6.1., with a photograph of the system shown in Figure 6.2.

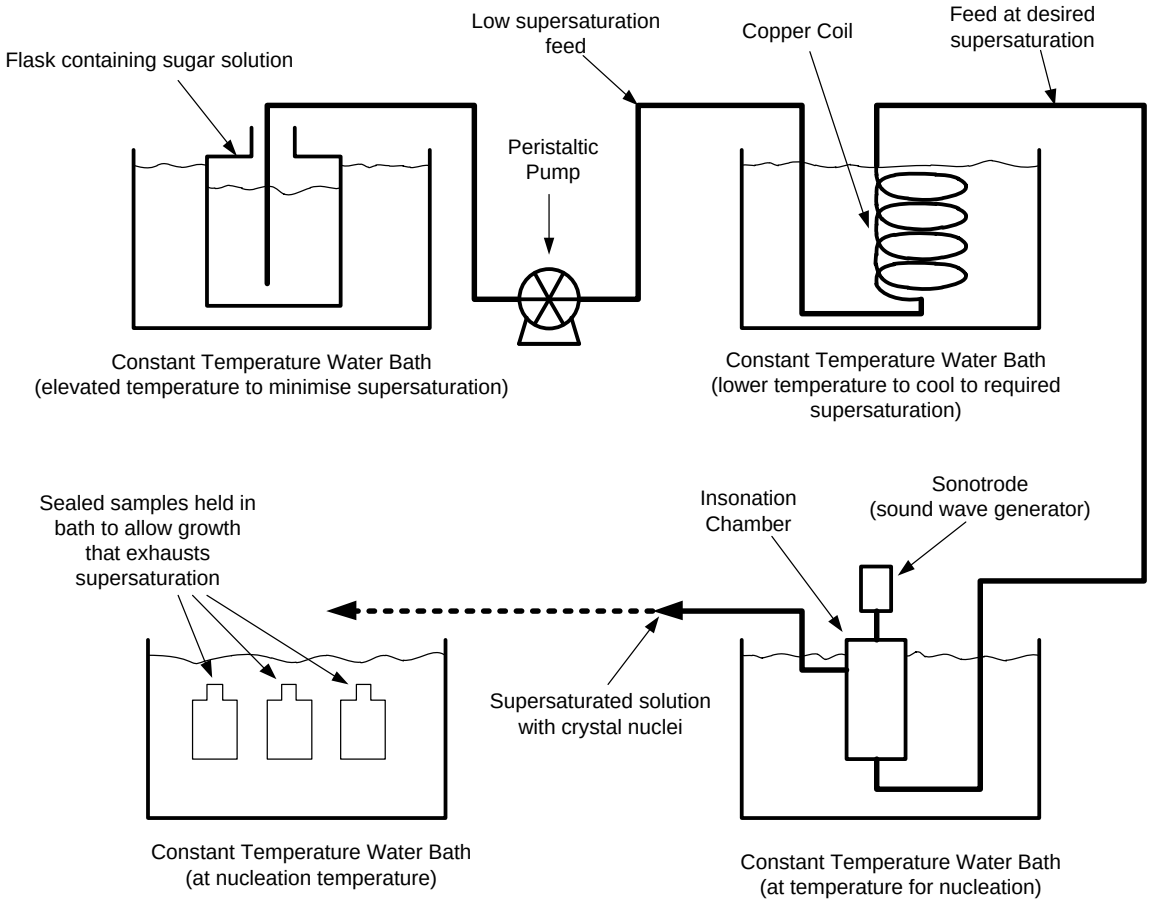

Figure 6.1. Schematic of bench-top scale continuous insonation system

Supersaturated technical solutions were prepared batchwise by dissolving refinery first boiling sugar into hot distilled water (95^{o}C). Data from Figure 3.2. was used to determine the desired SSCs. The solutions were then stored at a low level of supersaturation in a water bath (at least 20^{o}C above the test temperature to avoid false grain formation in storage), before being pumped through a heat exchanger (copper coil within a second water bath) to achieve the desired temperature and supersaturation for insonation. Once

the solution was exposed to the high frequency sound for the intended nucleation to occur, samples of the insonated stream were taken and sealed in small sample bottles. The samples were held in a constant temperature water bath for five minutes to allow completion of the crystal growth that exhausted the available supersaturation before taking a subsample for microscopic analysis.

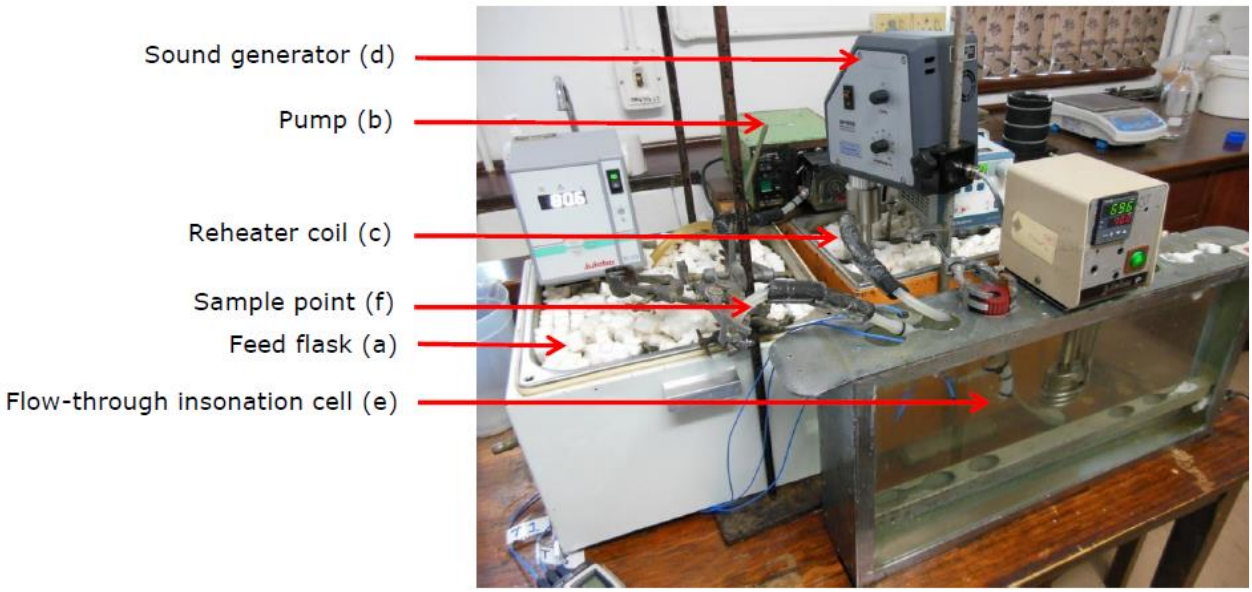

Figure 6.2. Bench-top scale continuous insonation system

The duration of the test runs was limited by the capacity of the auxiliary equipment available (waterbaths and feed flasks) and the time taken to prepare sufficient quantities of solution within a day (solutions stored overnight are not typical of the bulk feedstock to be treated in industry, due to the inversion of sucrose into glucose and fructose when stored at high temperatures for long retention times).

6.3. Experimental design rationale

Based on the literature survey and the requirements for an industrially suitable continuous seed production system, the following factors and levels were considered for investigation.

- Primary induced nucleation only by sound waves
- Primary induced nucleation by sound waves, followed by secondary induced nucleation by sound waves to maintain required quality specifications
- The effect of supersaturation on crystal quality (four levels)
- The effect of power intensity or amplitude on crystal quality (five levels)
- The effect of pressure on crystal quality (three levels)
- Temperature was fixed at 70^0C, as this is the temperature in most rawhouse and refinery pans
- The ultrasound frequency was fixed at 21 kHz, as the frequency could not be varied on the Hielscher 400W sonotrode system
- The pulse setting on the ultrasound unit was set at 35%, as tests showed that this setting limited the temperature rise across insonation and also gave the highest crystal number densities
- Repeatability of results obtained
- Flowrates (two levels)
- The influence of the presence of dissolves gases and gas bubbles were not investigated. It was assumed that the solutions tested were heterogeneous as no boiling or de-gassing has been performed (typical of factory feed stream to pans).

CHAPTER 7 – RESULTS AND DISCUSSION

In this chapter, the experimental results are presented and discussed. This includes the work done on primary-nucleation-only, induced by sound wave application on supersaturated sugar solutions, and also primary-induced-nucleation by sound waves, followed by secondary-induced-nucleation by sound waves to maintain required quality specifications.

The key quality requirements for the desired seed from the full continuous seed production system is given in **Table 4.1.** This is given here again for ease of reference:

- The crystal number density required should be greater than 7×10^4 crystals/mL of seed produced.
- The average crystal size should be greater than approximately 50 µm. Crystals slightly smaller than this are also acceptable as they can be grown with the addition of a supersaturated sugar solution.
- The crystal size CV should be less than 50%.

Also discussed in this chapter is the effect of SSC, amplitude, pressure, flow and impurities on the crystal quality. The repeatability of results is investigated and crystal growth is modelled. Scanning Electron Microscope (SEM) of various crystal types are also given, as are some comments on the quality of crystals presently obtained in the sugar industry.

7.1. Sound induced primary nucleation in flow through cell

The experimental setup in Figures 6.1. and 6.2. were used to investigate sound induced continuous primary nucleation. For each of the tests performed, a control test was also performed, where solution was run through the system at the test conditions, but without the application of a sound wave.

Sugar solutions at SSCs of 1.10, 1.20, 1.30, 1.35 and 1.40 (at temperatures of 70 and 80^{o}C) were prepared by dissolving refinery first boiling sugar into distilled water. The test procedure described in Section 6.2. was adhered to for flowrates of 75 and 200 mL/min, a pulse setting of 35% of a second and various sound wave amplitude settings. As per Section 6.2., samples of the insonated supersaturated solutions were taken and grown batch-wise in 20 mL closed sample bottles at the test temperature in a waterbath. The sample bottles were not stirred; stirring of the samples is expected to assist the crystal CV quality as a substantial amount of crystals had settled to the bottom of the sample bottom at the end of the five-minute growth period. The results of these tests is given in Table 7.1.

From the table it can be seen that no nucleation had occurred in any of the control tests, other than the 1.40 SSC solution at 80^{o}C, where crystals were formed in the prepared solution whilst it was in storage and prior to any test work being done on it.

There was no nucleation in any tests performed with the 1.10 and 1.20 SSC solutions. Nucleation did occur in the 1.30 and 1.35 SSC solutions when sound waves with peak-to-peak amplitudes of 50, 60 and 70 µm were applied. Crystal number densities ranging from 2.0 to 3.5x10^{6} crystals/mL of seed were obtained; however, the nucleation was not repeatable in other tests performed with the same conditions.

Nucleation was achieved with the application of sound waves in 1.40 SSC solutions (at 70^{o}C) with different flowrates and amplitude settings (highest densities with 60 µm peak-to-peak amplitude setting – see Figure 7.1. for photomicrograph of crystals obtained). Nucleation with these solutions was repeatable, however, the duration of tests runs was often limited due to blocking of pipelines from encrustation of crystals (very high sucrose concentrations at 1.40 SSC makes spontaneous nucleation around sharp edges, temperature probes, etc. a risk).

Table 7.4. Results - Sound induced primary nucleation in flow through cell

SSC	Temperature (°C)	Pulsing rate (% of second)	Peak-to-peak Amplitude (µm)	Flowrate (mL/min)	Crystal number density (crystal number /mL seed)	Comments
1.10, 1.20, 1.30, 1.35	70, 80	No ultrasound	No ultrasound	75, 200	0	Control tests with supersaturated solutions pumped through the flow through cells without any ultrasound being applied. No crystal nucleation was observed in any of the tests performed.
1.10, 1.20, 1.30, 1.35	70, 80	35	20-100 in increments of 10 µm	75, 200	0	No crystal nucleation was observed in all of the 1.10 and 1.20 SSC tests performed. Nucleation did occur in some of the 1.30 and 1.35 SSC tests performed (at both test temperatures, with crystal number densities ranging from 2.0-3.5 x 10^6 crystals/mL seed produced for amplitudes of 50, 60 and 70 µm); however, the nucleation was not repeatable in other tests performed, with no crystal formation with 1.30 and 1.35 SSC solutions at the given temperatures and ultrasound exposure).

SSC	Temperature (°C)	Pulsing rate (% of second)	Peak-to-peak Amplitude (µm)	Flowrate (mL/min)	Crystal number density (crystal number /mL seed)	Comments
1.40	70	No ultrasound	No ultrasound	75, 200	0	No crystals observed in control test.
1.40	70	35	40	75	2.0×10^6	After five minutes of crystal growth at 70°C (until saturation of surrounding solution) in an unstirred 20 mL sample bottle, the crystal sizes ranged from approximately 20-200 µm.
1.40	70	35	50	75	2.5×10^6	Same observation as above.
1.40	70	35	50	75	2.3×10^6	Same observation as above.

SSC	Temperature (°C)	Pulsing rate (% of second)	Peak-to-peak Amplitude (µm)	Flowrate (mL/min)	Crystal number density (crystal number /mL seed)	Comments
1.40	70	35	50	75	$2.6x10^6$	Same observation as above.
1.40	70	35	60	75	$2.2x10^6$	Same observation as above.
1.40	70	35	40	200	$1.6x10^6$	Same observation as above.
1.40	70	35	50	200	$2.0x10^6$	Same observation as above.
1.40	70	35	60	200	$1.9x10^6$	Same observation as above.
1.40	80	n/a	n/a	n/a	False nuclei formation	Poor quality crystals (conglomerates) formed spontaneously in the prepared solution prior to the tests commencing. The 1.40 SSC (at 80°C) control and ultrasound tests were not performed due to the false nucleation occurring.

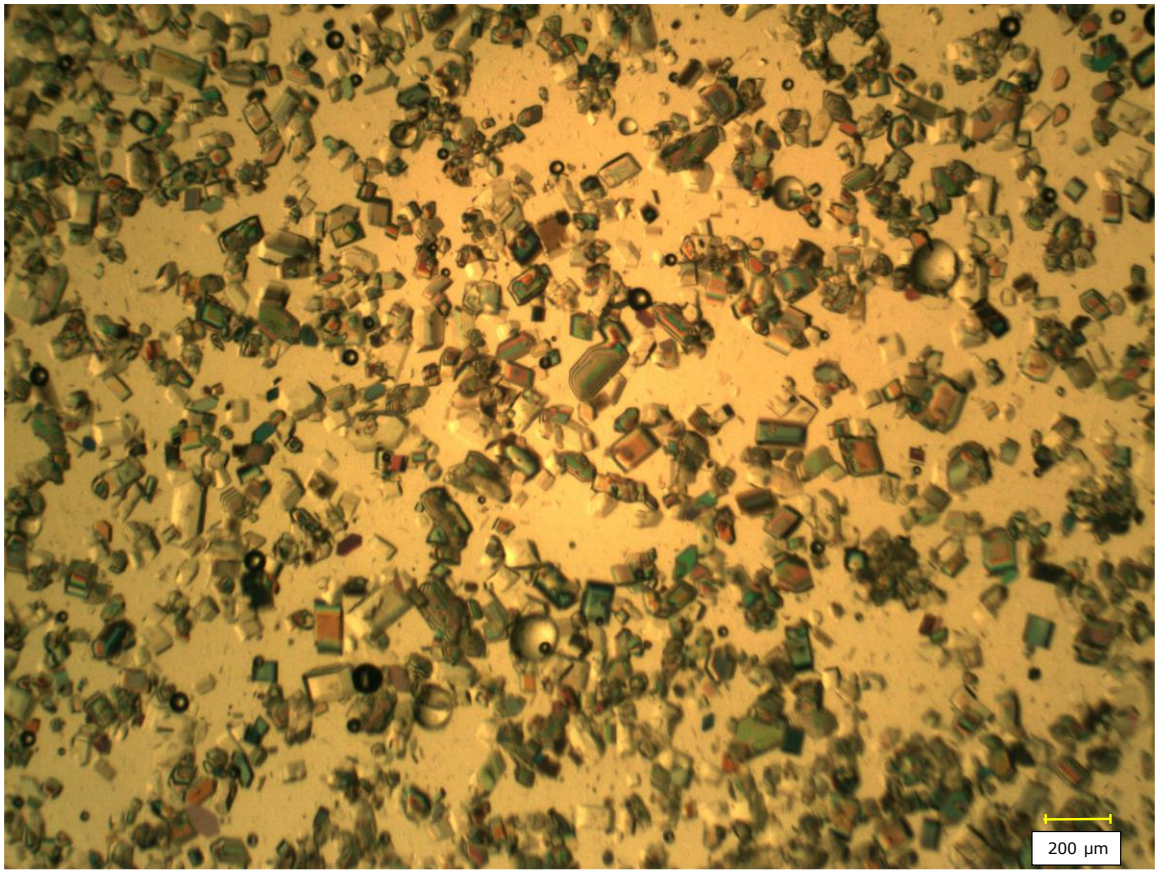

Figure 7.1. Photomicrograph of crystals obtained when 1.40 SSC refinery first boiling sugar solution (at 70ºC) was insonated with 60 µm peak-to-peak amplitude (primary induced sound nucleation).

7.2. Primary induced nucleation by sound waves, followed by secondary induced nucleation by sound waves to maintain nucleation

In these tests, primary nucleation was first established at low flowrates and high SSCs (1.4 SSC at test temperature), thereafter the test conditions were applied (flow changed to institute temperature and SSC changes) to maintain nucleation (by secondary nucleation). This section discusses the effects of SSC, amplitude, pressure, flow and impurities.

7.2.1. Effect of SSC

Refinery first boiling sugar solutions with SSCs of 1.20, 1.30, 1.35 and 1.40 (at 70ºC) were first subjected to primary nucleation induced by insonation, before secondary

nucleation pursued with application of a flow rate of 200 mL/min, pulse setting of 35% of a second and sound wave peak-to-peak amplitude of 60 µm. The results of these tests are given in Table 7.2. and Figure 7.2.

Table 7.2. Results - Sound induced secondary nucleation - effect of SSC

Prepared SSC (at 70°C)	1.20	1.30	1.35	1.40
Number of tests	3	3	5	3
Average temperature rise (°C) across insonation cell	4	5	5	5
SSC after insonation	1.14	1.23	1.28	1.33
Average crystal size (µm) after growth to saturation at 70°C	47	50	54	58
Standard deviation of crystal size	1	2	3	3
Average crystal size CV (%)	33	38	41	45
Standard deviation of crystal size CV	1	2	2	3
Crystal number density (number of crystals/mL of seed)	6.2×10^5	1.8×10^6	2.4×10^6	3.6×10^6
Standard deviation of crystal number density	5.3×10^4	4.0×10^5	4.0×10^5	4.5×10^5
Crystal number flow (number of crystals per hour)	7.5×10^9	2.2×10^{10}	2.9×10^{10}	4.3×10^{10}
Standard deviation of crystal number flow	6.4×10^8	3.7×10^9	4.8×10^9	6.0×10^9
Comments	Sample taken 30 minutes into test.	Sample taken 30 minutes into test.	Sample taken 30 minutes into test.	7 minute sample taken. Thereafter spontaneous nucleation occurred with feed vessel.

It was observed that for each of the SSCs tested, the crystal quality specification was met. There appeared to be direct relationships between the SSC used and the crystal number density, average crystal size and the crystal size CV obtained (linear trends with R^2 values of 0.9678, 0.9377 and 0.9873 were obtained, respectively). This was as expected. The higher the SSC, the greater the driving force for nucleation to occur, hence the higher the SSC the greater the crystal number densities expected and observed. The higher the SSC, the higher the crystal size expected – this is due to the increased amount of sucrose available for crystal growth. The CVs also increased with the higher SSCs – this too was expected, as experience with factory panboilings show similar trends. From Figure 7.2. it can also be seen that the crystal number densities appear to increase with time. Ideally longer test runs are desired to establish when the trend of increasing crystal number densities plateau; however, this was not possible due to limitations explained in Section 6.2.

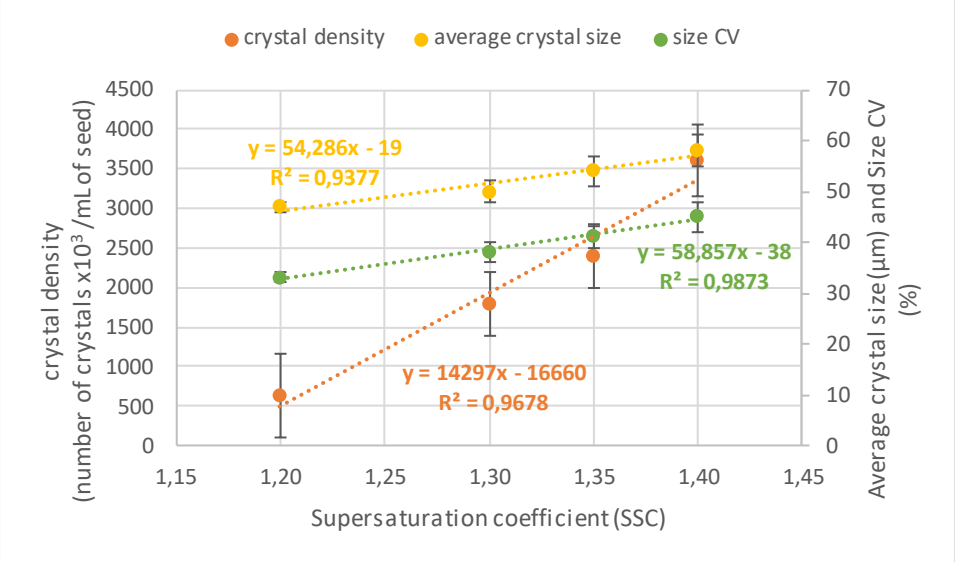

Figure 7.2. Crystal number density, average size and size CV observed with changes in SSC when secondary nucleation is induced by insonation

7.2.2. Effect of amplitude

To show the effect of amplitude, a 1.35 SSC refinery first boiling solution was prepared (at 70^{o}C). Primary nucleation was induced at a flowrate of 75 mL/min, pulse setting of

35% of a second and the test peak-to-peak amplitude, before the flowrate was raised to 200 mL/min. Peak-to-peak amplitudes of 20 to 90 µm were tested at increments of 10 µm. The results of the tests are given in Table 7.3. and Figure 7.3.

Very few crystals were obtained at 20 and 30 µm amplitude settings (determined visually to be below the desired crystal number density). The same was observed with the 90 µm setting. Figure 7.2. shows clearly that there is a direct relationship between the amplitude setting and the temperature rise observed across the insonation cell (R^2 of 0.9869). The highest crystal number density resulted when an amplitude of 50 µm was used. Section 2.7.1. describes the use of a calorimetric method to compute the power input to the solution from the temperature rise observed (and using one of the basic laws of thermodynamics $Q = mc_p\Delta T$). It can therefore be computed that the lowest power input to result in nucleation was observed at an amplitude of 40 µm and a power input of 40 W, or 31 W/cm^2 (from area of 1.4 cm diameter probe) and 0.2 W/cm^3 from 200 mL/min flowrate. Table 7.4. gives some other computed calorimetric power values.

It can also be observed from Figure 7.3. that the crystal number density decreases at amplitudes above 50 µm. This can be explained with the use of Figure 3.2. where it can be observed that for a given solution the higher the temperature rise, the lower the SSC, and therefore the lower the driving force for nucleation to occur (seen as lower crystal number densities) – to the extent of no crystal formation at 90 µm amplitude, due to the solution becoming undersaturated. Section 2.4.2. discusses a further reason why higher amplitudes or irradiation intensity may result in lower crystal numbers i.e. at the higher acoustic intensities or amplitudes used, a decoupling phenomenon occurs, leading to a loss of power transfer to the medium.

Table 7.3. Results - the effect of amplitude on crystal number density when a 1.35 SSC solution (70ºC) is insonated.

Amplitude setting on UP400S (%)	Peak-to-peak amplitude measured in air (µm)	Crystal number density (number of crystals/mL of seed)	Temperature rise across insonation flow through cell (ºC)
20	20	Few crystals formed (not quantified)	Not measured
30	30	Few crystals formed (not quantified)	Not measured
40	40	2.8×10^6	4.0
50	50	3.5×10^6	4.7
60	60	3.0×10^6	5.4
70	70	2.6×10^6	5.8
80	80	2.1×10^6	6.3
90	90	Few crystals formed (not quantified)	6.9

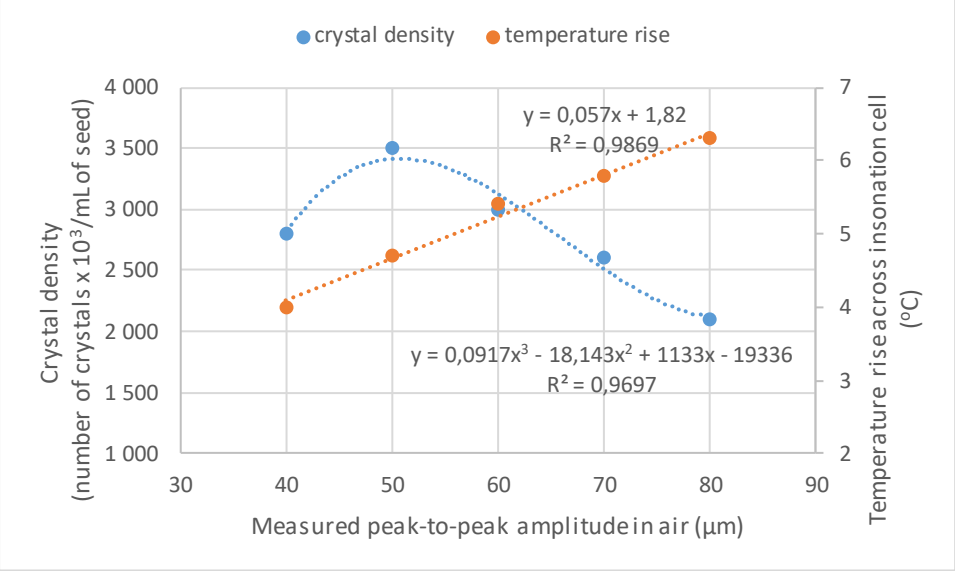

Figure 7.3. Crystal number density and temperature rise observed with changes in amplitude when secondary nucleation is induced by insonation

Table 7.4. Calorimetric power used for nucleation to proceed at different peak-to-peak amplitudes

Peak-to-peak amplitude (μm)	Calorimetric power (W)	Power/probe area (W/cm^2)	Power/flowrate (W/cm^3)
40	47	31	0,2
50	50	32	0,3
60	59	38	0,3
70	77	50	0,4

7.2.3. Effect of pressure (at a constant acoustic power)

The pressure in the flow through cell was varied using a throttle valve attached to the product line and by changing humified air flow introduced into the top of the flow cell. Tests were performed at gauge pressures of approximately 3, 40 and 60 kPa in the flow through cell. No tests were performed at pressures higher than 60 kPa $_{(gauge)}$ – for a typical pilot scale unit, it was approximated that the maximum pressure would not exceed 60 kPa $_{(gauge)}$ (determined from assuming a maximum height of three metres for a pilot scale crystalliser to further grow seed produced, and also using the density of the 1.35 SSC solution (at 70˚C) to obtain the hydrostatic pressure). The experiments were performed using the following conditions: 1.35 SSC solution (70˚C) prepared using refinery first boiling refined sugar, 60 μm sound peak-to-peak amplitude, 35% pulsing and a flow rate of 200 mL/min. Primary nucleation was initiated by insonation before proceeding with the test conditions maintaining secondary nucleation by insonation. Samples of the seed were taken 20 minutes into the test and grown for five minutes at 70˚C in a water bath; thereafter the seed quality and quantity were quantified using image analysis. Table 7.5. and Figure 7.4. summarises the results obtained.

Table 7.5. Results showing the effect of external pressure on the quality and quantity of seed when secondary nucleation is induced by insonation

External pressure kPa (gauge)	Crystal number density (number of crystals /mL seed)	Crystal number flow (number of crystals/h)	Average crystal size (µm)	Crystal size CV (%)
3	$2.5x10^6$	$2.8x10^{10}$	51	45
40	$2.0x10^6$	$2.4x10^{10}$	64	42
60	$1.0x10^6$	$1.2x10^{10}$	66	43

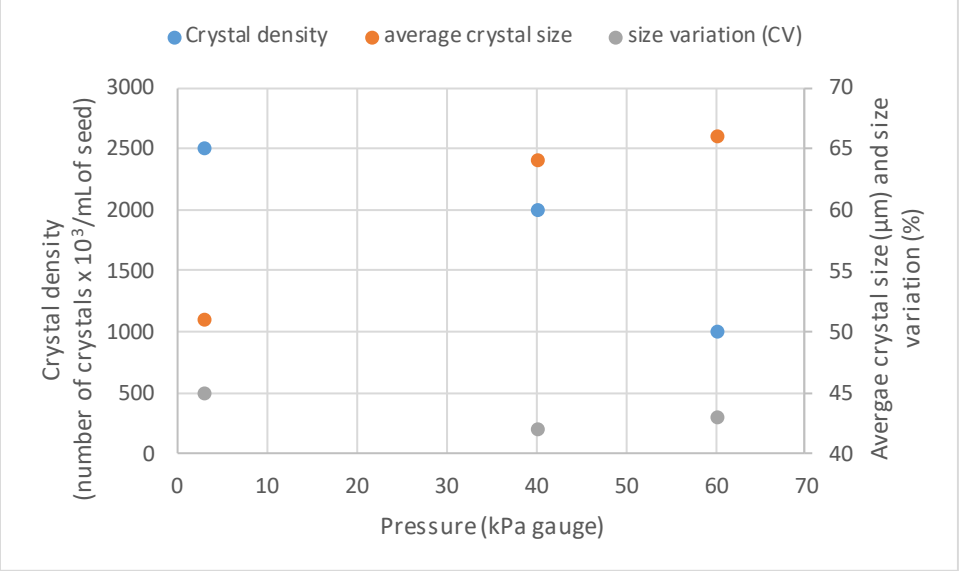

Figure 7.4. Results showing the effect of external pressure on the average crystal size and size variation when secondary nucleation is induced by insonation

It can be observed from Table 7.5. and Figure 7.4. that all the specified seed specifications were met at the different tests conditions. It can also be seen that the crystal number density decreased as the pressure was increased. The average crystal size

appeared to increase with increasing pressure; this is to be expected with the decrease in the crystal number density. This trend was expected (discussed in Section 2.4.2.). Mason (1990) reported that for larger external pressures, a greater acoustic power will need to be applied to provide the necessary cavitation.

7.2.4. Effect of flow

The effect of flow was not extensively tested. For the equipment available it was essential to determine if the crystal quality specifications could still be met with the maximum flowrate possible with the pump used (i.e. 200 mL/min). For these tests, nucleation was first established as per previous tests and then the test conditions applied for the 1.35 SSC refinery first boiling sugar solution. Table 7.6. shows the results obtained. It can only be deduced from the results that at the higher flowrate, lower crystal number densities were obtained for each amplitude used. The crystal number densities at the higher flowrates still satisfied the crystal seed density requirement. The trend was expected (Section 2.4.2.), as the increased flow would have reduced the power intensity (W/m^3), thereby decreasing the cavitation or nucleation effect.

Table 7.6. Crystal number densities obtained with sound induced secondary nucleation at flowrates of 75 and 200 mL/min for peak-to-peak amplitude settings of 50, 60 and 70 µm.

Description of test settings and results obtained	Settings used and results obtained					
Flowrate (mL/min)	75	200	75	200	75	200
Amplitude (µm)	50	50	60	60	70	70
Crystal number density (number of crystals/mL of seed)	$5.0x10^6$	$2.8x10^6$	$5.0x10^6$	$3.5x10^6$	$3.2x10^6$	$3.0x10^6$

7.2.4. Repeatability of results

If the seeding technique under study is to be used in industry, it would have to be a robust process that produces repeatable results. With current practices in mind, an industry committee stipulated that the new seeding technique can be deemed repeatable if the seed characteristics from the continuous process show less than 10% relative standard deviation (RSD) from the desired values for crystal sizes and CV, and less than 20% deviation for crystal number density. RSD is commonly used in statistics as a measure of precision in data analysis. The RSD is calculated by dividing the standard deviation of a series of values by the average of the values.

To investigate the repeatability of results, the 1.35 SSC solution (at 70˚C) was used. This was prepared using refinery first boiling refined sugar and subjected to a sound wave with 60 μm sound peak-to-peak amplitude and 35% of a second pulsing, at a flow rate of 200 mL/min. Primary nucleation was initiated by insonation at a lower flowrate and higher SSC, before proceeding with the test conditions maintaining secondary nucleation by insonation. The results of these tests are shown in Tables 7.7., 7.8. and 7.9., showing crystal number density, average crystal sizes and size CVs, respectively (together with the RSDs).

Table 7.7. shows that for each run performed, the crystal number density increased from the first sample to the last sample taken. For industrial applications, this increase in crystal densities needs to be considered as a constant crystal number density would be preferred. There are several means of maintaining a constant crystal number density, for example one such method may be by increasing the flowrate through the insonation chamber; this will effectively lower the power intensity (W/cm^3) and give more control over the crystal number density. A batch of seed could also be prepared and stored; the crystal number density of the batch could be determined and the appropriate amount of seed then fed into the pan for full seeding to occur.

Table 7.7. Crystal number densities at different sampling intervals for repeated tests – secondary nucleation induced by insonation at specified conditions

Test number	Crystal number density (crystals/mL)			
	5 min	10 min	20 min	30 min
1	1.7×10^6	2.1×10^6	2.2×10^6	2.4×10^6
2	1.9×10^6	2.1×10^6	2.5×10^6	3.0×10^6
3	1.5×10^6	1.7×10^6	2.0×10^6	2.5×10^6
4	1.8×10^6	1.5×10^6	1.9×10^6	2.4×10^6
5	1.8×10^6	1.7×10^6	1.6×10^6	1.9×10^6
Average (crystals/mL)	1.7×10^6	1.8×10^6	2.0×10^6	2.4×10^6
Standard deviation (crystals/mL)	1.8×10^5	2.5×10^5	3.5×10^5	4.0×10^5
Crystal number RSD (%)	11	14	18	17

The seed crystal content was calculated using the crystal number densities of the 30 minute samples taken and was taken to be the mass of the crystals as a percentage of the mass of the seed. The length of the crystal was determined to be about 1.4 times the width of the crystal. The crystal height was assumed to be the same as the crystal width (generally accepted assumption by sugar technologists). The crystal content average was found to be about 22%. This agrees with the correlations shown in Figure 4.1. and suggests that an equilibrium saturation limit of about 1.05 was achieved. For a more detailed calculation of the crystal content, the volume shape factor (discussed in Section 3.4.) and the distribution of crystal sizes would have to be taken into consideration.

Table 7.8. Average crystal sizes at different sampling intervals for repeated tests – secondary nucleation induced by insonation at specified conditions

Test number	Average crystal size (µm)			
	5 min	10 min	20 min	30 min
1	52	55	53	57
2	60	57	51	52
3	57	57	54	52
4	60	57	56	54
5	60	56	56	57
Average (µm)	58	57	54	54
Standard deviation (µm)	3.8	1.0	2.1	2.6
Crystal size RSD (%)	7	2	4	5

Table 7.9. Crystal sizes CV at different sampling intervals for repeated tests – secondary nucleation induced by insonation at specified conditions

Test number	CV (%)			
	5 min	10 min	20 min	30 min
1	43	41	42	44
2	39	40	40	40
3	41	37	41	41
4	41	38	42	41
5	37	39	41	40.1
Average	40	39	41	41
Standard deviation	2	2	1	2
Crystal size CV RSD (%)	5	5	2	5

Figure 7.5. shows the crystal number densities for the repeatability tests performed, together with the standard deviations for samples taken at the specific time. Figure 7.6. gives the average crystal sizes and the size CVs. For each of the tests performed it can be seen that all of the desired crystal quality specifics were met. From the Tables 7.7. to 7.9. it can be seen that all of the RSD requirements were satisfied. Figure 7.7. is a typical photomicrograph of the type of crystals obtained in the repeatability tests.

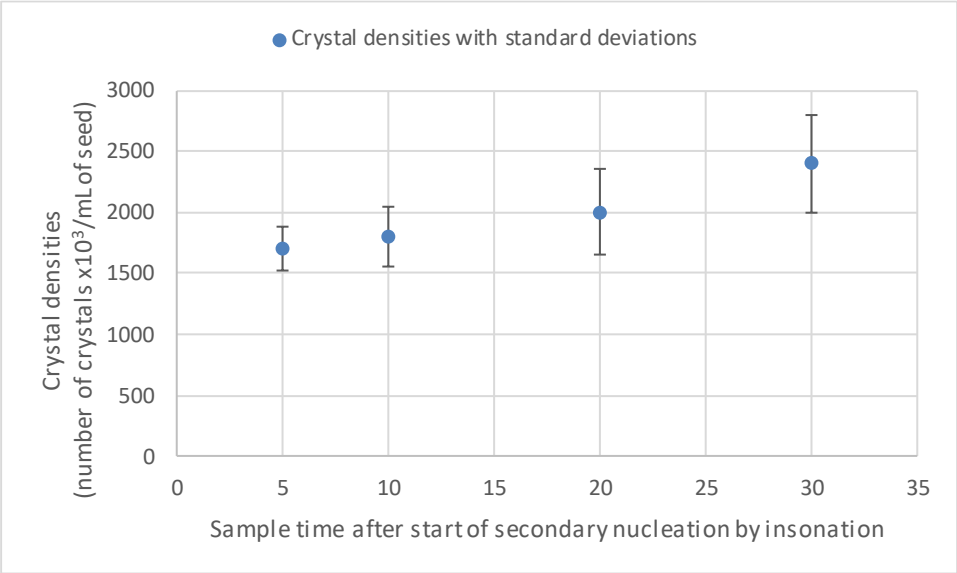

Figure 7.5. Crystal number densities with standard deviations at different sampling intervals for repeated tests – secondary nucleation induced by insonation at specified conditions

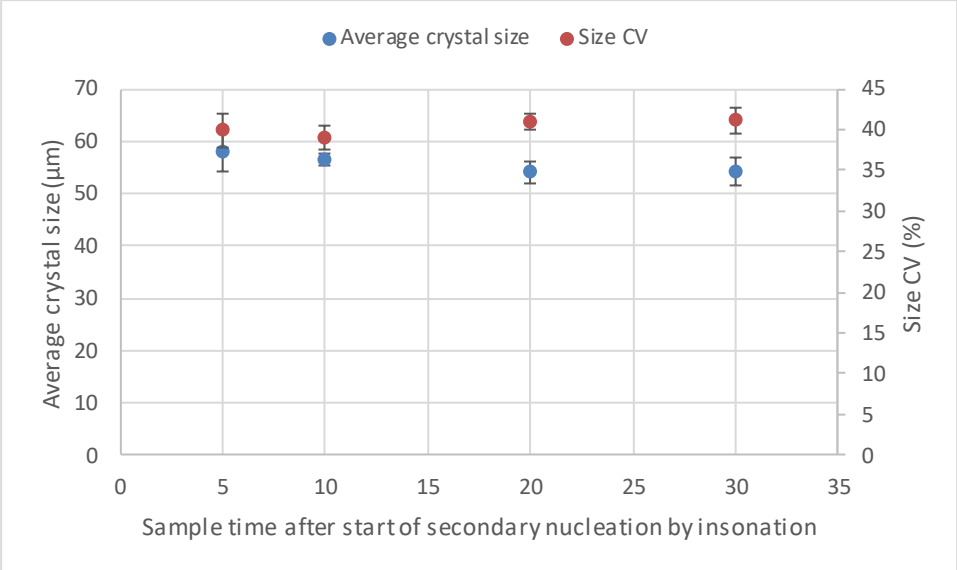

Figure 7.6. Average crystal sizes and CVs with standard deviations at different sampling intervals for repeatability tests – secondary nucleation induced by insonation at specified conditions

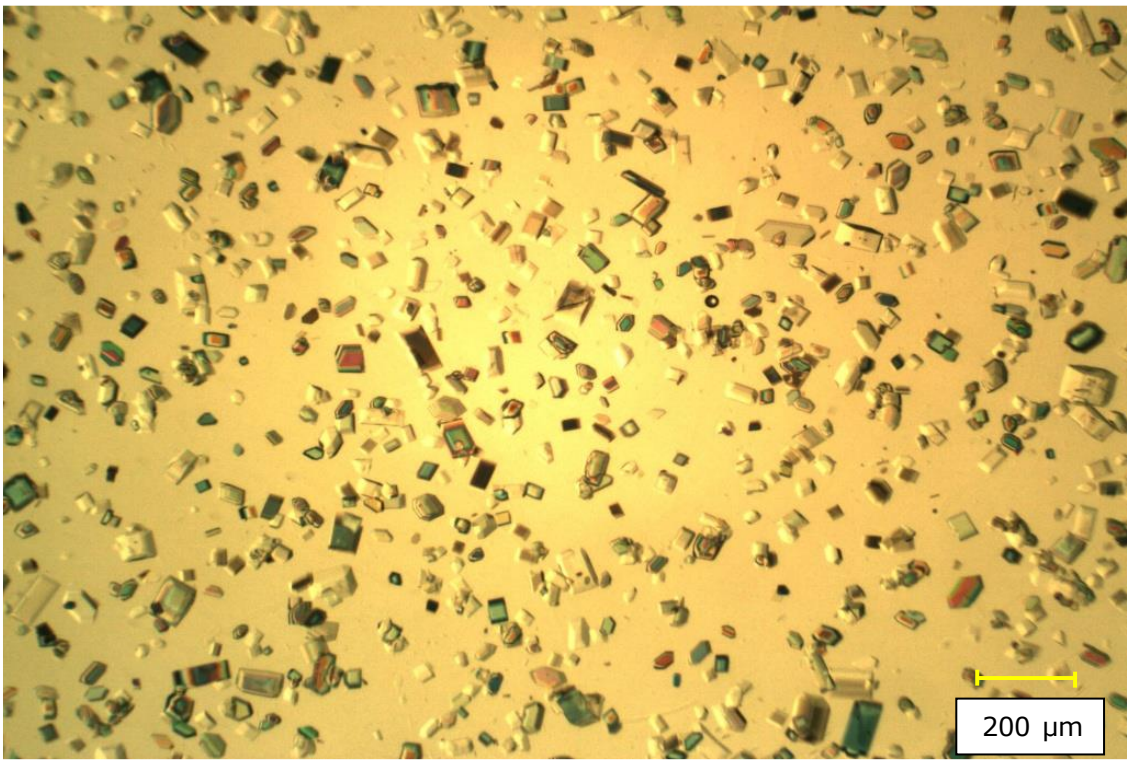

Figure 7.7. Photomicrograph of type of crystals obtained in repeatability tests.

7.2.5. Crystal growth kinetics

For the crystal growth tests, a 1.35 SSC (70^{o}C) refinery first boiling sugar solution was insonated using the same procedure for the other secondary nucleation tests describes in this section. Samples of the insonation solution were collected and allowed to grow in a waterbath held at 70^{o}C in closed sample bottles. The crystal growth data obtained is given in Table 7.10. and Figure 7.8. This experimental data was modelled on Matlab® and compared to classic crystallisation growth models for batch systems, as described in Section 3.5. Volumetric and surface shape factors of 0.34 and 2.90 respectively, were assumed (Lionnet, 1998[a]) and a regression performed for the crystal number density (includes the initial mass of crystals). The results of the nth-order kinetics modelling are shown in Figures 7.9. For this model, the crystal number density was found to be approximately 1.5 x 10^{6} crystals/mL of seed. This compares closely with experimental data obtained. The value of the constant k in Equation 3.16. was found to be

approximately 0.0009 and n was found to be approximately 0.48. The programming code for the Matlab® n^{th}-order kinetics and the regressions performed is included in Appendix C.

All of the other models gave low crystal number densities (1.1-1.2 x 10^6 crystals/mL of seed) that did not agree with the experimental data.

Table 7.10. Average crystal size growth for 1.35 SSC (70ºC) refinery first boiling sugar solution grown at 70ºC in an unstirred batch reactor

Time (minutes)	0.5	1	2	3	4	5	6	7	9	11
Average crystal size (µm)	26	27	33	43	53	61	69	67	76	72
Standard deviation of average crystal size (µm)	11	13	14	19	26	29	30	33	38	40

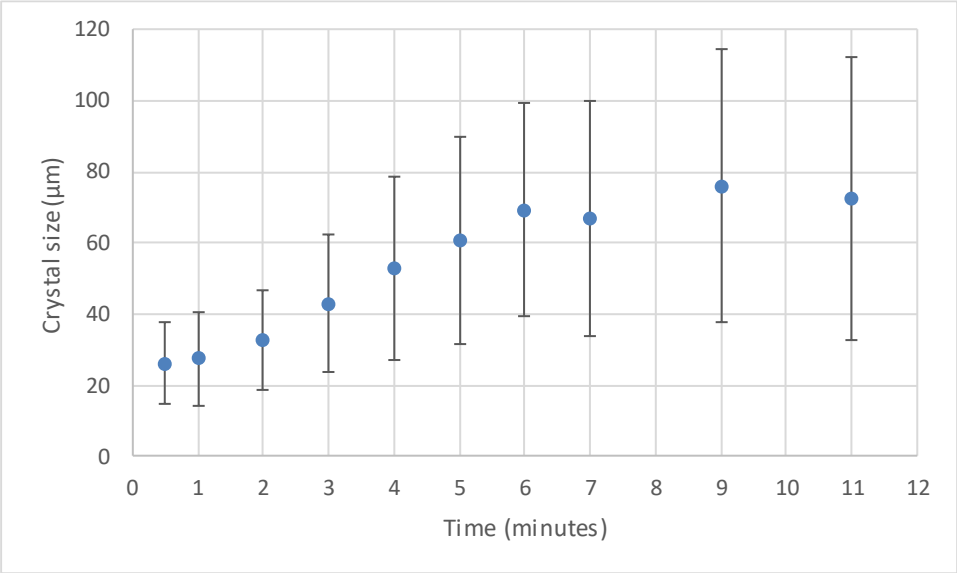

Figure 7.8. Average crystal size growth for 1.35 SSC (70ºC) first refinery sugar solution grown at 70ºC in an unstirred batch reactor

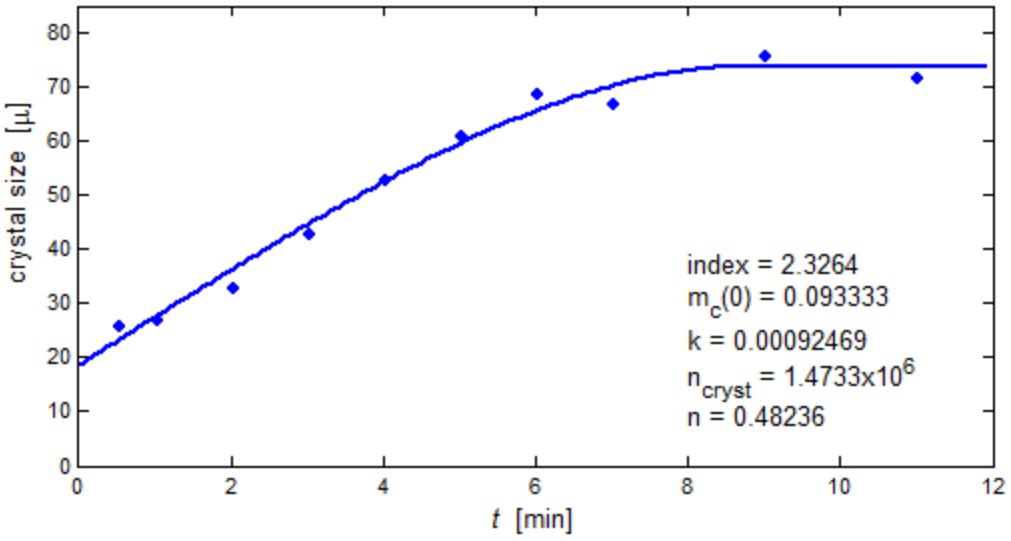

Figure 7.9. Results of the nth-order kinetics modelling

7.2.6. Effect of impurities

Table 7.11. and Figures 7.10., 7.11. and 7.12. show the results of the secondary nucleation tests using 1.35 SSC solutions (70ºC) of different purities viz. refinery first boiling sugar solution (99.9% purity), raw sugar solution (99.8% purity) and a technical third refinery runoff solution (97.5% purity, prepared by dissolving the appropriate amount of factory 4th sugar into factory 4th runoff). The procedure for the insonation was the same for the other secondary nucleation tests described in this section. Thieme's solubility data for the different purities was used (Hugot, 1986). For the refinery first boiling sugar solution tests, five runs were performed. For both the raw sugar and third runoff tests, triplicate runs were performed.

It was observed that the time to create the primary nuclei induced by sound waves varied substantially for the different solutions. This ranged from five minutes for the refinery first boiling sugar solution, to ten minutes for the raw sugar solution and about 16 minutes for the technical third runoff solution. The point of primary nucleation was determined visually with crystals observable in the flow through cell. Due to the darker nature of the raw sugar and technical refinery third run-off solutions, the point of primary

nucleation was more difficult to determine visually than the previous tests performed with refinery first boiling solutions.

Table 7.11. The effect of impurities on the quality of crystal seed obtained from insonation induced secondary nucleation

1st refinery boiling sugar (99.9% purity)				
Sample time after secondary nucleation	5 min	10 min	20 min	30 min
Average crystal number densities (number of crystals/mL seed)	1.7 x10^6	1.8 x10^6	2.0 x10^6	2.4 x10^6
Standard deviation crystal no. densities	1.8 x10^5	2.5 x10^5	3.5 x10^5	4.0 x10^5
Average crystal sizes (µm)	58	57	54	54
Standard deviation crystal sizes	4	1	2	3
Average crystal size CV (%)	40	39	41	41
Standard deviation CV	2	2	1	2
VHP sugar (99.8% purity)				
Sample time after secondary nucleation	5 min	10 min	20 min	30 min
Average crystal number densities (number of crystals/mL seed)	8.1 x10^5	8.7 x10^5	9.8 x10^5	1.4 x10^6
Standard deviation crystal no. densities	2.0 x10^5	2.5 x10^5	3.0 x10^5	2.8 x10^5
Average crystal sizes (µm)	65	63	61	59
Standard deviation crystal sizes	4	1	3	2
Average crystal size CV (%)	37	34	37	37
Standard deviation CV	2	1	1	3
Refinery 3rd molasses (97.5% purity)				
Sample time after secondary nucleation	5 min	10 min	20 min	30 min
Average crystal number densities (number of crystals/mL seed)	3.9 x10^5	6.6 x10^5	1.1 x10^6	1.0 x10^6
Standard deviation crystal no. densities	1.9 x10^5	3.9 x10^5	3.7 x10^5	3.1 x10^5
Average crystal sizes (µm)	52	49	49	49
Standard deviation crystal sizes	1	1	3	2
Average crystal size CV (%)	32	28	30	33
Standard deviation CV	2	1	1	3

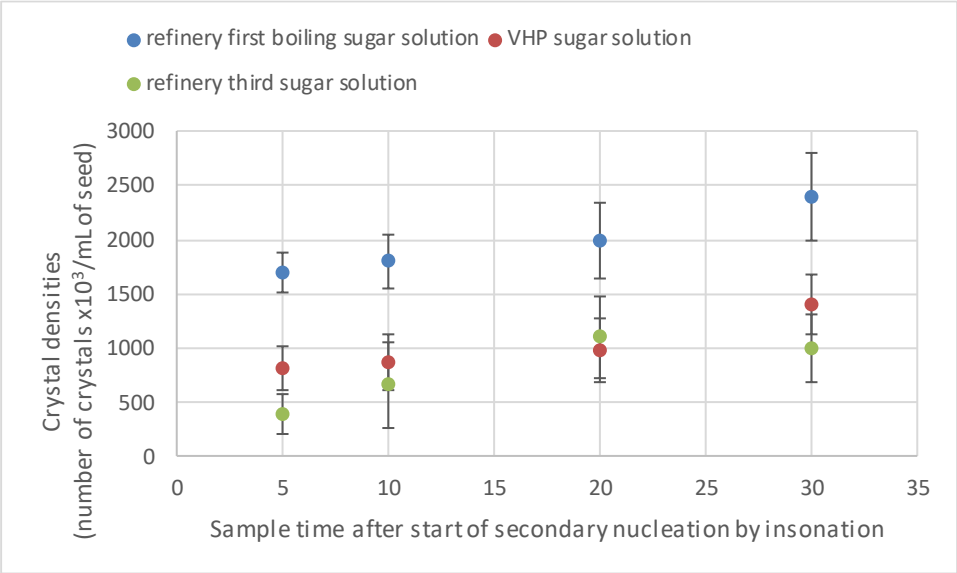

Figure 7.10. Crystal seed densities obtained from insonation induced secondary nucleation in different feed streams

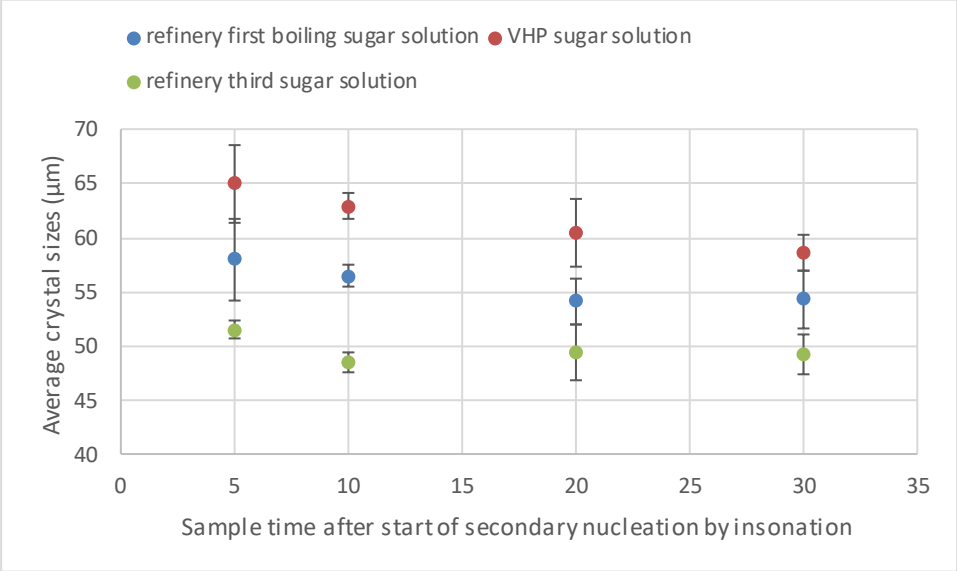

Figure 7.11. Average crystal sizes obtained from insonation induced secondary nucleation in different feed streams

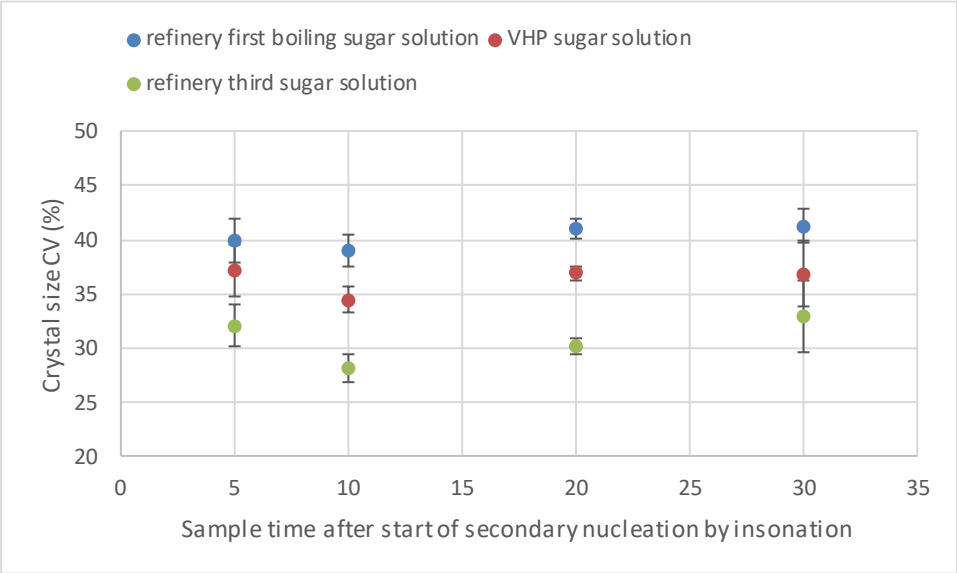

Figure 7.12. Crystal size CVs obtained from insonation induced secondary nucleation in different feed streams

From Figure 7.10. it can be seen that the crystal number densities achieved with each of the solutions meet the requirements of a continuous full seeding process. The crystal number densities obtained were the highest with the refinery first boiling sugar solution and lowest with the technical refinery third runoff solution; this corresponds to the purity of the solutions – the higher the purity of the solution at a specific supersaturation, the higher the crystal number density achieved.

The seed crystals nucleated were allowed to grow at 70^{o}C for a period of five minutes before a sample was taken for image analysis. Figure 7.11. shows that the crystals in each of the tests can be considered to have reached a stable size (specified to be greater than about 50 µm) after the five minutes of growth at the constant temperature. For the similar purity refinery first boiling sugar and raw sugar solutions it can be observed that the substantially lower crystal number density achieved with the raw sugar crystals had resulted in a larger crystal size, as can be expected. With the lowest purity technical

refinery third runoff, the lowest crystal sizes were obtained despite the lowest crystal number densities – this is presumably directly influenced by the purity of the solution.

The CV of the size of the crystals obtained appears in Figure 7.12. and follows the purity profile of the feedstocks i.e. a drop in the purity of the feedstock is accompanied by a drop in the CV of the crystals achieved. All of the CVs obtained are substantially lower than the 50% CV target specified.

7.3. Comparison of the seed crystals from sound wave induced nucleation to ball-milled slurry and final refined sugar product

Ideally the seed crystals, from sound wave induced nucleation, should be compared to conditioned and unconditioned crystals from a refinery pan that is of a similar density and size; the crystal size distribution or CV can be compared. This was not possible as the refinery pans boil with very high supersaturations and when samples are taken out, there is immediate false nucleation due to the change in temperature of the pan to the ambient temperature. The relevant crystal number density, size and CV information was also not found in any literature. In order for some comparison to be done, Figures 7.13. and 7.14. are given. These are photomicrographs of a typical ball-milled slurry (added as the start seed crystals for some refinery pans) and the seed crystals from sound wave induced nucleation, respectively. The ball-milled slurry was found to have a CV of 72%, whilst the seed crystals from the sound wave induced nucleation was found to have a CV of 43%. Refined sugar (Figure 7.15.) produced from ball-milled slurry nuclei was found to have a CV of 75%, similar to the start material.

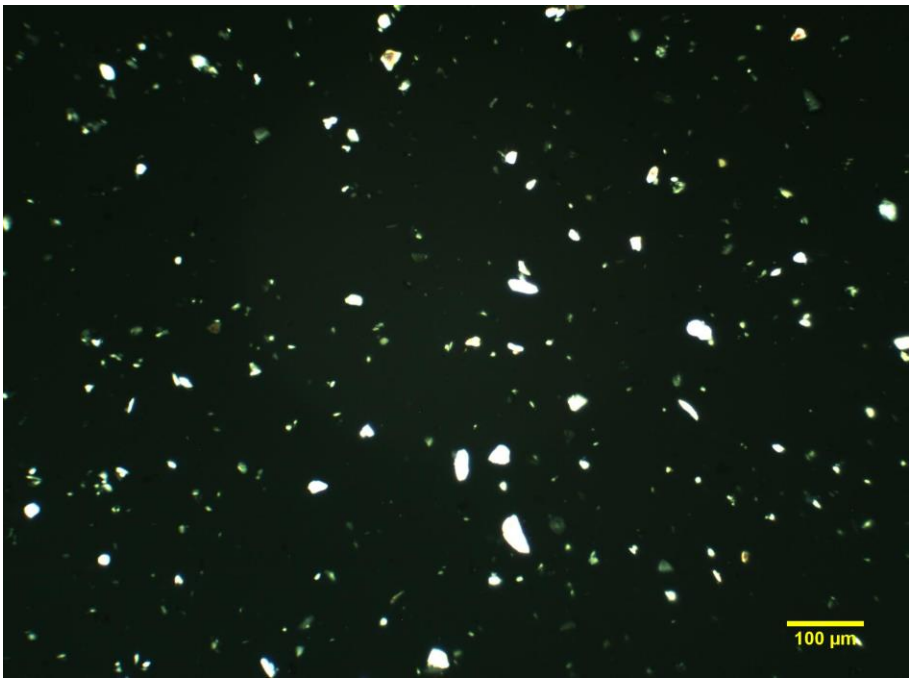

Figure 7.13. Photomicrograph of a typical ball-milled slurry used in some refinery pans for crystallisation nuclei (CV=72%)

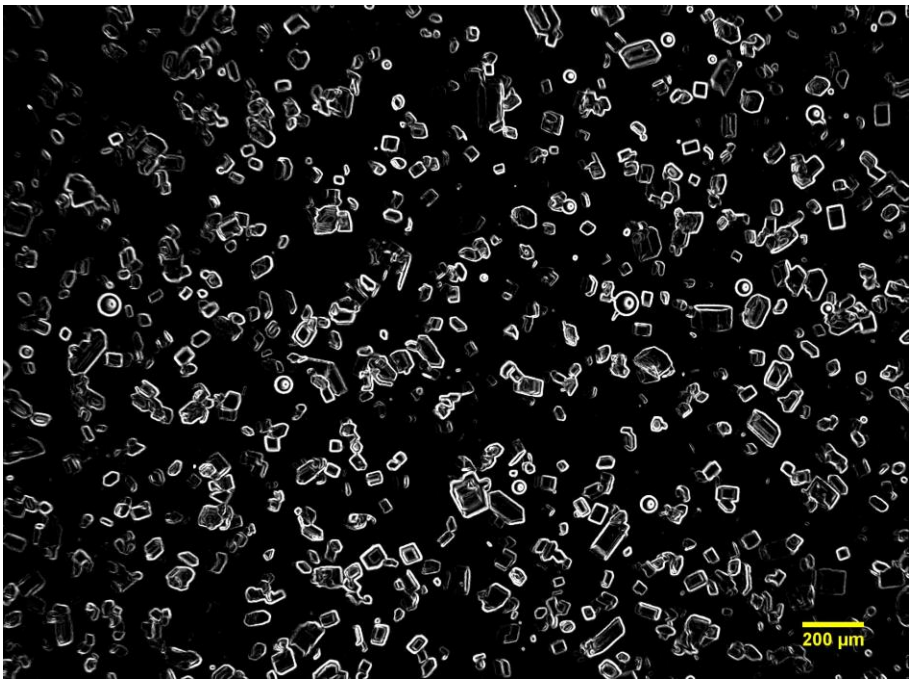

Figure 7.14. Photomicrograph of seed crystals produced from sound induced nucleation (CV = 43%)

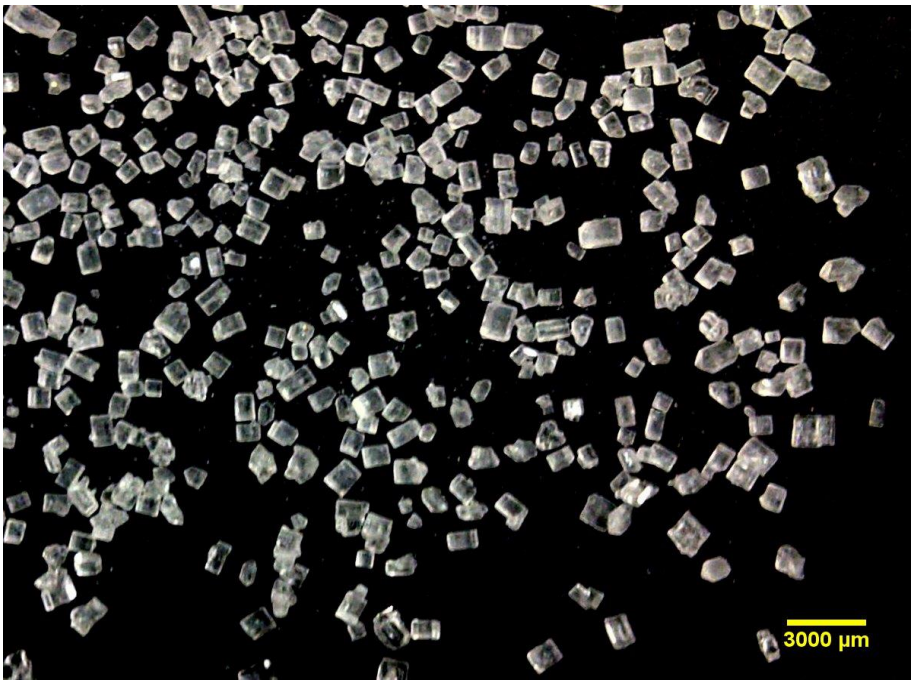

Figure 7.15. Photomicrograph of typical refined sugar product (CV = 75%) grown from ball-milled slurry nuclei.

Figures 7.16., 7.17., and 7.18. are Scanning Electron Microscope (SEM) images (done at the University of KwaZulu Natal) of ball-milled slurry crystals, affinated refined sugar crystal and an affinated seed crystal from sound wave induced nucleation, respectively. The samples were affinated at the SMRI by removing the molasses layer around the crystals, using a standard technique developed by the SMRI using firstly a saturated sugar solution wash, followed by alcohol rinsing.

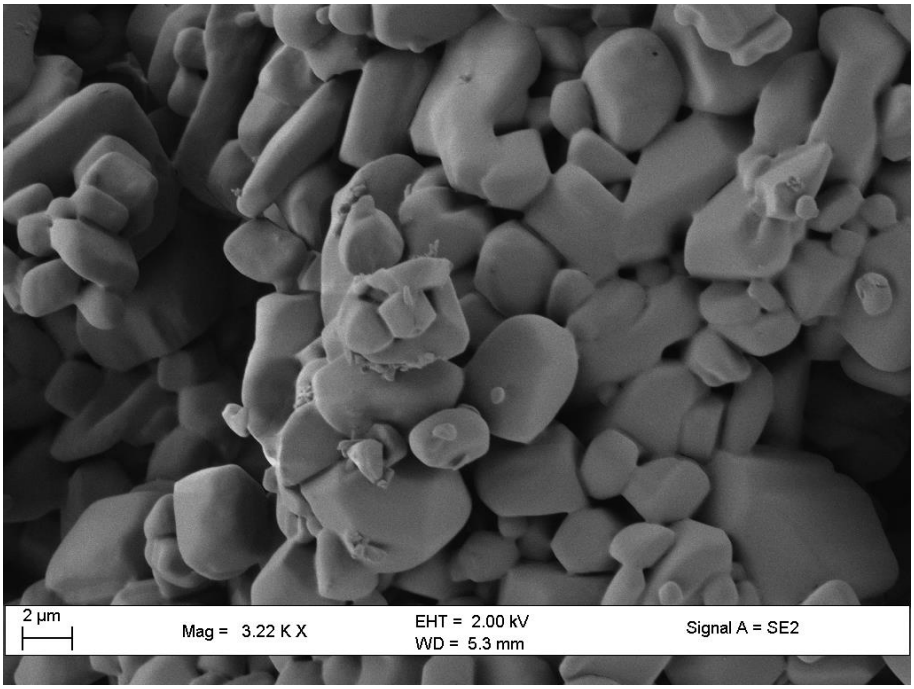

Figure 7.16. SEM image of a ball-milled slurry

Figure 7.16. shows very smooth surfaces on the surface of the ball-milled slurry nuclei for crystal growth.

Figure 7.17. shows the SEM image of a refined sugar crystal that was grown from a ball-milled slurry seeded pan. The crystal surface is also smooth but with evidence of crystal growth centres.

Figure 7.18. which is an SEM image of an affinated seed crystal from sound wave induced nucleation, shows many smooth surfaces and sites available for crystal growth.

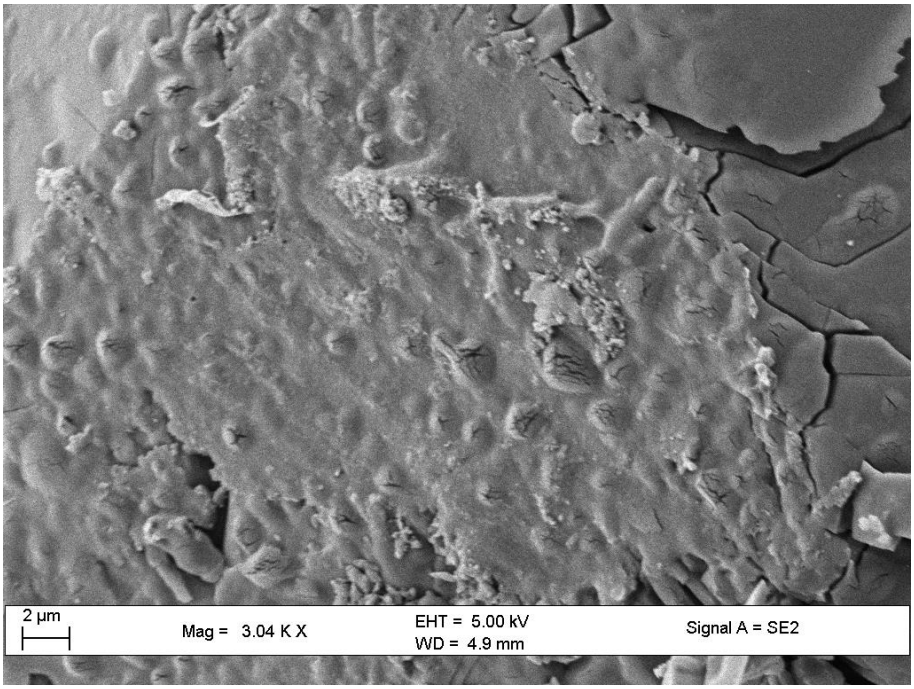

Figure 7.17. SEM image of an affinated refined sugar crystal

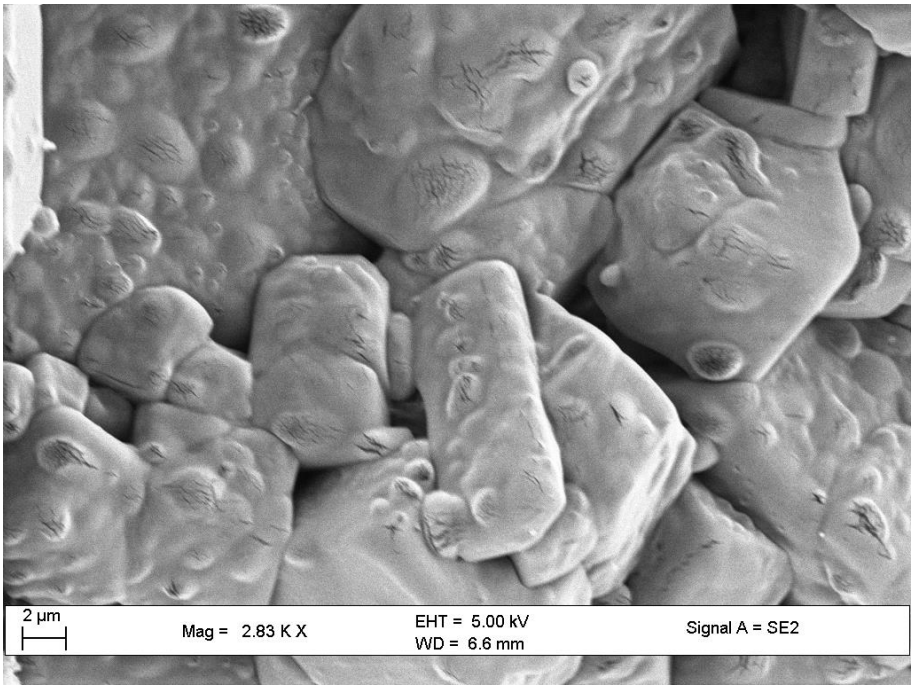

Figure 7.18. SEM image of an affinated seed crystal from sound wave induced nucleation

CHAPTER 8 – CONCLUSIONS AND RECOMMENDATIONS

The objective of this study was to determine if high frequency sound could be used to induce nucleation in supersaturated solutions for the production of sugar refinery seed crystals. It was determined by means of calculations, and communications with experienced sugar refinery personnel, that the seed to be produced will have to meet the following characteristics: (1) Crystal number density > $7x10^4$ crystals/mL of seed, (2) crystal size > 50 µm and (3) size coefficient of variance (CV) < 50%. For industrial usage, the seeding technique would also have to be a robust process that produces repeatable results. With this in mind, the industry committee further stipulated that the new seeding technique can be deemed repeatable if the seed characteristics from the continuous process show less than 10% relative standard deviation (RSD) from the desired values for crystal sizes and CV, and less than 20% deviation for crystal number density.

The study describes work led by the author of this dissertation, that was undertaken as a research project at the Sugar Milling Research Institute NPC (SMRI). Tongaat Hulett Sugar (THS) collaborated in this project as a technology and commercial partner. The work reported here was performed on a bench-top scale but at throughputs capable of producing sufficient amounts of crystals to fully seed factory-scale production pans. Using this calculated range of operating conditions as a specification, an extensive benchtop scale laboratory investigation identified the equipment and operating conditions that are capable of producing acceptable seed crystals in a continuous process. As part of the investigation it was been necessary to develop appropriate techniques for measuring crystal sizes, size distributions and number densities.

The results of the laboratory tests have shown that acceptable seed crystal sizes, with an acceptable crystal size distribution, can be achieved by growth at constant temperature as the nuclei exhaust the available supersaturation of the mother liquor from which they have been nucleated. The crystal number densities achieved are high enough to allow a

range of acceptable densities to be achieved by the addition of extra mother liquor after nucleation if desired. It was concluded that the process is technically feasible for refinery seed production.

It was also found that the desired specifications could only be achieved with a high intensity sonotrode sound application system (power intensity of about 130 W/cm^2) and not with lower intensities systems viz. flange-type transducer and clamp-on flow through system with power intensities of 3 and 6 W/cm^2, respectively.

The bench-top tests performed showed that it was possible to induce primary nucleation in sugar solutions with high frequency sound waves, however, these were at very high supersaturations which was deemed to be unsuitable for an industrial process. When the sugar solutions were stored for extended periods during test runs, false nucleation occurred before insonation, proving that the conditions were not robust enough for industrial usage.

A series of tests were performed with primary nucleation induced by the high frequency sound waves and then crystal formation maintained by secondary nucleation at different operating conditions. Refinery first boiling sugar solutions with supersaturation coefficients (SSCs) of 1.20, 1.30, 1.35 and 1.40 (at 70^{o}C) all resulted in crystal seed formation meeting the required specifications. The results for a series of repeatability tests performed on a 1.35 SSC (70^{o}C) refinery first boiling sugar solution is given in Table 8.1. For these tests, the sound wave peak-to-peak amplitude was set at 60 µm and the pulse setting was 35% of a second.

For the secondary nucleation tests, the effects of SSC, amplitude, pressure, flowrates and purity of feedstock were investigated. These tests can be summarised as follows:

- When the SSC was increased, the crystal number density, size and CV all increased.

- When the peak-to-peak amplitude was increased, there was an increase in crystal number density up to 70 μm, but with further increases the crystal number density decreased.
- When the pressure was increased, the crystal number density decreased, the crystal size increased and the CV remained approximately the same.
- When the flow was increased, the crystal number density decreased.
- When the purity of the feedstock was increased, the crystal number density, size and CV all increased.

Table 8.1. Results of repeatability tests for secondary nucleation on refinery first boiling sugar solution (1.35 SSC at 70°C)

Description	Value	Relative Standard Deviation
Achieved crystal no. density	2.4×10^6 ($\pm 4 \times 10^5$) crystals/mL seed	17%
Specification for crystal no. density	$> 7 \times 10^4$ crystals/mL seed	< 20%
Achieved average crystal size	54 μm	5%
Specification for average crystal size	> 50 μm	< 10%
Achieved crystal size coefficient of variance (CV)	41%	5%
Specification for average size CV	< 50%	<10%

Various classical crystal growth theories were modelled on Matlab®. The predicted results for the theory of empirical n^{th}-order kinetics with concentration-based driving force, compared well with the experimental results for growth of crystals obtained from sound induced secondary nucleation.

It is recommended to those continuing studies in this area, to perform longer test runs than reported here. The crystal number density appeared to still be increasing at the end of the test runs; it would be ideal to establish when this increase plateaus. The increasing densities is not seen as a showstopper to an industrial unit though, as the crystal number densities can be diluted with sugar solutions to give a consistent crystal content. The length of the test runs was limited mostly due to the capacity of auxiliary equipment. Another limitation was the degradation of prepared solutions when stored at high temperatures in holding water baths. This can be avoided by continuous evaporative concentration of sugar solutions to the desired SSCs.

The sonotrode system used in the tests reported had a fixed frequency of 21 kHz. It may be possible to use lower frequency systems to achieve similar results with lower SSCs (as was reported by Tai-quin, 1993).

REFERENCES

Allen AJ, Wood RM and McDonald MP (1974). Molecular association in the sucrose-water system. *Sugar Technol Reviews* Vol. 2: 165-180.

Amara N, Ratsimba B, Wilhem A and Delmas H (2001). Crystallization of potash alum: effect of power ultrasound. *Ultrasonics Sonochemistry* 8: 265-270.

Anon (1985). Slurry Preparation Apparatus. *SASTA Laboratory Manual* 3rd Ed 5.21: 160-162.

Anon (2011). Pan Boiling. *Sugar Milling Research Institute, 10 week course in Sugar Engineering*: p. 7.

Anon (2012). Image J®: Image Processing and Analysis in Java. http://rsbweb.nih.gov/ij/index.html [accessed January 2012].

Archibald RD and Smith IA (1975). The effect of low purities at Darnall on boiling house capacity. *Proc S Afr Sug Technol Assoc* 49: 63-73.

Austmeyer KE and Schliephake D (1983). Solution flow and exchange and heat transfer in a heating tube of an evaporation-crystalliser, *Int. Sug. Journal*, Vol. 85, No. 1019: 328-333.

Bachan L and Sanders RR (1987). Evaluation of a refinery pan stirrer. *Proc. S Afr Sug Technol Assoc* 61: 65-69.

Batterham RJ, Frew JA and Wright PG (1973). The use of boiling point rise for the control of pans. *Proc Queensland Soc Sug Cane Technol* 40: 187-192.

Bueche FJ (1986). Introduction to physics for scientists and engineers. McGraw-Hill Publishers, Singapore: 550-597.

Broadfoot R (2005). Design and operation criteria for maximizing the benefit of continuous vacuum pans. *Proc Int Soc Sug Cane Technol* 25: 31-39.

Broadfoot R and Hutchinson RT (1980). Development of a Continuous Seed Crystal Preparation Technique, *Proc. Aust. Soc. Sugar Cane Technol*.: 211-219.

Broadfoot R and Petersen G (2005). Improving the quality of C-sugar magma for use as seed crystal material, *Proc. Int. Soc. Sugar Cane Technol*., 25th Congress: 63 - 72.

Broadfoot R and Steindl RJ (1987). A seed crystal initiation pan, *Proc. Aust. Soc. Sugar Cane Technol* 9.: 235-244.

Broadfoot R and Wright PG (1972). Nucleation Studies. *Proc Queensland Soc Sug Cane Technol* 39: 353-362.

Broadfoot R and Wright PG (1992). Continuous Seed Preparation. *Proc. Int. Soc. Sugar Cane Technol*. *Symposium*, 11 pp.

Bubnik Z and Kadlec P (1992). Sucrose shape factors. *Zuckerind*. 117 No. 5: 345-350.

Culp EJ (1981). The magic of small numbers – molecules of water per molecule of sucrose. *Sug J*, September 1981: 7-10.

Faria N, Pons MN, Feyo de Azavedo S, Rocha F and Vivier H (2003). Quantification of the morphology of sucrose crystals by image analysis. *Powder Technol* 133: 55-67.

Fogler HS (2006). *Elements of Chemical Reaction Engineering*. Prentice Hall, 4th Edition, New Jersey, USA: p. 179.

Hugot E (1986). Handbook of Cane Sugar Engineering – 3rd edition. Elsevier, New York.

Gao DW, Chen SG, Min YG and Li GJ (1992). A new nucleation method: combination of organic solvent and ultrasonic wave (OSUW). *Proc Int Soc Sugar Cane Technol* 21: 853-864.

Grut EW (1937). *Zuckerindustrie Tschechosi Rep* 61: p. 356.

Harvey EN (1939). Sololuminescence and sonic chemiluminescence. *Journal American Chem Soc*, 61 (9): 2392-2398.

Hedrick WR, Hykes DL and Starchman DE (1995). Ultrasound Physics and Instrumentation – 3rd edition. Mosby, Missouri: 1-30.

Horiba Scientific (2012). A guidebook to particle size analysis. http://www.horiba.com/fileadmin/uploads/Scientific/Documents/PSA/PSA_Guidebook.pdf [accessed March 2012].

Hugot E (1986). Handbook of Cane Sugar Engineering – 3rd edition. Elsevier, New York: p. 628.

James GP and Maslen G (1964). Seeding Low Grade Massecuites – True or False, *Proc. Qld. Soc. Sugar Cane Technol*. 31: 297-299.

Jensen ED (1967). True Seeding – Let's be Critical!, *Proc. Qld. Soc. Sugar Cane Technol.* 34: 61-67.

Lichtenhaler FW, Immel S and Kreis U (1991). Carbohydrates as organic raw materials. Wiley VCH, Welheim: 1-32.

Lionnet GRE (1998)[a]. Impurity transfer rates during the crystallisation of sucrose. *Proc S Afr Technol Assoc* 72: 261-268.

Lionnet GRE (1998)[b]. The incorporation of impurities into sucrose crystals during the crystallisation process. PhD Thesis, University of Natal, Durban, South Africa: 33-35.

Lionnet GRE (1999). A Continuous vacuum pan for refinery massecuites. *Sugar Milling Research Institute Technical Report* No. 1823.

Love DJ (2002). Dynamic Modelling and Optimal Control of Sugar Crystallisation in a Multi-compartment Continuous Vacuum Pan. *PhD thesis*, University of KwaZulu Natal, South Africa.

Love DJ, Peacock SD and Schumann GT (2004). Quantification of crystal conglomerates using image analysis. *Proc S Afr Sug Technol Assoc* 78: 531-542.

Love DJ, Rahiman SN and Madho S (2016). The continuous production of seed crystals using sound induced nucleation. To be published in *International Society of Sugar Cane Technologists 2016 proceedings*.

Madho S (2016). Sugar refining – one week course presentation. *Sugar Milling Research Institute*.

Neppiras EA (1984). Acoustic cavitation: an introduction. *Ultrasonics*, 22 (1): 25-28.

Mason TJ (1990). Sonochemistry: The uses of ultrasound in chemistry. Royal Soc of Chem, Cambridge: 2-3.

Mason TJ and Lorimer JP (1988). Sonochemistry: Theory, applications and uses of ultrasound in chemistry. Ellis Horwood Publishers Ltd.

Mason WP (1976). Sonics and ultrasonics: early history and applications. *IEEE Trans Sonics and Ultrasonics*, 23(4): 224-232.

Mathlouthi M (1981). X-ray diffraction study of the molecular association in aqueous solution of d-fructose, d-glucose and sucrose. *Carbohydrate Res* 91: 113-123.

Maurandi V, Mantovani G and Vaccari G (1988). Kinetic studies on low grade boiling. *Sugar Technol Reviews* Volume 14: 29-118.

McCausland LJ, Cains PW and Martin PD (2001). Use the power of sonocrystallisation for improved properties. *Chem Eng Prog*, July: 56-61.

McCausland LJ and Cains PW (2003). Ultrasound to make crystals. *Chemistry and Industry*, 5 May 2003: 15-17.

Miller KF and Broadfoot R (1997). Crystal growth rates in high grade massecuite boilings. *Proc Aust Soc Sug Cane Technol*: 441-447.

Murphy A, Punter GA and Thompson PD (1991). Enhancements to a three boiling scheme. *Int. Sug. Journal* 93: 79-81, 86, 95-96, 97-98.

Myerson AS (2002). Handbook of Industrial Crystallization, 2nd edition. Butterworth Heinemann Publishers, Boston: 33-65.

Payne JH (1984). Correspondence, *Int. Sug. Journal* 86 (1023): p. 83.

Peacock SD (1995). Selected physical properties of sugar factory process streams. *Sugar Milling Research Institute Technical Report* No. 1714.

Perry RH (1999). Perry's Chemical Engineers' Handbook. McGraw-Hill, USA: 18-54.

Pillay JV (1994). Essential sugar technology. *Sugar Milling Research Institute*.

Price CJ (1997). Ultrasound – the key to better crystals for the pharmaceutical industry. *Pharm Technol Europe*, 9 (10): 78.

Pugin B (1987). Quantitative characterization of ultrasound reactors for heterogeneous sonochemistry. *Ultrasonics*, 25 (1): 49-55.

Rahiman SN, Madho S and Davis SB (2012). Assessing the quality of ball-milled slurries. *Proc S Afr Technol Assoc* 85: 312-328.

Randolph AD and Ziebold SA (1974). Continuous sucrose nucleation, *Int. Sug. Journal* 76: 8-12, 35-38, 73-76.

Rein PW (2007). Cane Sugar Engineering. Bartens, Berlin.

Sugartech (2012). Density of sugar factory products.
http://www.sugartech.co.za/density/index.php [accessed March 2012].

Tai-quin Q (1993). Nucleation of sucrose solution by sound field. *Int Sugar J* 95 (1140): 513-519.

Taiqui Q, Ximei Z and Yuehua L (1994). The treatment of saturated sugar solution with a sonic field. *Int Sugar J* 96 (1152): 523-526.

Trottier R, Dhodapkar S and Wood S (2010). Particle sizing across the CPI: This survey of modern measurement technologies demonstrates how selection criteria vary by application. *Chemical Engineering* 4: 62-63.

Rahiman SN, Muir BM and Madho S (2010). Finalisation of the Tachy-X 1L batch work. *Sugar Milling Research Institute Technical Report* No. 2102 (RC).

Richards WT and Loomis AL (1927). The chemical effects of high frequency waves I – a preliminary survey. *Journal of the American Chemical Society*, 49 (12): 3086-3100.

Ruytings D (2005). Equipment and factory experiences with seed magma production by cooling crystallisation, *Int. Sug. Journal*, Vol. 107 (1284): 666-677.

Schwikkard GW (2001). An investigation of advanced oxidation processes in water treatment. *PhD thesis*. University of KwaZulu Natal, South Africa.

Starzak M (2016). Modelling of batch crystallization with programmed temperature. Unpublished.

Suslick KS (1989). The chemical effects of ultrasound. *Scientific American*, February 1989: 80-86.

Suslick KS (1990). Sonochemistry. *Science*, 247: 1439-1445.

Tinke AP, Vanhoutte K, Vanhoutte F, De Smet M and De Winter H (2005). Laser diffractometry and image analysis as a supportive analytical tool in the pharmaceutical development of immediate release direct compression formulations. *Int Journal Pharm* 4: p. 88.

van der Poel PW, de Schutter MAM, Bleyenberg CC and van Heeschvelde PMT (1985). A new approach to full seeding. *La Sucrerie Belge* 103: 15-24.

van der Poel PW, Schiweck H and Schwartz T (1998). Sugar Technology. Beet and Cane Sugar manufacture. Verlag Dr A Bartens, Berlin.

van Hook A (1959) in: Honig P. Principles of Sugar Technology, Volume 2. Elsevier, Amsterdam: p. 176.

van Hook A (1964). Nucleation in supersaturated sucrose solutions. In: Honig P. Principles of Sugar Technology, Vol II, Elsevier, Amsterdam, Chapter 3: 113 - 148.

Vavrinecz G (1960). *Cukoripar*, 13: 182-183.

Wei NX (2008). Bridging the gap. *The Chemical Engineer* No 800 (February): 36-38.

Wilson BP (1997). Ultrasound, cavitation and cleaning. *PhD thesis*. University of Wales, Swansea.

Wright PG (1983). Pan and pan stage control. *Sug Technol Reviews* 10: 39-96.

APPENDIX A – CALCULATION OF SUITABLE OPERATING CONDITIONS FOR FULL CONTINUOUS SEED PRODUCTION SYSTEM

Supersaturation in aqueous sucrose solutions

The solubility of sucrose in water is well described by the equation of Charles (1960):

$$C_s = 64.397 + 0.07251 \cdot t + 0.0020569 \cdot t^2 - 9.035 \cdot 10^{-6} \cdot t^3$$

Where: C_s is the sucrose concentration at saturation as a percent by mass

t is the temperature in ºC

The mass ratio of sucrose to water (*S/W*) can be calculated from the concentration as a mass percentage (*C*) as follows:

$$S/W = \frac{C}{100 - C}$$

The supersaturation coefficient (SSC) is defined as

$$SSC = \frac{S/W}{(S/W)_s}$$

where: *S/W* is the sucrose to water ratio of a given solution

$(S/W)_s$ is the sucrose to water ratio of a saturated solution at the same temperature

Crystal content of aqueous sucrose solutions at equilibrium

If the total sucrose concentration of a sample is known, and it is assumed that if there is any crystal present it is in equilibrium with its surrounding mother liquor, the crystal content of the sample can be calculated.

Assume that:

C is the sucrose concentration in the sample as a percent by mass

From the temperature of the sample and the solubility relationship, the concentration of a saturated mother liquor can be calculated, C_s %. Clearly if C is less than C_s, the solution is undersaturated and there can be no crystal present at equilibrium.

However, if C is greater than C_s, the solution would be super-saturated and crystal would need to be deposited to bring the solution to equilibrium. Performing calculations on the basis of one mass unit of water:

Total mass of sucrose = $C/(100 - C)$

Mass of sucrose dissolved in water = $C_s/(100 - C_s)$

(Because the mother liquor is assumed to be at saturation i.e. in equilibrium with the crystal)

Thus mass of sucrose present as crystal = $C/(100 - C) - C_s/(100 - C_s)$

Thus mass percent of crystal present, or crystal content is given by:

$CC = (C/(100 - C) - C_s/(100 - C_s)) / (C/(100 - C) + 1) \times 100$

Where: CC is the crystal content in the sample as a percent by mass

A convenient approach to produce a graph of crystal content against sucrose content with contours of constant temperature (as shown in Figure 2) is to use the solver function within a spreadsheet to determine the value of C which gives the required crystal content (using the appropriate value for C_s at the temperature of interest).

Number density of crystals in a sample of known crystal content

To calculate a reasonable approximation of the number density of crystals in a sample of known crystal content, the following are assumed:

The crystals are all cubes of a uniform size described by the length of a side, d m.

Density of the massecuite = 1400 kg/m^3

Density of crystals = 1580 kg/m^3

The mass of an individual crystal is then given by: $1580 \cdot d^3$ kg

The mass of crystals in a 1 kg sample is: $CC/100$ kg

(where *CC* is the crystal content as a mass percentage)

The number of crystals in a 1 kg sample is thus: $(CC/100) / (1580 \cdot d^3)$

The volumetric density of crystals is thus:
$(CC/100) / (1580 \cdot d^3) \cdot 1400$ crystals per m^3

Or more conveniently:
$(CC/100) / (1580 \cdot d^3) \cdot 1400 / 10^6$ crystals per mL

APPENDIX B – THE DEVELOPMENT OF AN IMAGE ANALYSIS METHOD FOR THE ASSESSMENT OF CRYSTAL QUALITY

Work done by Love *et al*. (2004) encouraged the use of the Image J® software package to automatically size and count crystals. The software is available in the public domain (http://rsbweb.nih.gov/ij/index.html [accessed 2012]) at no charge.

A challenge using the software was to create a distinct contrast between the crystals and their background. This was overcome by means of polarisation and light manipulation (well known microscope techniques using standard equipment). For the assessment of the proposed method, three images of the slurry (with crystals dispersed in saturated glycerol) were captured and collectively measured using Image J®. The mean (average size), median (middle value of a distribution) and CV (ratio of standard deviation to mean size expressed as a percentage) were then determined. A method of estimating the crystal number density was also investigated using the settled volume of slurry crystals and the size distribution of the sample. This developed technique of estimating the crystal number density is more time efficient than the initial method, and greatly reduced the effect of glycerol, and heat from the microscope light.

The development of this proposed method is described fully below and includes the development of the sampling technique, crystal number density measurement and use of the image analysis tool. The repeatability of the sampling technique and the analyses are also reported.

Sub-sampling

The factory slurries were sampled as follows:

- The entire amount of slurry from a ball-mill was shaken until all the settled crystals were visually suspended.

- One litre of the slurry was then emptied into a separating funnel by intermittently shaking and decanting small amounts of the slurry.
- The sample from the funnel was shaken 20 times and inverted ten times before 10 g of sample was discharged into a sample bottle. This was repeated until a total sample mass of 30 g was obtained.

Microscope and Image J® analysis

The sub-sample was analysed as follows:

- The sub-sample was shaken manually for one minute. Thereafter 0.5 mL of the sample was withdrawn using a medicine dropper and emptied into a smaller vial.
- Approximately 6 mL of saturated glycerol was added to the slurry in the vial, followed by swirling of the mixture.
- A drop of the glycerol-slurry mixture was placed onto a large slide; thereafter an identical slide was placed on top of the sample to disperse the slurry.
- Once the slurry was dispersed, three photomicrographs were captured at three different points on the slide.
- Each picture was converted into a binary image (Image J® function that creates a white background and fills in solids in black) that was automatically analysed using Image J® to determine the Feret's diameter of all particles. The Feret's diameter, also referred to as the 'maximum calliper' by Image J®, is defined as the longest distance between parallel tangents to the projected area of the particle (Anon, 2012). The use of the maximum calliper replaces the manual measurement of the longest distance across the projected crystal area, as in the initial investigations.
- The raw data was processed in Microsoft Excel® to determine the mean, median and CV, defined as the ratio of standard deviation to mean.

Determining the minimum number crystal size measurements

Work carried out by Lionnet (1998)[b] on C-massecuites involved determining the minimum number of crystals to be sized, based on the standard deviation of the width and

length of the crystals. A similar method was employed to estimate the minimum number of crystals to be measured when assessing slurries. The length of the slurry crystals (assumed to be equal to the Feret's diameter) was measured for 20 crystals followed by increments of 20 until the standard deviation value became constant. Figure B1 illustrates the findings.

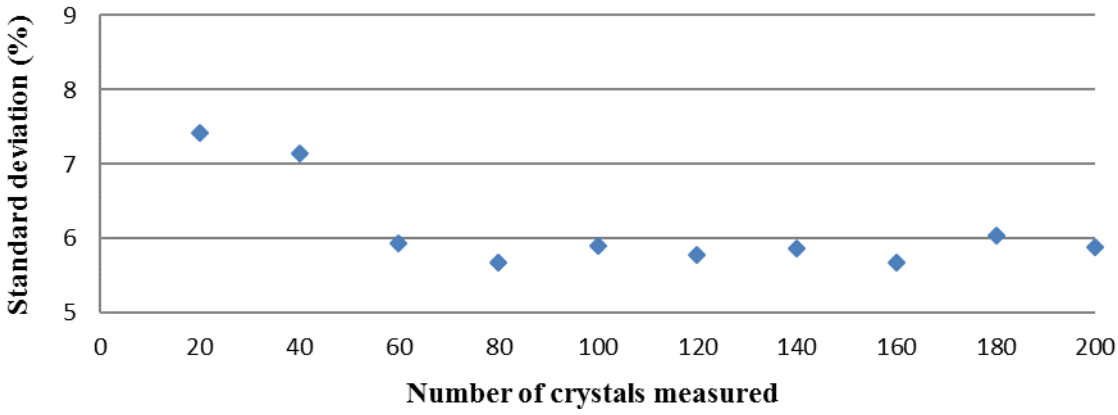

Figure B1. Standard deviations of slurry crystals as a function of sample size.

The standard deviations were determined using manual sizing of the crystals, and it is expected that an automatic sizing would not deviate substantially from the test performed. For the manual count, as can be seen in Figure B1, the standard deviation became constant after 60 crystals were counted and a sample size of at least 100 crystals was thought necessary for any slurry evaluations. For the Image J® analyses proposed, more than 1000 crystals are analysed for every image taken (usually three images per analysis).

Repeatability

Repeatability in sampling from the ball-mill contents and then the subsequent sampling from the sub-sample were tested as illustrated in Figure B2. The results of the measurements are shown in Table B1. Differences in means were tested using the Student's t-test, and differences in variances were tested using the F-test, both at a 95%

confidence interval, between samples 1a, 1b and 1c, and between 1a-c combined, and samples 2 and 3, with the results shown below. There were no significant differences in means between any pair of tests, apart from between 1abc and 2, and in some cases the differences in variances were significant at the 95% confidence level. However, as can be seen in Table B1, the actual differences were very small, and thus it was concluded that the sampling, sub-sampling and analysis procedures with Image J® are repeatable.

Having shown repeatability of the image software and sampling technique, evaluation of the various factory slurries involved only a single analysis.

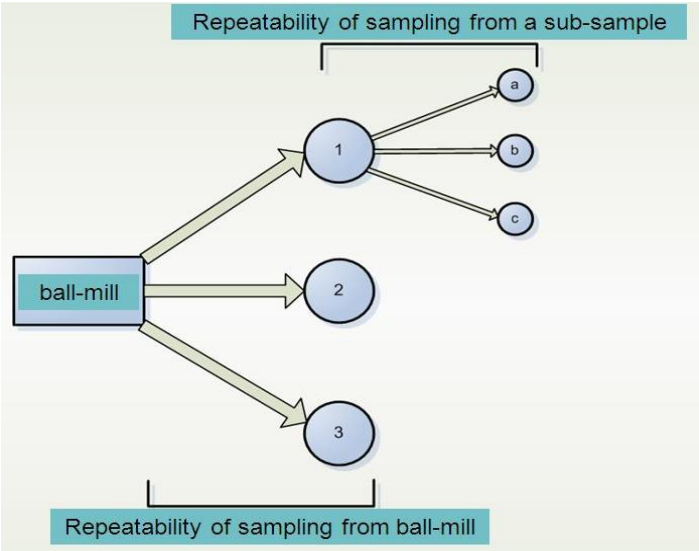

Figure B2. The method used to evaluate repeatability in sampling (analysis of 1-3), sub-sampling (analysis of a-c) and the use of the Image J® technique.

Table B1. Repeatability test results for slurry analyses - Image J® technique.

Slurry quality parameters	Sample 1			Sample 1abc combined	Sample 2	Sample 3
	a	b	c			
Mean (μm)	9.05	9.23	9.26	9.18	9.52	9.27
σ (standard deviation)	6.72	6.76	6.67	6.72	6.50	6.55
CV (%)	74.29	73.20	71.98	73.18	68.33	70.68

Settled volume of slurry

The settled volume (V_{ST}) of slurry crystals was obtained by pouring 500 mL of a well-mixed sample into a volumetric cylinder followed by reading off the settled volume of crystals after approximately six hours or once all crystals had settled.

Crystal number density

An estimate of the crystal number density may be obtained by utilising the CSD data and the settled volume of crystals. Image J® additionally provides the minimum Feret's diameter which is the shortest distance between parallel tangents across the particle projected area. It is assumed that the maximum and minimum Feret's diameters are the mean length and width of a crystal respectively (Faria *et al.*, 2003). Furthermore, from general microscope observations, it is assumed that the crystals are fairly flat; hence it will be assumed that the width of the crystal is equal to the height of the crystal. The volume of a single crystal may be estimated, as in the CSD analyses of C-massecuite by Equation B1.

$$V_C = L \times W^2 \qquad \text{…Equation B1}$$

where L = length of the crystals (μm)
W = width of the crystals (μm)
V_C = volume of a single crystal (μm^3).

Therefore the mean crystal volume, given the CSD data, may be determined by Equation B2.

$$V_m = \frac{\sum_{i=1}^{n} V_{Ci}}{n} \qquad \text{…Equation B2}$$

where V_m = the arithmetic mean volume (μm^3)

n = the number of crystals analysed.

The settled volume of slurry crystals (V_{ST}) comprised the volume of the crystals alone, and the organic solvent volume occupying the voids present between the settled crystals. The volume fraction of the abovementioned voids is critical in determining the crystal number density which will be observed later on; however, the void fraction is directly dependent on the bulk density of the slurry crystals. The bulk density was determined experimentally by measuring the settled volume of a known mass of slurry crystals in an organic solvent, as in the procedure which follows.

Approximately 250 g of slurry from each mill was centrifuged for 15 minutes at 1500 rpm, followed by decanting of the solvent. The paste-like crystals were dried at 105°C for approximately four hours. After one hour of drying, the slurry-cake was gently separated into individual smaller crystals using a pestle (referred to as 'conditioning'). When drying was complete, the crystals were further conditioned so that no agglomerates could be felt. A fixed mass of slurry (20 g) was deposited into a 250 mL volumetric cylinder that initially was filled to the 150 mL mark with saturated colourless methylated spirits, followed by additional methylated spirits to the 250 mL mark. The crystals were allowed to settle freely for 16 hours to obtain a settled volume of crystals. It is assumed that the density of the colourless methylated spirits is approximately the same as the density of the organic solvent used by the individual mills.

The bulk density (ρ_b) of the slurry crystals from the above experiments can be determined by simply dividing the known mass of crystals by the volume obtained after 16 hours of settling. According to Fogler (2006), the voidage percentage can be determined by Equation B3.

$$\phi = \left(1 - \frac{\rho_b}{\rho_c}\right) \times 100 \qquad \text{…Equation B3}$$

where ϕ = voidage (%)

ρ_b = bulk density of slurry crystals (g/cm^3)

ρ_c = sucrose crystal density = 1.5862 g/cm^3 (Sugartech, 2012).

The settled volume of crystals obtained from 500 mL of slurry can be used to determine the no-void volume. The number of crystals may be determined by Equation B4.

$$N_C = \frac{V_{ST} \times \phi}{V_m} \qquad \text{…Equation B4}$$

where N_C = total number of crystals

V_{ST} = settled volume crystals in 500 mL of slurry (μm^3).

The crystal number density (nuclei/mL slurry) of slurry can be determined using Equation B5.

$$\frac{N_C}{V_T} \qquad \text{…Equation B5}$$

where V_T (mL) is the total volume of slurry used to determine the settled volume of crystals (500 mL).

Duration of slurry assessment tests

Once the mill staff have become familiar with the methodology involved in assessing slurry quality as suggested, it can be estimated that the test duration will be as follows:

- Sampling and subsampling (25 minutes)
- Taking of photomicrographs (5 minutes)
- Image J® processing (10 minutes).

Thus, in about 40 minutes, a slurry quality can be assessed with regards to its CSD, mean size, CV and habit. For the habit (or shape) of the crystal, a simple classification system or comment can be used, e.g. Class 1 = regular, well-formed crystals, Class 2 = defaced crystals, and so forth.

In order to determine the crystal number density, a duration of five minutes is estimated for data processing once the settled volume is known (the settled volume determination is dependent on the crystal mean size and could span from three to six hours). However, it is envisaged that this test would not be done routinely.

Statistical analysis of repeatability tests

The results of the t-tests for samples 1a, b and c are shown in Table B2 and results of F-tests for samples 1a, b and c are shown in Table B3. The results of the t-tests for samples 1a, b and c combined, 2 and 3 are shown in Table B4 and results of F-tests for samples 1a, b and c combined, 2 and 3 are shown in Table B5.

Table B2. Results of t-test for samples 1a, b and c (ball-milled slurry analyses).

Comparison	**1a vs 1b**		**1a vs 1c**		**1b vs 1c**	
Sample	**1a**	**1b**	**1a**	**1c**	**1b**	**1c**
Mean	9.05	9.23	9.05	9.26	9.23	9.26
Variance	45.19	45.67	45.19	44.4	45.69	44.44
Observations	4066	4827	4066	3754	4827	3754
Df	8891		7818		8579	
Hypothesized mean	0		0		0	
t stat	**-1.29**		**-1.40**		**-0.18**	
P(T<=t) two-tail	0.20		0.16		0.85	
t Critical two-tail	1.96		1.96		1.96	

Table B3. Results of F-test for samples 1a, b and c (ball-milled slurry results).

Comparison	**1a vs 1b**		**1a vs 1c**		**1b vs 1c**	
Sample	**1a**	**1b**	**1a**	**1c**	**1b**	**1c**
Mean	9.05	9.23	9.05	9.26	9.23	9.26
Variance	45.19	45.67	45.19	44.4	45.69	44.44
Observations	4066	4827	4066	3754	4827	3754
Df	4065	4826	4065	3753	4826	3753
F	**1.01**		**1.02**		**1.03**	
P(F<=f) one-tail	0.36		0.30		0.19	
F Critical one-tail	1.05		1.05		1.05	

Table B4. Results of t-test for samples 1a, b and c combined, 2 and 3 (ball-milled slurry results).

Comparison	**1abc vs 2**		**1abc vs 3**		**2 vs 3**	
Sample	**1abc**	**2**	**1abc**	**3**	**2**	**3**
Mean	9.18	9.52	9.18	9.27	9.52	9.27
Variance	45.16	42.28	45.16	42.91	42.29	42.91
Observations	12647	3001	12647	4044	3001	4044
Df	15646		16689		7043	
Hypothesized mean	0		0		0	
t stat	**-2.46**		**-0.70**		**1.58**	
P(T<=t) two-tail	0.01		0.48		0.11	
t Critical two-tail	1.96		1.96		1.96	

Table B5. Results of F-test for samples 1a, b and c combined, 2 and 3 (ball-milled slurry results).

Comparison	**1abc vs 2**		**1abc vs 3**		**2 vs 3**	
Sample	**1abc**	**2**	**1abc**	**3**	**2**	**3**
Mean	9.18	9.52	9.18	9.27	9.52	9.27
Variance	45.16	42.28	45.16	42.91	42.29	42.91
Observations	12647	3001	12647	4044	3001	4044
Df	12646	3000	12646	4043	3000	4043
F	**1.07**		**1.05**		**1.01**	
P(F<=f) one-tail	0.01		0.02		0.34	
F Critical one-tail	1.06		1.04		1.06	

APPENDIX C – MATLAB® PROGRAM CODE FOR NTH-ORDER KINETICS MODELLING WITH CRYSTAL NUMBER DENSITY REGRESSION

```
%  Identification of the batch crystallisation model
%  for nth-order "Solid-on-Solid" kinetics

  clear all
  close all

  global V00 n_cryst N_cryst phiV phiA tC ms00 ms0 mw mc0 L0 Ac0 k n ...
       rho_s rho_c ms mc Brix Brix_s L0 L sigma Rc Ac ts L_median tf

%  Temperature, C
  tC = 70;
%  Solubility Brix at tC
  Brix_s = 64.447+(((-4.63e-8*tC-1.558e-6)*tC+1.6169e-3)*tC+0.08222)*tC;
%  Density of liquor at saturation, g/cm3
  rho_s = emmerich('sucrose', tC, Brix_s);
%  Total batch time [min]
  tf = 12;
%  Crystal size data [min, cm]
  ts = [0.5, 1, 2, 3, 4, 5, 6, 7, 9, 11];
  L_median =  [26, 27, 33, 43, 53, 61, 69, 67, 76, 72]*1e-4;
  L_mean = [28, 31, 36, 47, 58, 65, 73, 75, 84, 82]*1e-4;
%  Crystal density, g/cm3
  rho_c = 1.5862;
%  Crystal dimension ratios
  ab = 0.64/1.31;
  ac = 0.64;
%  Crystal shape factors (Bensouissi et al., Cryst. Eng. Comm., 2010, 12, 579–584)
%  Note:  not used in this calculation
  phiV = 1-ab/2.434-ac/3.920+ab*ac/7.174;
  phiA = (2+1.226*ac+0.958*ab-0.748*ab*ac)*(ab*ac)^(-1/3);
%  Crystal shape factors according to Lionnet (1998)
  phiV = 0.34;
  phiA = 2.9;

%  Brix of liquor before starting ultrasound (no crystals), %
  Brix00 = 81.4;
%  Volume of liquor before starting ultrasound (no crystals), cm3
  V00 = 20;
%  Density of liquor before starting ultrasound (no crystals), g/cm3
  rho00 = emmerich('sucrose', tC, Brix00);
%  Mass of liquor before starting ultrasound (no crystals), g
```

```
  m00 = rho00*V00;
%  Mass of dissolved sucrose before starting ultrasound (no crystals), g
  ms00 = Brix00/100*m00;
%  Mass of water (does not change), g
  mw = m00-ms00;

%  Initial guess for mass of crystals, g
  mc0 = 0.2;
%  Initial guess for crystallisation rate constant
  k = 0.01;
%  Initial guess for log10[number density of crystals] (does not change), crystals/cm3
  logn = 6.23;
%  Initial guess for the kinetics order
  n = 0.8;

%  ====================
%  PARAMETER ESTIMATION
%  ====================
  p0 = [mc0, k, logn, n];
  N_opt = 500;
  LB = [1e-6, 0, 5.8, 0.1];
  UB = [80, 100, 6.4, 2];
  options = optimset('Display', 'iter', 'MaxIter', N_opt, 'TolX', 1e-9);
  [p, fval, exitflag, output] = fminsearchbnd(@index3, p0, LB, UB, options);
  I = index3(p);
  mc0 = p(1);
  k = p(2);
  n_cryst = 10^p(3);
  n = p(4);

%  Initial volume of crystals, cm3
  Vc0 = mc0/rho_c;
%  Initial volume of a single crystal, cm3
  V_c0 = Vc0/N_cryst;
%  Initial crystal size, cm
  L0 = (V_c0/phiV)^(1/3);
%  Mass of dissolved sucrose at t=0, g
  ms0 = ms00-mc0;
%  Total number of crystals (does not change)
  N_cryst = n_cryst*V00;
%  Initial total crystal surface area, cm2
  Ac0 = N_cryst*phiA*L0^2;

%  Initial ODE state vector
  t0 = 0;
  u0 = [ms0];
```

```
  balances3(0, u0);
  ms_ = ms;
  mc_ = mc;
  Brix_ = Brix;
  Brix_s_ = Brix_s;
  sigma_ = sigma;
  Rc_ = Rc;
  Ac_ = Ac;
  L_ = L;
  t_ = t0;

%  Numerical integration of ODEs using a variable-order method
%  for stiff ODEs:  Shampine & Reichelt, SIAM J. Sci. Comput, 18, 1 (1997)
%  -  Number of time subintervals for result display
  NN = 200;
%  -  Max. size of the integration step [h]
  hmax = 0.001*tf;
%  -  Integration tolerance
  tol = 1e-7;

%  Integration of ODEs
  dt = tf/NN;
  opt = odeset('MaxStep', hmax, 'RelTol', tol);
  t = t0;
  u = u0;
  for i=2:NN,
    [t1, u1] = ode15s('balances3', [t, t+dt], u, opt);
    t = t1(end);
    u = u1(end, :)';
    balances3(t, u);
    ms_ = [ms_; ms];
    mc_ = [mc_; mc];
    Brix_ = [Brix_; Brix];
    Brix_s_ = [Brix_s_; Brix_s];
    sigma_ = [sigma_; sigma];
    Rc_ = [Rc_; Rc];
    Ac_ = [Ac_; Ac];
    L_ = [L_; L];
    t_ = [t_; t];
  end

  FS = 10;
  LW = 1.7;
  tyt = ['Solid-on-Solid model with nth-order kinetics'];
```

```
close all
figure(1)
subplot(2,2,1)
plot(t_, 1e4*L_, 'b-', 'LineWidth', LW)
xlabel('{\it{t}}  [min]', 'FontSize', FS)
ylabel('Median crystal size  [\mu]', 'FontSize', FS)
vv = [t0, tf, 0, 85];
axis(vv)
hold on
plot(ts, 1e4*L_median, '.b', 'MarkerSize', 10)
set(gca, 'FontSize', 8)
title([blanks(118), tyt], 'FontSize', 13, 'VerticalAlignment', 'bot')
text(8,37, ['index = ', num2str(I)])
text(8,30, ['m_c(0) = ', num2str(mc0)])
text(8,23, ['k = ', num2str(k)])
s1 = floor(p(3));
s2 = 10^(p(3)-s1);
s3 = num2str(s1);
text(8,16, ['n_{cryst} = ', num2str(s2), 'x10^', s3])
text(8,9, ['n = ', num2str(n)])

subplot(2,2,2)
plot(t_, ms_, '-r', 'LineWidth', LW)
xlabel('{\it{t}}  [min]', 'FontSize', FS)
ylabel('Mass of sucrose in liquor [g]', 'FontSize', FS)
vv = [t0, tf, 0, 25];
axis(vv)
set(gca, 'FontSize', 8)

subplot(2,2,3)
plot(t_, Brix_, 'b-', 'LineWidth', LW)
xlabel('{\it{t}}  [min]', 'FontSize', FS)
ylabel('Solution brix  [%]', 'FontSize', FS)
vv = [t0, tf, 75, 85];
axis(vv)
set(gca, 'FontSize', 8)
hold on
plot(t_, Brix_s, 'r:')

subplot(2,2,4)
plot(t_, mc_, 'r-', 'LineWidth', LW)
xlabel('{\it{t}}  [min]', 'FontSize', FS)
ylabel('Mass of sucrose crystals  [g]', 'FontSize', FS)
vv = [t0, tf, 0, 10];
axis(vv)
set(gca, 'FontSize', 8)
```

```
  fscreen

  figure(2)
  subplot(1,3,1)
  plot(t_, sigma_, 'b-', 'LineWidth', LW)
  hold on
  xlabel('{\it{t}}  [min]', 'FontSize', FS)
  ylabel('Sigma driving force,  \sigma', 'FontSize', FS)
  vv = [t0, tf, 0, 0.1];
  axis(vv)
  set(gca, 'FontSize', 8)

  subplot(1,3,2)
  plot(t_, Ac_, 'b-', 'LineWidth', LW)
  xlabel('{\it{t}}  [min]', 'FontSize', FS)
  ylabel('Total crystal surface area  [cm^2]', 'FontSize', FS)
  vv = [t0, tf, 0, 6000];
  axis(vv)
  set(gca, 'FontSize', 8)
  title(tyt, 'FontSize', 13, 'VerticalAlignment', 'bot')

  subplot(1,3,3)
  plot(t_, Rc_, 'b-', 'LineWidth', LW)
  xlabel('{\it{t}}  [min]', 'FontSize', FS)
  ylabel('Rate of crystallization  [g/cm^2 min]', 'FontSize', FS)
  vv = [t0, tf, 0, 0.0008];
  axis(vv)
  set(gca, 'FontSize', 8)
  fscreen

  figure(1)
  saveas(1, 'Figure 03-1.emf')
  saveas(2, 'Figure 03-2.emf')



function I = index3(p)

  global V00 n_cryst rho_c N_cryst phiV phiA ms00 ms0 mc0 mw L0 L Ac0 k n ts
L_median tf

  mc0 = p(1);
  k = p(2);
  n_cryst = 10^p(3);
  n = p(4);
```

```
%  Initial volume of crystals, cm3
   Vc0 = mc0/rho_c;
%  Total number of crystals (does not change)
   N_cryst = n_cryst*V00;
%  Initial volume of a single crystal, cm3
   V_c0 = Vc0/N_cryst;
%  Initial crystal size, cm
   L0 = (V_c0/phiV)^(1/3);
%  Mass of dissolved sucrose at t=0, g
   ms0 = ms00-mc0;
%  Initial total crystal surface area, cm2
   Ac0 = N_cryst*phiA*L0^2;

%  Initial ODE state vector
   u0 = [ms0];
%  Numerical integration of ODEs using a variable-order method
%  for stiff ODEs:  Shampine & Reichelt, SIAM J. Sci. Comput, 18, 1 (1997)
%  -  Number of time subintervals for result display
   NN = length(ts);
%  -  Max. size of the integration step [h]
   hmax = 0.001*tf;
%  -  Integration tolerance
   tol = 1e-7;
%  Integration of ODEs
   opt = odeset('MaxStep', hmax, 'RelTol', tol);
   t = 0;
   u = u0;
   I = 0;
   for i=1:NN,
      [t1, u1] = ode15s('balances3', [t, ts(i)], u, opt);
      t = t1(length(t1));
      u = u1(size(u1,1),:)';
      balances3(t,u);
      s = (L-L_median(i))*1e4;
      I = I+s*s;
   end
   I = sqrt(I/NN);



 function du_dt = balances3(t, u)

   global ms0 mw mc0 L0 Ac0 k n tC rho_s rho_c ms mc Brix Brix_s L sigma Rc Ac

   ms = u(1);
```

```
  mc = mc0+ms0-ms;
  Brix = 100*ms/(ms+mw);
  rho = emmerich('sucrose', tC, Brix);
  sigma = max([0, Brix*rho/(Brix_s*rho_s)-1]);
  Rc = k*sigma^n*rho_c;
  L = L0*(mc/mc0)^(1/3);
  Ac = Ac0*(L/L0)^2;
  du_dt(1,1) = -Rc*Ac;


function  rhosug = emmerich(sugar, t, Brix)
%  Density of sucrose/glucose/fructose-water solutions [g/cm3]
%  References:
%  [1] Bettin, H., Emmerich, A., Spieweck, F. & Toth, H.:
%     Density data for aqueous solutions of glucose, fructose and invert sugars.
%     Zuckerindustrie, 123(5), 341–348 (1998)
%  [2] Emmerich, A. & Emmerich, L.:
%     Die Dichte waßriger Lösungen von Glucose, Fructose und Invertzucker sowie
%     ihre Messung. Zuckerindustrie, 111, 441–447 (1986)
%  [3] Emmerich, A.:
%     Density data for sucrose solutions. Contribution to the application of
%     the new values adopted by ICUMSA.
%     Zuckerindustrie, 119, 120-123 (1994)
%  [4] Emmerich, A.:
%     Proceedings of the 21st Session of ICUMSA, Subject 11 - Density (1994)
%  Inputs:
%  sugar - type of sugar [string]:  sucrose, glucose or fructose
%  t - temperature [C], scalar
%  Brix - mass percentage of sugar, allowed to be a vector
%  Output:
%  rhosuc - density [g/ml], in general a column vector

  rhow = (999.83952+t*(16.952577+t*(-7.9905127e-3+t*(-46.241757e-6+...
        t*(105.84601e-9-281.03006e-12*t)))))/(1+16.887236e-3*t);
  h = 1;
  if strcmp(sugar, 'sucrose'),
    b = [ 385.1761,    135.3705,    40.9299,    -3.9643,    13.4853,   -17.2890;
         -46.2720,     -7.1720,     1.1597,     5.1126,    17.5254,    0;
          59.7712,     7.2491,     12.3630,    -35.4791,    0,         0;
         -47.2207,    -21.6977,    27.6301,    0,         0,         0;
          18.3184,    12.3081,     0,          0,         0,         0 ];
    h = 100;
  elseif strcmp(sugar, 'glucose'),
    b = [ 382.3089,    122.8456,    33.7382,    -10.9724,    15.7115,   -17.0990;
         -0.55131,    -0.01651,    0.12055,    0.06328,    0.13662,    0;
          0.0075748,  -0.0005640,  -0.0002244,  -0.0024582,  0,         0;
```

```
        -4.3945e-5,  -1.6701e-5,  -6.554e-6,    0,          0,          0;
         0,          0,           0,           0,          0,          0 ];
elseif strcmp(sugar, 'fructose'),
  b = [ 389.9822,    128.5980,     41.2216,    -20.4398,    30.0894,   -32.4503
        -0.73991,    -0.16423,     0.17736,    -0.06407,    0.20928,    0;
         0.0077259,   0.0013194,  -0.0064035,   0.0011841,  0,          0;
        -6.9542e-5,  -2.5768e-5,   7.7592e-5,   0,          0,          0;
         3.033e-7,    1.919e-7,    0,          0,          0,          0 ];
else
  halt
end
tau = (t-20)/h;
w = Brix/100;
[m,n] = size(Brix);
if n>m,
  w = w';
end
w1 = w;
w2 = w1.*w;
w3 = w2.*w;
w4 = w3.*w;
w5 = w4.*w;
w6 = w5.*w;
w = [w1, w2, w3, w4, w5, w6];
rhosug = rhow+w(:,1:6)*b(1,1:6)'+tau*(w(:,1:5)*b(2,1:5)'+tau*...
        (w(:,1:4)*b(3,1:4)'+tau*(w(:,1:3)*b(4,1:3)'+w(:,1:2)*...
        b(5,1:2)'*tau)));
rhosug = 0.001*rhosug;
if n>m,
  rhosug = rhosug';
end
```